National University of Science and Technology
Politehnica Bucharest

Doctoral School of Mechanical and Mechatronic Engineering

DOCTORAL THESIS

STUDIES ON THE VERTICAL BENDING VIBRATIONS OF THE RAILWAY VEHICLE CARBODY
SUMMARY

Ph.D supervisor
Prof.Dr. Eng. Mădălina Dumitriu

Ph.D Student
Dihoru Ioana Izabela

Bucharest
2024

Contained

1. Introduction

1.1. Relevance of the research topic

Railway transport has an important role in today's society, where mobility is a pressing necessity both economically and socially. In the general set of transports, railway transport stands out by satisfying the requirement of the mobility of passengers and goods in safety conditions, economic efficiency and with a low impact on the environment. All of these contribute to the creation of an attractive, efficient and sustainable transport system, competitive on the transport market marked by strong competition from the air and road transport system.

The position that railway passenger transport occupies today is due to the evolution of the last 40 years, which has been marked by the increase in speed. From this perspective, railway transport has become a field of interest in scientific research with applications in engineering, in which exceptional achievements have been achieved. The appearance of high-speed trains, because they are referred to here, completely changed the concept regarding the construction of railway vehicles, giving, at the same time, a new perspective on the technical possibilities and economic advantages of the railway transport system.

The general trend, which characterizes the development of the railway transport system, is further directed towards increasing speed, reducing fuel consumption and manufacturing costs. These desired goals can be achieved through a permanent research-innovation activity, ever more refined and complex, which requires a systemic approach in identifying the best technical solutions to ensure at the same time the dynamic performance of railway vehicles – ride comfort, ride quality and safety, at high speeds.

In the context of the above, the railway vehicle was and is constantly subject to innovations in order to maintain dynamic performances, it must ensure in order to respond to the constantly changing requirements on the transport market. The innovation activity starts from the careful study of the phenomena that occur during the running of the vehicle, in this way it is possible to establish the important factors that influence the behaviour of the vehicle and the theoretical foundation of the proposed technical solutions.

One of the phenomena that manifests permanently during the running of the railway vehicle is vibrations, which are a result of the interaction between the vehicle and the track [35, 65]. In general, the level of vibrations to which a railway vehicle is exposed depends on its type and constructive characteristics, on the operating conditions and on the interaction phenomena between the vehicle and the track. The increase in speed leads to an amplification of the vibration level and, consequently, to numerous challenges related to the design of vehicles whose dynamic behaviour satisfies the performance criteria mentioned above [28].

The railway vehicle represents a complex oscillating system, which makes it difficult to address vibration problems, which present specific characteristics [32]. First, it should be stated that the eigenfrequencies of the main vibration modes of the railway vehicle, relevant from the point of view of passenger comfort or ride quality, are in the low frequency range, below 20 Hz. It is also mentioned that the vibrations of the railway vehicle develop both in the vertical plane and in the horizontal plane, but applying the principle of vibration decoupling, the vertical vibrations can be studied separately from the horizontal vibrations. This hypothesis is adopted based on the fact that, from a constructive point of view, the railway vehicle is, in general, symmetrical, both geometrically and inertially and elastically [5 – 7, 45, 46].

Regarding the vibration modes of the railway vehicle, respectively of its suspended masses (carbody and bogies), a distinction is made between rigid modes or simple vibration modes and flexible modes (structural modes) or complex vibration modes.

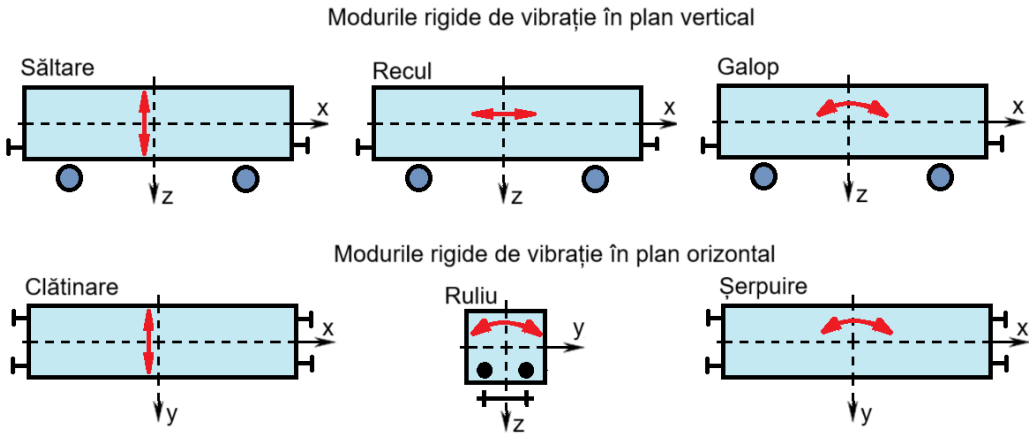

Fig. 1.1. Rigid vibration modes of the railway vehicle carbody [27].

Rigid modes of vibration develop as independent, translational and rotational motions. In the vertical plane, two translational movements are distinguished - the bounce and the rebound, and a rotational movement - the pitch, and in the horizontal plane, the rigid modes of vibration are manifested in the form of a translational movement - the sway, and two rotational movements - the roll and yaw. A schematic illustration of the rigid vibration modes of the vehicle body is shown in figure 1.1.

Regarding the flexible vibration modes of the railway vehicle, the flexible vibration modes of the carbody are considered. They become important in the case of long carbodies of railway vehicles intended for the transport of passengers, in the design of which weight reduction is imposed as a basic criterion.

The weight reduction criterion is a general valid criterion in the design of railway vehicles so that they travel at the highest possible speeds and the energy consumption is as low as possible. At the same time, by reducing the weight of railway vehicles, other benefits are obtained, such as reducing vibrations transmitted through the ground, reducing manufacturing costs or maximizing the use of axle loads [25, 38, 63]. To apply this criterion, one of the following solutions can be chosen during the design stage of railway vehicles: the use of light materials or the modification of the mechanical structures of the vehicle.

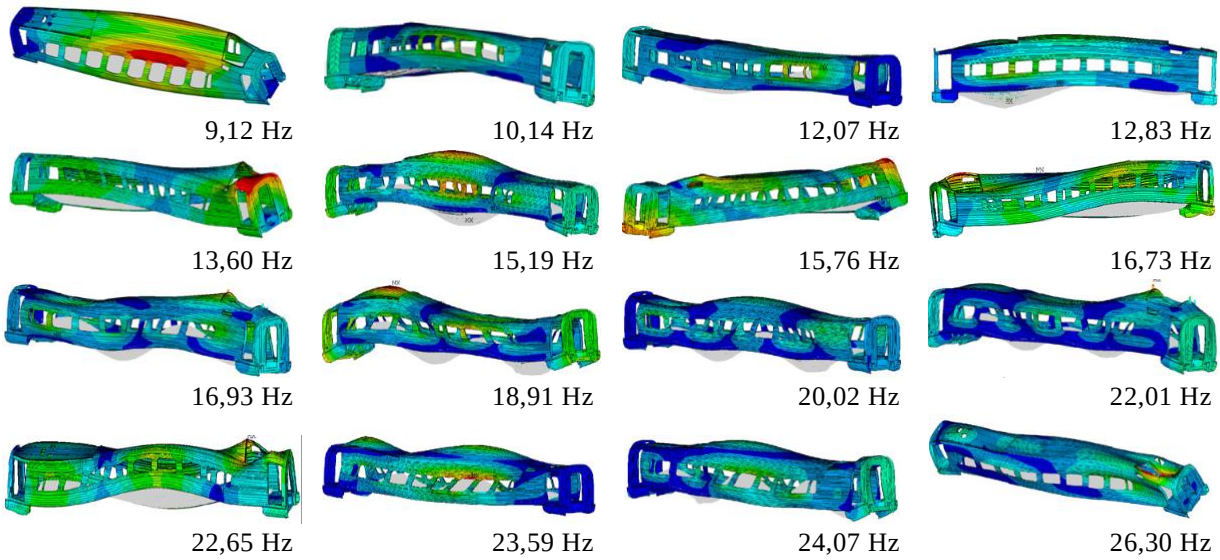

Fig. 1.2. Examples regarding the modal shapes of the structural vibrations of the railway vehicle carbody, after [34].

The use of light materials for the manufacture of the carbody resulted in a significant decrease in its structural rigidity. Favourable conditions were thus created for the excitation of structural vibrations in the long carbodies of passenger vehicles, which thus became much more flexible [34].

The structural vibrations of the railway vehicle carbody are particularly complex, with local and global modes, which can have different modal shapes and eigenfrequencies, as shown in figure 1.2.

The results of numerous research have shown that the vibration behaviour of the carbody is strongly influenced by structural vibrations [1, 4, 12, 26, 47, 66], with important effects on the comfort of the passengers [2, 15, 38, 51, 67]. Also, structural vibrations stress the carbody to fatigue, which leads to the reduction of its service life [39, 40].

Narrowing the discussion to the structural vibrations of the carbody that affect the comfort of passengers, the structural vibration modes of the carbody are important, whose frequencies are in the low frequency range, below 20 Hz, in which the human body shows a high sensitivity to vibrations [41]. The first mode of vertical bending of the carbody is of particular importance because, usually, its eigenfrequency is found in the range of 7 ... 12 Hz, a range in which the human body shows greater sensitivity to vertical vibrations [4, 15, 47, 68, 72].

Based on the considerations presented above, the conclusion can be summarized that, to reduce the structural vibrations of long carbodies for passenger vehicles, the weight criterion must be correlated with the stiffness criterion. Obtaining a greater rigidity with a lower weight is also the "key" to the design of the structure of the railway vehicle carbody [68].

The simplest solutions for reducing the structural vibrations of the carbody of railway vehicles involve reducing the length of the carbody, increasing the cross-section or increasing the rigidity of the carbody. However, these solutions are nowhere near as effective as they are simple, being in contradiction with other requirements imposed in the design of long carbodies of passenger vehicles.

The first of the solutions, which refers to reducing the length of the carbody, is in contradiction with the requirement to maximize the number of passengers, for example, in relation to the number of bogies. The second solution, aimed at increasing the cross-section, can lead to problems of stability of the carbody under the action of the side wind or registration in the gauge. Regarding the possibility to increase the stiffness of the carbody, the reinforcements used for stiffening lead to an increase in the weight of the carbody, which contradicts the weight reduction criterion. Moreover, this solution leads to constructive complications of the carbody and to the increase of the manufacturing price [42]. In search of the most effective solutions for reducing structural vibrations of flexible carbodies of passenger railway vehicles, numerous research has been developed throughout the world in the last 20-30 years. Thus, a vast area of research was opened, in which new concepts were introduced, and different methods were developed, all following the same direction – the reduction of structural vibrations of the carbody of passenger railway vehicles, relevant from the point of view of ride comfort.

In the brief presentation above can be found the motivation for choosing the research theme developed in this doctoral thesis, as well as its importance from a scientific and technical point of view. By the nature of the problem it deals with, the doctoral thesis entitled *Studies on the vertical bending vibrations of the railway vehicle carbody* represents a current theme, which is part of the area of research on the possibilities of reducing the structural vibrations of the flexible carbodies of railway passenger vehicles in to improve comfort both on high-speed trains [3, 19, 20, 26, 47, 67, 70] and on suburban trains or on metro trains [2, 42, 43, 48, 49, 63, 64].

The results presented in this thesis bring relevant contributions regarding, on the one hand, the modelling of the vehicle-track system in addressing the problems related to the vibrations of the flexible carbodies of the railway vehicle, and on the other hand, the possibility of reducing the bending vibration vertical of the carbody and increasing the eigenfrequency of this mode of vibration through a simple and effective method that involves the use of a system of anti-bending bars. These results become useful further both in the activity of scientific research with applications in the railway field, as well as in the activity of designing railway vehicles, constituting a real basis in the development and implementation of a technical solution leading to the improvement of ride comfort.

1.2. Objectives of the doctoral thesis

The research topic of the doctoral thesis - *Studies on the vertical bending vibrations of the railway vehicle carbody*, was defined in a broad sense, to be specified by defining the general objective and several specific objectives.

The general objective of the thesis is to develop research on the possibilities of reducing the vertical bending vibrations of the carbody of railway vehicles by using a system of anti-bending bars. The concept of anti-bending bars mounted on the longitudinal beams of the carbody chassis was introduced by the PhD supervisor in an innovative method from the scientific point of view and simple from the technical point of view [14]. The functionality of this method has been demonstrated both theoretically and experimentally on a scale laboratory model [8, 10, 36], which justifies further research to make the transition to a higher scientific and technical level.

Concretely, the general objective of the doctoral thesis consists in the development of a complex model of the carbody - anti-bending bars system and its integration into the general system model of the carbody with anti-bending bars - bogies - track used to evaluate the effect of anti-bending bars on vibrations vertical of the vehicle carbody. Furthermore, the specific objectives of the thesis were established and, depending on them, the directions to be followed to reach the proposed targets were drawn.

In establishing the specific objectives of the thesis, it was considered that in order to achieve the general objective, preliminary studies are necessary, based on which the degree of complexity of the model of the vehicle - track system necessary for the evaluation of the vertical vibration behaviour of the vehicle carbody can be established.

Considering the specifics of the problem addressed, it was started from the premise that in the modelling of the vehicle-track system, the important factors that can influence the vertical vibration behaviour of the carbody must be considered and that lead to sufficiently accurate results, but without complicating analysing the results and synthesizing the relevant conclusions. These factors can be represented by the models adopted for the railway vehicle subsystem and the track subsystem.

Thus, the first specific objectives of the thesis were established, which consist in the development of three different studies, in which the influence of the carbody model, the secondary suspension and the track in the simulation of the vertical vibration behaviour of the railway vehicle carbody is analysed, as appropriate. The scientific challenges that the proposed objectives raise are highlighted here, and which primarily refer to the development of several theoretical models of the vehicle-track system, which include different models of the carbody, the secondary suspension or the track, as follows: the model "rigid carbody", "flexible carbody "model, "reference model" and four "analysis models" of the secondary suspension, "rigid track" model, "elastic track" model. Then, there is the problem of developing different software applications for each of these models to simulate the vertical vibration behaviour of the railway vehicle carbody. The analysis of the vertical vibration behaviour of the vehicle carbody constitutes an important stage of each of the three studies, following which the structure of the model of the vehicle – track system is established, into which, in the next stage, the model of the carbody - anti-bending bars system will be integrated.

The following two specific objectives are in close agreement with the general object of the thesis. The first of these consists in the study of the dynamic response of the carbody - anti-bending bar system. To achieve this objective, an important step must first be completed, namely the modelling of the carbody - anti-bending bars system for several analysis scenarios: the "carbody without anti-bending bars" model, the "carbody with anti-bending bars without inertia" model, the “carbody with anti-bending bars with inertia” model. By this approach, the initially proposed simple model for the representation of the anti-bending bars – the inertia-free model, and their rigid attachment to the supports fixed to the vehicle carbody is to be developed to take into account the effect of the elastic parameters of the fastening elements, as well as the effect of the rigid and bending modes of the anti-bending bars on the dynamic response of the vehicle carbody. The second objective consists in the analysis of the effect of anti-bending bars on the vertical vibrations of the railway vehicle carbody generated by track irregularities, which implies the development of a new model, namely the model of the integrated system of the carbody with anti-bending bars – bogies – track.

The last specific objective of the thesis consists in carrying out experimental determinations to verify the results obtained through numerical simulations, based on which, on the one hand, basic characteristics of the vertical vibration behaviour of the railway vehicle carbody were highlighted, and on the other hand, important effects of anti-bending bars on the vertical vibrations of the railway vehicle carbody. In order to achieve this goal, several steps must be taken, starting from the establishment of the measurement conditions – real physical conditions or laboratory conditions, to the choice of equipment, measurement and data acquisition systems and their integration into a measurement chain, the development of software applications for control, acquisition, processing, representation and storage of data and continuing with making experimental determinations, synthesizing the results and comparing them with the results obtained through numerical simulations.

1.3. Overview of the doctoral thesis

The doctoral thesis is organized by chapters, which have been established in accordance with the specific objectives presented above. Dedicating a distinct chapter to each of the six specific objectives, to which were added two chapters of introduction and presentation of the problem addressed and a chapter of conclusions, personal contributions and future research directions, the structure of the present thesis was reached, which includes 9 chapters.

Chapter 2 provides a synthesis of the current state of research on vertical vibrations of railway vehicles, with a focus on the structural vibrations of flexible carbodies of passenger vehicles and their effect on ride comfort. The purpose of this chapter is to provide an overview of previous studies that include research results on the characteristics and possibilities of reducing structural vibrations of the carbody of railway vehicles relevant from the ride comfort to vertical vibrations. A section of the chapter is devoted to the presentation of the method of reducing the bending vibrations of the railway vehicle carbody, in which the concept of anti-bending bars was introduced. This presentation aims to highlight the current state of research developed in this direction, which is also the starting point in establishing the general objective of the doctoral thesis.

In Chapter 3, the results of a study are presented in which the influence of the first bending mode of the railway vehicle carbody on its vertical vibration behaviour is analysed. The study is based on comparisons between the results of numerical simulations developed based on two mechanical models of the vehicle. In the first model - the "rigid carbody" model, the carbody is represented by a rigid body, and in the second model - the "flexible carbody" model, the carbody is represented by an equivalent Euler-Bernoulli beam. Both vehicle models are described in the first part of the chapter, where the equations of motion corresponding to each model are also included. The following sections of the chapter are dedicated to establishing the calculation relations, customized according to the two models, for the frequency response functions, the acceleration power spectral density and the root mean square of the acceleration in three points relevant to the vibration regime of the carbody. The chapter concludes with the analysis of the vertical vibration behaviour of the "rigid carbody" and the "flexible carbody " and the influence of the first vertical bending mode on the vertical vibration level of the carbody.

In Chapter 4, the influence of the secondary suspension model on the evaluation of the vertical vibration behaviour of the carbody is investigated based on the results of numerical simulations. Numerical simulation applications are developed based on a rigid-flexible coupled vehicle model with seven degrees of freedom, corresponding to the vertical vibration modes of the carbody – bounce, pitch and first vertical bending mode, and the vertical vibration modes of the bogies – bounce and pitch. Four different secondary suspension models are integrated into the vehicle model. The first model is a simple model, considered the "reference model", consisting of a single Kelvin-Voigt system for vertical translation by which the stiffness and vertical damping of the secondary suspension are represented. The other three models are "analysis models", which are obtained by composing in various variations the reference model with Kelvin-Voigt systems for rotation or longitudinal translation through which the pitch vibrations of the bogies are transmitted to the carbody, influencing its vibration behaviour. The vehicle model and its equations of motion, corresponding to the four secondary suspension models, are presented in the first part of the chapter. The second part of the chapter is focused on the frequency response functions of the vehicle carbody and the dynamic response of the vehicle to random track irregularities. The influence of the secondary suspension model on the evaluation of the vertical vibration behaviour of the railway vehicle carbody is carried out based on the analysis of the results of numerical simulations on the frequency response functions of the acceleration, the power spectral density of the acceleration and the root mean square of the acceleration calculated at the relevant points for the behaviour of vibrations of the carbody. This analysis is presented in the last part of the chapter.

The purpose of Chapter 5 is to establish the influence of the track model on the evaluation of the vertical vibration behaviour of the railway vehicle carbody based on the results obtained through numerical simulations. For this, the frequency response functions, the power spectral density and the root mean square of the acceleration at the relevant points of the vibration behaviour of the carbody are compared for two models of the vehicle-track system, namely the "rigid track" model and the "elastic track". The model referred to here as "rigid track" is a model analysed in the previous chapter as well, which brings together the track model, considered rigid, and the rigid-flexible coupled model of the vehicle, with 7 degrees of freedom, in which the secondary suspension is represented by one of the three "analysis models", composed of the "reference model" and a Kelvin-Voigt system for longitudinal translation that models the longitudinal force transmission system between the carbody and the bogies. The "elastic track" model is developed in this chapter and includes the same rigid-flexible coupled model of the vehicle and the track, which is represented by an equivalent model with concentrated parameters. Assuming the hypothesis of linear Hertzian contact between the wheel and the rail, the connection between the vehicle model and the track model, respectively the elasticity of the contact between the wheel and the rail is considered by a Hertzian elastic element with linear characteristic. The "elastic track" model is a 15-degree-of-freedom model corresponding to the vertical vibration modes of the carbody - bounce, pitch and the first vertical bending mode, the vertical vibration modes of the bogies – bounce and pitch, and the vertical displacements of the wheelsets and rails. This model is described in detail in the second section of the chapter, where the equations of motion of the carbody, bogies, wheelsets and rails are also presented.

Chapter 5 follows the same structure as Chapters 3 and 4, respectively after the presentation of the model of the vehicle– track system, the relationships of the frequency response functions, the acceleration power spectral density and the root mean square of the acceleration at the relevant points of the vibration behaviour of the carbody. In the last section, the results of the numerical simulations for the two models of the vehicle-track system are analysed, through which the influence of the track model in the simulation of the vertical vibration behaviour of the railway vehicle carbody is highlighted.

Chapter 6 constitutes the first stage in the development of research on the possibilities of reducing vertical bending vibrations of the carbody of railway vehicles by using anti-bending bars. Thus, for the study of the dynamic response of the carbody - anti-bending bars system, a simplified model of the railway vehicle was developed, which includes the carbody, considered a Euler-Bernoulli beam supported on the secondary suspension elements, and equipped with anti-bending bars. The simple model proposed in previous research to represent the anti-bending bars by linear elastic elements and neglecting their mass in relation to the mass of the carbody – the "carbody with anti-bending bars without inertia" model, rigidly fixed in the supports on the longitudinal beams of the carbody chassis, was developed to consider both the effect of the rigid and bending modes of the anti-bending bars, as well as the effect of the elastic parameters of the fastening elements on the dynamic response of the vehicle carbody. To represent the vertical movements, the anti-bending bars were modelled as Euler-Bernoulli free-free equivalent beam at the ends but related to the elastic elements of the support. The attachment system of the anti-bending bars to the supports was modelled by ideal elastic elements that take both vertical and longitudinal translations, as well as rotations in the vertical-longitudinal plane. In order to achieve the purpose of this chapter, which is to highlight the basic properties of the dynamic response of the carbody - anti-bending bar system and to evaluate the influence of the first two vibration modes of the anti-bending bars and the stiffness of the elastic fastening elements of the support anti-bending bar system on the frequency response functions of the carbody and anti-bending bars, the results of numerical simulations developed on the basis of three distinct models: " carbody without anti-bending bars" model, " carbody with anti-bending bars without inertia", " carbody with anti-bending bars with inertia" model. The chapter is structured in four sections, the first of which is an introductory section in which the working principle of the anti-bending bar system and the method of reducing vertical bending vibrations of the carbody developed on this principle are briefly described. In the next two sections, the model of the carbody – anti-bending bar system is described, the equations of motion of the carbody and anti-bending bars are derived, and the displacement frequency response functions for the carbody – anti-bending bar system and for the anti-bending bars are determined. The analysis of the dynamic response of the carbody - anti-bending bar system is presented in the last section of the chapter.

In Chapter 7, the scientific steps carried out in Chapters 4, 5 and 6 initiated to build the theoretical model for the study of the vibrations of the integrated system of the carbody with anti-bending bars – bogies – track are exploited. Thus, starting from the results obtained in Chapters 4 and 5, the most suitable mechanical representations of the carbody, the secondary suspension of the vehicle and the track are established, so that the numerical simulations performed based on the model of the integrated system of the carbody with anti-bending bars – bogies – track to provide sufficiently correct results, on

the one hand, and on the other hand, to simplify the analysis of these results by reducing the number of model parameters to the strictly necessary. At the same time, the model of the carbody with anti-bending bars is taken from Chapter 6 which allows the study of coupled bending vibrations of the carbody and anti-bending bars, considering the stiffness in three directions of the attachment of the anti-bending bars to the supports fixed to the longitudinal beams of the chassis the carbody. Once the model of the integrated system of the carbody with anti-bending bars – bogies – track has been finalized, we move on to writing its motion equations and deducing the frequency response functions. The dynamic response of the carbody with anti-bending bars to the running of the railway vehicle on a track with harmonic irregularities is then analysed. In the final part of the chapter, the parametric study on the effect of anti-bending bars on the vertical vibrations of the carbody when running on a track with random irregularities is presented. The influence of the bending vibrations of the anti-bending bars on the vertical vibration of the carbody is highlighted, evaluated by the root mean square of the acceleration and by the ride comfort index.

In the previous chapters, the problem of vibrations of the railway vehicle carbody was approached from a theoretical point of view, and numerical simulation software applications were used as an investigation tool. Thus, in the studies developed based on the results of numerical simulations, on the one hand, basic characteristics of the vertical vibration behaviour of the carbody were highlighted, and on the other hand, important effects of the anti-bending bars on the bending vibrations of the railway vehicle carbody. However, being observations that are based only on theoretical studies, to be synthesized in the form of conclusions, it is necessary that they be corroborated with experimental results. For this, Chapter 8 was included in the structure of the thesis, in which the experimental determinations made both in real physical conditions and in laboratory conditions are described, to verify the theoretical results. The first part of the chapter is dedicated to the experimental determinations carried out under real physical conditions, on a passenger vehicle traveling in a current line. Two distinct sections are included here, a section in which the characteristics of the vehicle, the conditions of making the measurements, the equipment and software applications used are described, and another section in which the experimental results are presented and analysed. Based on the spectral analysis and the root mean square of the measured acceleration, the most important characteristics of the vertical vibrations of the vehicle carbody are highlighted, which were also emphasized in the analysis of the results obtained through numerical simulations in Chapters 3, 4 and 5. The experimental determinations described in the second part of Chapter 8 were carried out to verify the results obtained through numerical simulations regarding the effect of anti-bending bars on the vertical vibrations of the railway vehicle carbody, presented in Chapter 6. These determinations were conducted under laboratory conditions on a scale model of the carbody with/without anti-bending bars. The second part of the chapter is structured in three sections. In the first section, the demonstrative experimental system and the measurement and control chain components of this system are described. The second section presents the structure of the software application for the control, acquisition, processing, representation and storage of the measured data. The last section is reserved to the analysis of the vertical accelerations of the experimental carbody model with/without anti-bending bars and to summarize the conclusions regarding the agreement between the theoretical and experimental results.

2. Current state of research on vertical vibrations of the passenger railway vehicle

2.1. Thematic area of research

The research topic addressed in this doctoral thesis, "*Studies on the vertical bending vibrations of the railway vehicle carbody*", is a current topic, which is part of the research area with applications in the railway field, which have enriched in the last 20-30 years specialized literature with numerous scientific publications. In this framework, new concepts were proposed, and innovative methods were developed which, however different they may be and regardless of the approach, converge in the same direction – identifying the possibilities of reducing the structural vibrations of the light carbodies of railway passenger vehicles in the view of improving ride comfort in both high-speed trains and suburban or metro trains.

As it was also shown in the brief presentation in the first chapter of the thesis, the problem of structural vibrations of the light carbodies of passenger railway vehicles has become a research topic of interest as a result of the effect that these modes of vibration have especially on passenger comfort. It is about those flexible modes of vibration whose eigenfrequencies decrease in the case of reducing the structural rigidity of the carbody as a result of reducing its weight, thus reaching the area of sensitivity of the human body to vibrations [38]. For example, the eigenfrequency of the first mode of vertical bending of the carbody is, as a rule, in the range of 7 ... 12 Hz, where the human body shows a greater sensitivity to vertical vibrations. According to the results of several research, the first mode of vertical bending affects comfort, especially in the middle of the carbody [12, 26]. In some situations, high speeds or/and high flexibility of the carbody, repositioning of the critical points for comfort from the extremities of the carbody to its middle [17, 51, 67].

Following a detailed analysis of the specialized literature, representative of the topic of the doctoral thesis, several scientific articles, book chapters, doctoral theses and research reports were identified, in which the problem of reducing the vertical bending of the carbody is treated with predilection or it is included in the broader framework of reducing flexible vibration modes relevant from the point of view of ride comfort. Regarding the proposed methods, in general, they can be grouped, depending on the approach, into "vibration isolation" methods or "vibration damping" methods. The methods that fall into the first category aim to isolate the carbody from the vibrations that are transmitted from the wheelsets and bogies through the vehicle suspension [3, 18, 29, 37, 52 – 56, 66, 69, 70]. In the second category can be included the methods that lead to the increase of the structural damping of the carbody [13, 14, 21, 24, 30, 31, 52 - 57]. Regardless of the category they fall into, these methods can be developed based on passive, semi-active or active concepts [33, 43, 44, 71].

Research on the vibrations of flexible carbodies of passenger vehicles has, however, been extended to other related directions, which have been developed on topics such as modelling the structural flexibility of the carbody or simulating its vibration behaviour. Also, in the specialized literature, numerous papers are found in which the characteristics of the vertical vibrations of flexible carbodies are analysed or the influence of flexible modes of vibration on ride comfort, respectively on the ride quality, is studied. Last but not least, the experimental research carried out for the validation of the concepts or the effectiveness of the proposed methods for reducing the flexible vibration modes of the railway vehicle carbody or the numerical simulation models should be mentioned. What is important to emphasize here is that this issue of flexible carbody vibration, particularly important from the point of view of the impact it has on the dynamic performance of railway vehicles, has opened a vast area of research, which has developed over time, as research directions have diversified, and investigative methods and tools have become increasingly complex and refined.

The purpose of this chapter is to present synthetically a series of representative scientific papers, which contain the results of research on the vibrations of the flexible carbodies of railway passenger vehicles, structured on three general topics: (a) the characteristics of the flexible modes of vibration of the carbody of railway vehicles and their influence on ride comfort; (b) reducing the flexible modes of vibration of the railway vehicle carbody; (c) experimental validation of the effectiveness of methods to reduce the flexible vibration modes of the railway vehicle carbody. An important section of this chapter is the one in which the method of reducing vertical bending vibrations of the carbody of railway vehicles is presented, based on a system of anti-bending bars mounted on the longitudinal beams of the carbody chassis. In accordance with the general objective of the thesis, research on the possibilities of reducing vertical bending vibrations of the carbody of railway vehicles by using the anti-bending bar system will be developed in Chapters 6 and 7. In principle, the general objective of the doctoral thesis aims to develop a complex model of the carbody - anti-bending bars system and its integration into the general system model of the carbody with anti-bending bars - bogies - track, which will be used to evaluate the effect anti-bending bars on the vertical vibrations of the railway vehicle carbody and on the ride comfort.

3. Study on the influence of bending vibrations on the vertical vibration behaviour of the railway vehicle carbody

3.1. Introduction

In this chapter they are presented the results of a study in which the influence of the first vertical bending mode on the vibration behaviour of the railway vehicle carbody is analysed, in correlation with the bending stiffness of the carbody, velocity and suspension damping. The study is based on comparisons between the results of numerical simulations developed based on two different mechanical models of a railway vehicle.

In the first model - the "rigid carbody" model, the carbody is represented by a rigid body, and in the second model - the "flexible carbody" model, the carbody is represented by an equivalent Euler-Bernoulli beam. The "flexible carbody" model allows the consideration of the carbody's own vibration modes due to bending. Both models are described in the first part of the chapter, where the equations of motion corresponding to each model are also found. The following sections of the chapter are dedicated to establishing the calculation relations for the frequency response functions in the permanent harmonic vibration regime, the power spectral density of the acceleration and the root mean square acceleration of the three-point of the carbody, considered relevant to its vibration behaviour. One of the points is fixed in the middle of the carbody, and the other two points are positioned above to the two bogies, respectively above to the points where the carbody rests on the secondary suspension. The calculation relationships are particularized according to the two vehicle models.

The chapter ends with the study dedicated to the vertical vibration behaviour of the vehicle carbody. In the first part of the study, the characteristics of the vertical vibration behaviour of the "rigid carbody" and the "flexible carbody" are analysed based on the frequency response functions and the power spectral density of the vertical acceleration, calculated at the relevant points for the vibration behaviour of the carbody. In the second part of the study, the influence of the first vertical bending mode on the vertical vibration level of the carbody is analysed, using the root mean square of the acceleration.

3.2. Mechanical models of the railway vehicle

For the proposed study, we consider the case of a passenger vehicle on bogies, with two suspension stages, which traveling at constant speed V on a track in alignment. It is represented from a mechanical point of view both by a "rigid carbody" type model and by a "flexible carbody" type model, as shown in figure 3.1. Both models include seven bodies, through which the carbody, the chassis of the two bogies and the four wheelsets are modelled, linked together by Kelvin-Voigt type systems with the help of which the two suspension stages are modelled. In the case of the "rigid carbody" model, all bodies are considered rigid bodies. The "flexible carbody" model is a rigid-flexible coupled model, where the bogies and wheelsets are represented by rigid bodies and the carbody is represented by an equivalent Euler-Bernoulli beam.

The rigid modes of vibration of the carbody and bogies, common to both models, are bounce and pitch. Figure 3.1 shows the vertical displacements of the carbody (z_c) and bogies ($z_{b1,2}$) corresponding to the bounce and the rotation angles corresponding to the pitch of the carbody (θ_c), respectively the pitch of the bogies ($\theta_{b1,2}$). The inertia of the carbody and bogie in relation to their rigid modes of vibration are represented by the mass and inertia moment related to the two bodies, denoted as follows: m_c – carbody mass; m_b - bogie mass; J_c - inertia moment of the carbody; J_b - inertia moment of the bogie.

The Kelvin-Voigt system through which the primary suspension related to an wheelset is modelled has the elastic constant $2k_{zb}$ and the damping constant $2c_{zb}$. Each bogie is connected to the carbody by means of a Kelvin-Voigt system with elastic constant $2k_{zc}$ and damping constant $2c_{zc}$.

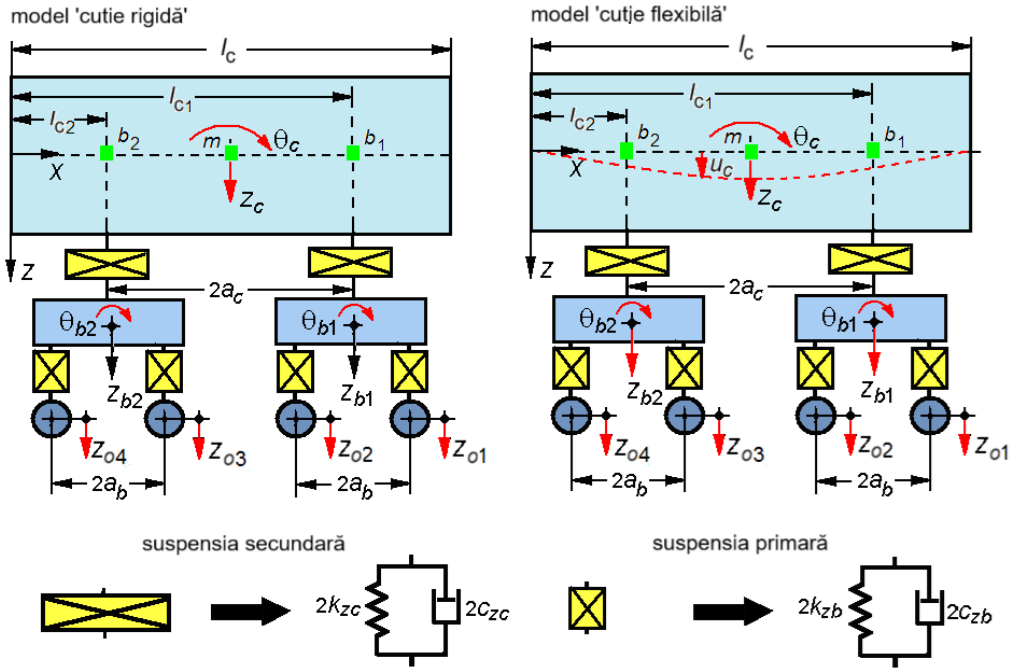

Fig. 3.1. Mechanical model of the railway vehicle:
"rigid carbody" model; "flexible carbody" model.

Other common elements of the two models, marked on figure 3.1, are the length of the carbody, denoted by l_c, the wheelbase of the carbody $2a_c$ and the wheelbase of the bogie $2a_b$. With $l_{c1,2}$ the distances that fix the position of the support points of the carbody on the secondary suspension were noted. Also, three points are marked on the carbody model, one in the middle of the carbody - point *m*, and two others above to the bogies, respectively above to the supporting points of the carbody on the secondary suspension - points b_1 and b_2. These three points are considered relevant points for the vibration behaviour of the carbody. The track is considered rigid, and in this hypothesis the vertical irregularities of the track are transmitted to the wheelsets, which require vertical displacements marked on figure 3.1 with $z_{o1...4}$.

3.3. Analysis of the vertical vibration behaviour of the vehicle carbody

This section is dedicated to the analysis of the influence of the first vertical bending mode on the vertical vibration behaviour of the railway vehicle carbody. For this, results obtained through numerical simulations developed in the Matlab programming environment are used for the two mechanical models of the railway vehicle presented in section 3.2 - the "rigid carbody" type model and the "flexible carbody" type model. To carry out the proposed study, the frequency response functions of the acceleration, the power spectral density of the acceleration and the root mean square of the acceleration, calculated in the three points relevant to the vibration carbody - point *m* located in the middle of the carbody, are analysed in parallel and points b_1 and b_2 positioned above to the two bogies, for the reference values of the parameters of the numerical model of the vehicle, to which are added analysis values for the bending stiffness of the carbody and for the damping ratio of the secondary suspension and the primary suspension.

The eigenfrequencies of the vertical vibration modes of the carbody corresponding to the reference values of the parameters of the numerical model of the vehicle are: the eigenfrequency of the bounce vibration f_s = 1,17 Hz; eigenfrequency of pitch vibration f_g =1,46 Hz; eigenfrequency of vertical bending f_{iv} = 8 Hz.

For the reference parameters of the numerical model of the vehicle, the damping ratio of the two suspension stages have the following values: ξ_{zc} = 0.12 for the secondary suspension; ξ_{zb} = 0.22 for the primary suspension. Regarding the analysis values, for the bending stiffness of the carbody, they are adopted so that the bending frequency of the carbody takes the values shown in Table 3.1. For the damping ratio of the two suspension floors, 50 values are adopted in the range of 0.05 ... 0.5.

Table 3.1. Vertical bending frequency as a function of carbody bending stiffness.

The bending stiffness of the carbody [MNm^2]·10^3	1,776	3,158	4,934
Frequency of vertical bending of the carbody [Hz]	6	8	10

Figure 3.2 shows the response functions of the acceleration of the carbody at its middle and above to the two bogies, calculated for the reference values of the two vehicle models - the "rigid carbody" model and the "flexible carbody " model, taking considering the undamped case (c_{zc} = 0; c_{zb} = 0; c_m = 0). The curves of the response functions thus obtained show a series of peaks corresponding to the resonance frequencies of the vibration modes of the carbody and several minima corresponding to some anti-resonance frequencies. The peaks corresponding to the resonance frequencies of the rigid vibration modes of the carbody - bounce at 1.17 Hz and pitch at 1.46 Hz (diagrams a and b) and vertical bending at 8 Hz (diagram b) are highlighted. On both diagrams, the peak of the response functions corresponding to the resonance frequency of the bounce vibrations of the bogies at 6.65 Hz is also identified.

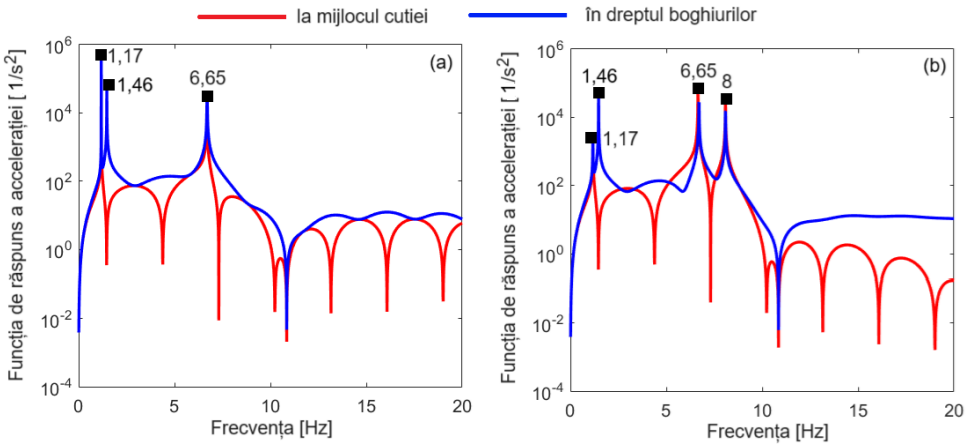

Fig. 3.2. Frequency response functions of the carbody acceleration for the undamped case: (a) for the "rigid carbody" model; (b) for the "flexible carbody " model.

The anti-resonance frequencies, which are identified on the frequency response curve of the carbody as minima, are due to the geometric filtering effect. This effect is an important characteristic of the vertical vibration behaviour of railway vehicles.

According to several studies [16, 22, 23, 50, 72, 73], the geometric filtering has a selective character, depending on the speed, and a differentiated efficiency along the vehicle carbody. As seen in the diagrams in figure 3.2, the frequency response function at the middle of the carbody exhibits more anti-resonant frequencies than the frequency response functions above the bogies, which means that the geometric filtering effect is more effective at the middle of the carbody. A final observation based on the diagrams in figure 3.2 is related to the fact that, in the absence of damping, the frequency response of the carbody above the two bogies is symmetrical.

The diagrams in figure 3.3 show the response functions of the acceleration at the relevant points of the carbody for the "rigid carbody "model and the "flexible carbody " model. These are to show that, for the damped case, the response of the carbody above to the two bogies is not symmetrical. The significant differences between the response functions of the acceleration of the two bogies are particularly noticeable of the eigenfrequencies of the carbody vibration modes, which are also highlighted here, namely 1.17 Hz for the bounce vibrations, 1.46 Hz for the pitch and 8 Hz for vertical bending. It is also possible to observe the anti-resonance frequencies corresponding to the geometric filtering effect given by the wheelbases of the vehicle.

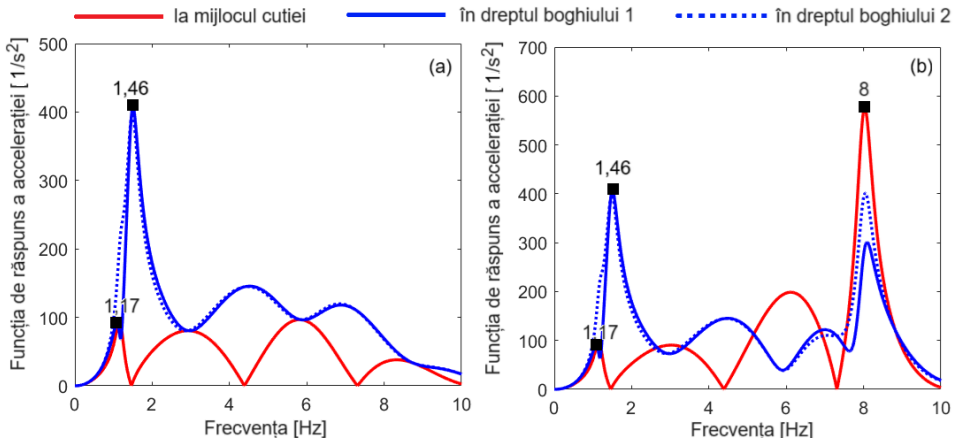

Fig. 3.3. Frequency response functions of the carbody acceleration for the damped case: (a) for the "rigid carbody" model; (b) for the "flexible carbody" model.

Figures 3.4 – 3.6 show the power spectral density of the acceleration at the relevant points for the vibration behaviour of the carbody – figure 3.4 at the point located in the middle of the carbody, figure 3.5 at the point located above to bogie 1, figure 3.6 for the point located above to the bogie 2, calculated for the two vehicle models - the "rigid carbody" model (diagrams a) and the "flexible carbody" model (diagrams b – for f_{iv} = 6 Hz; diagrams c – for f_{iv} = 8 Hz; diagrams d – for f_{iv} = 10 Hz).

In the case of the "rigid carbody" model, the vibration behaviour at the middle of the carbody is due to bounce vibrations only (figure 3.4 - diagram a). Above the bogies, both bounce and pitch vibrations of the carbody are manifested, but the power density spectrum is dominated by pitch vibrations (figures 3.5 and 3.6 – diagrams a).

In the case of the "flexible carbody" model it is observed that the bending vibrations especially influence the vibration behaviour at the middle of the carbody and less above the two bogies. Bending vibrations become important in the high-speed range as seen in diagrams (b) and (c) of the three figures.

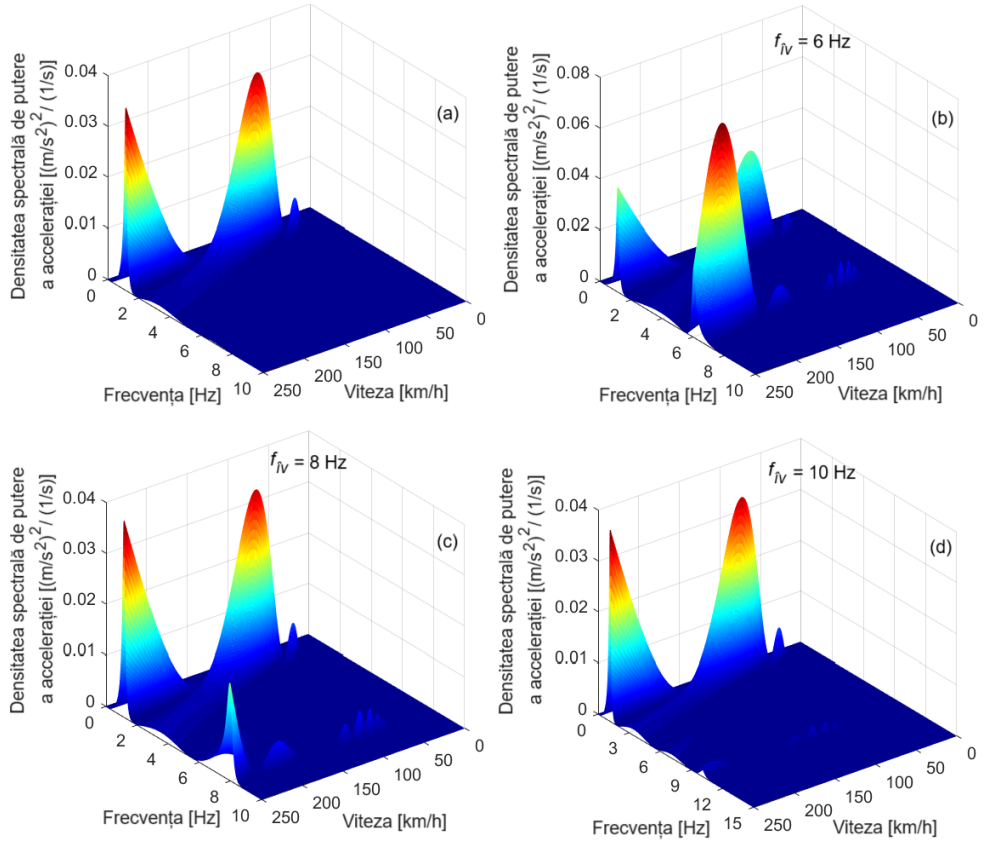

Fig. 3.4. Power spectral density of the acceleration at the middle of the carbody:
(a) for the "rigid carbody" model; (b), (c) and (d) for the “flexible carbody” model.

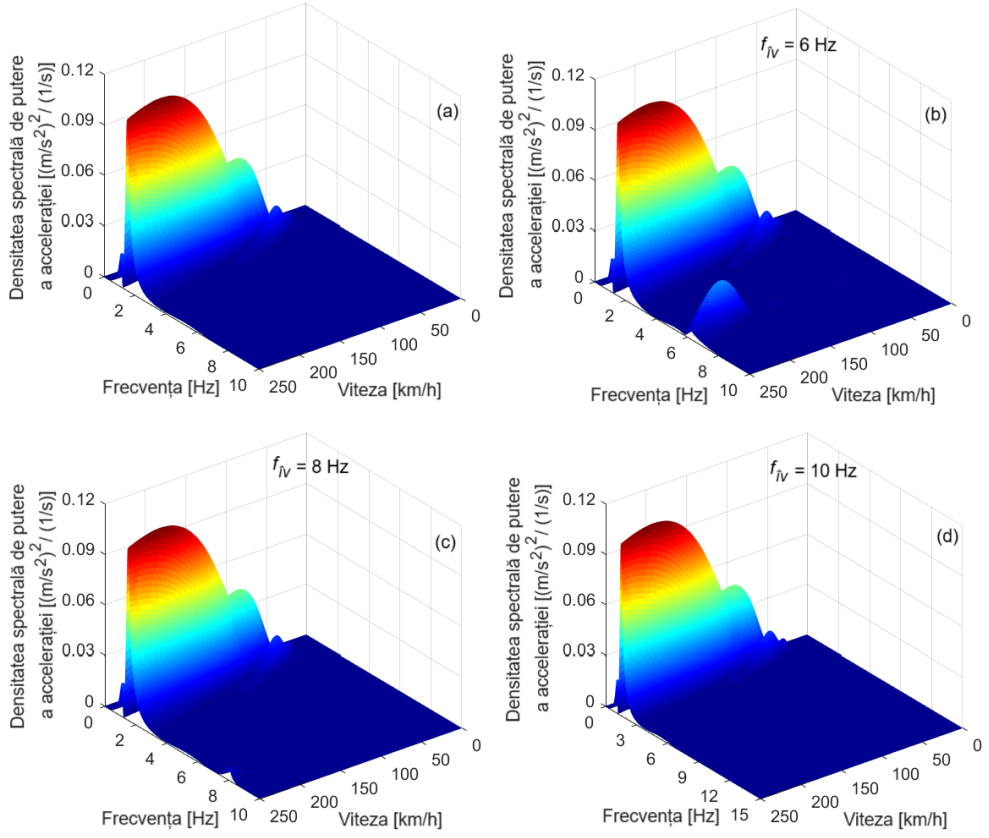

Fig. 3.5. Power spectral density of the acceleration above the bogie 1:
(a) for the "rigid carbody" model; (b), (c) and (d) for the “flexible carbody” model.

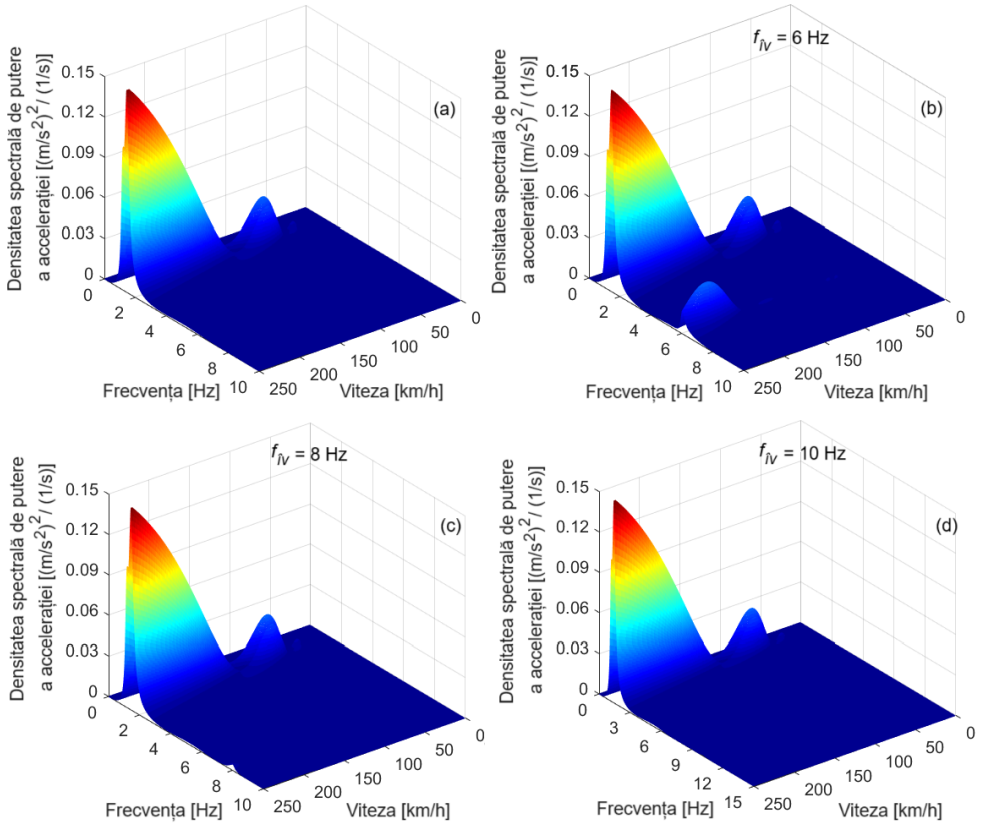

Fig. 3.6. Power spectral density of the acceleration above the bogie 2:
(a) for the "rigid carbody" model; (b), (c) and (d) for the “flexible carbody” model.

For example, according to diagrams (b), for f_{iv} = 6 Hz, at speeds higher than 200 km/h, bending becomes the dominant mode of vibration in the middle of the carbody (figure 3.4), and above the two bogies it has an important contribution (figures 3.5 and 3.6). The weight of bending vibrations decreases as the bending stiffness of the carbody increases. For f_{iv} = 8 Hz – diagrams (c), bending vibrations are important only in the middle of the carbody at high speeds (figure 3.4), and above the bogies their contribution is insignificant (figures 3.5 and 3.6). For f_{iv} = 10 Hz - diagrams (d), the weight of bending vibrations in all relevant points of the carbody is insignificant (figures 3.4 - 3.6).

Based on the diagrams in figures 3.4 – 3.6, the following observations can be made regarding the dominant modes of vibration: excluding the situation presented above (figure 3.4 – diagram b), at the middle of the carbody, the dominant mode of vibration is bounce; above to the bogies, the vibration of the carbody is dominated by pitch vibrations. It should also be noted that, throughout the speed range, the power spectral density shows a series of minima at certain speeds, respectively at geometric filtering speeds. It is observed that the geometric filtering effect is more effective at the middle of the carbody under certain conditions: at the vertical bending resonance frequency; at low speeds.

To analyze the influence of bending vibrations on the vertical vibration level of the carbody in correlation with the speed, the diagrams in figure 3.7 are analyzed. Comparing the values of the root mean square of the acceleration for the "flexible carbody" model with those corresponding to the "rigid carbody" model, it is observed that the vertical bending causes a significant increase in the vibration level only at the middle of the carbody.

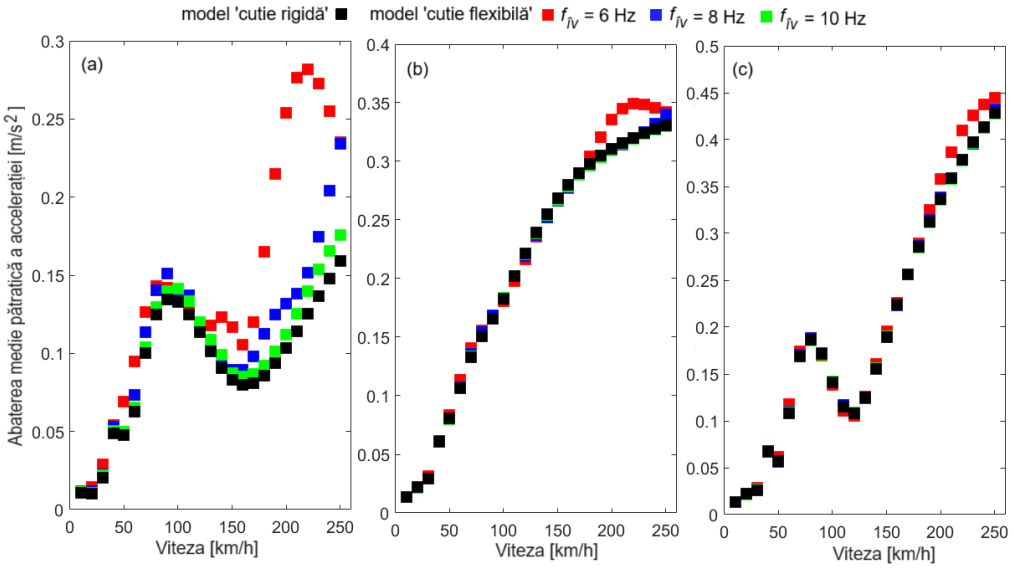

Fig. 3.7. Influence of bending vibrations on the root mean square of the carbody acceleration in relation to speed: (a) at the middle of the carbody; (b) above to bogie 1; (c) above to bogie 2.

Another interesting aspect to analyse is related to how vertical bending influences the maximum level of vibration along the carbody. This analysis can be done with the help of figure 3.8, which shows the root mean square of the acceleration at the relevant points of the carbody for the "rigid carbody" model and for the "flexible carbody" model. In all four cases presented, the maximum vibration level of the carbody is recorded in one of the points located above the two bogies. The position of the point where the vibration level of the carbody is maximum changes according to the speed but is not influenced by the bending vibrations.

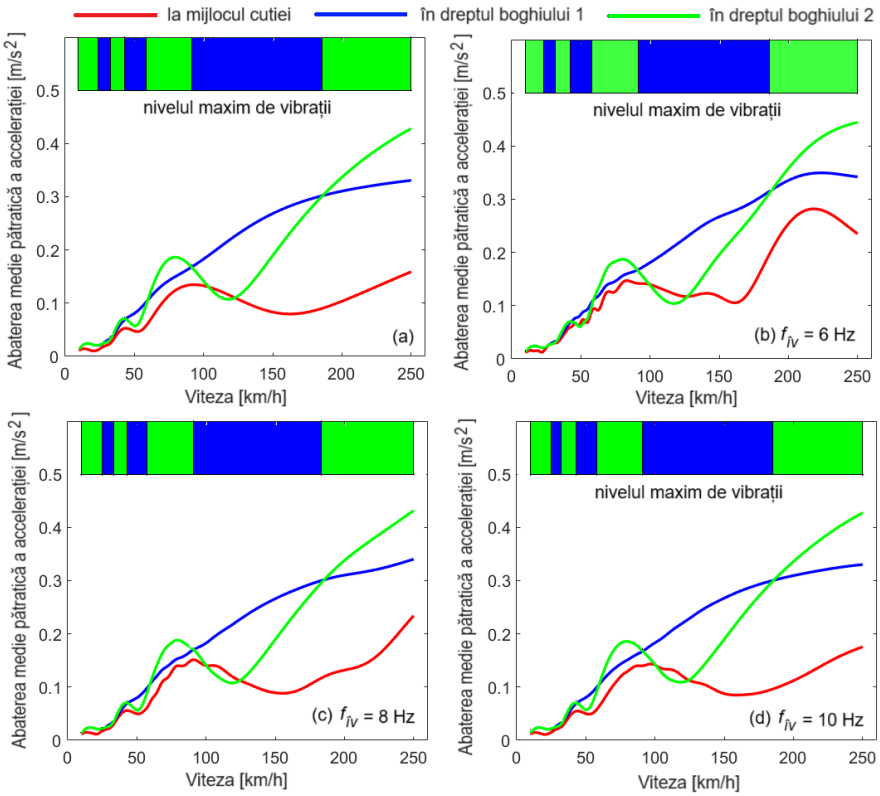

Fig. 3.8. The maximum vibration level of the carbody:
(a) for the "rigid carbody " model; (b), (c) and (d) for the “flexible carbody” model.

Figure 3.9 highlights the influence of the vertical carbody bending on the root mean square of the acceleration in correlation with the damping ratio of the secondary suspension. It is observed that in the case of both models of the vehicle - the "rigid carbody" model, respectively the "flexible carbody" model, when the damping ratio of the secondary suspension increases to a certain value, the root mean square of the acceleration decreases continuously until it reaches a minimum. This value depends on the position of the relevant point for the vibration behaviour of the carbody and the type of model - "rigid carbody" model or "flexible carbody" model.

The diagrams from figure 3.10 highlight the influence of the vertical bending of the carbody on the root mean square of the acceleration, in correlation with the damping ratio of the primary suspension. The presented results show that for both the "rigid carbody" and the "flexible carbody" model, the root mean square of the acceleration decreases continuously as the damping of the primary suspension increases.

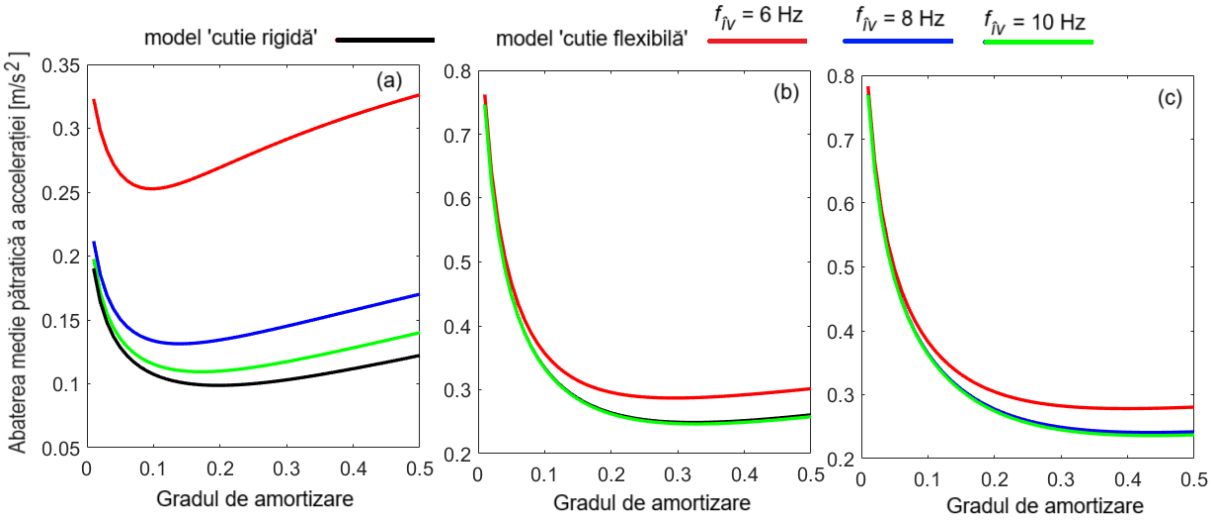

Fig. 3.9. The influence of bending vibrations on the root mean square of the carbody acceleration in correlation with the damping ratio of the secondary suspension:
(a) at the middle of the carbody; (b) above to bogie 1; (c) above to bogie 2.

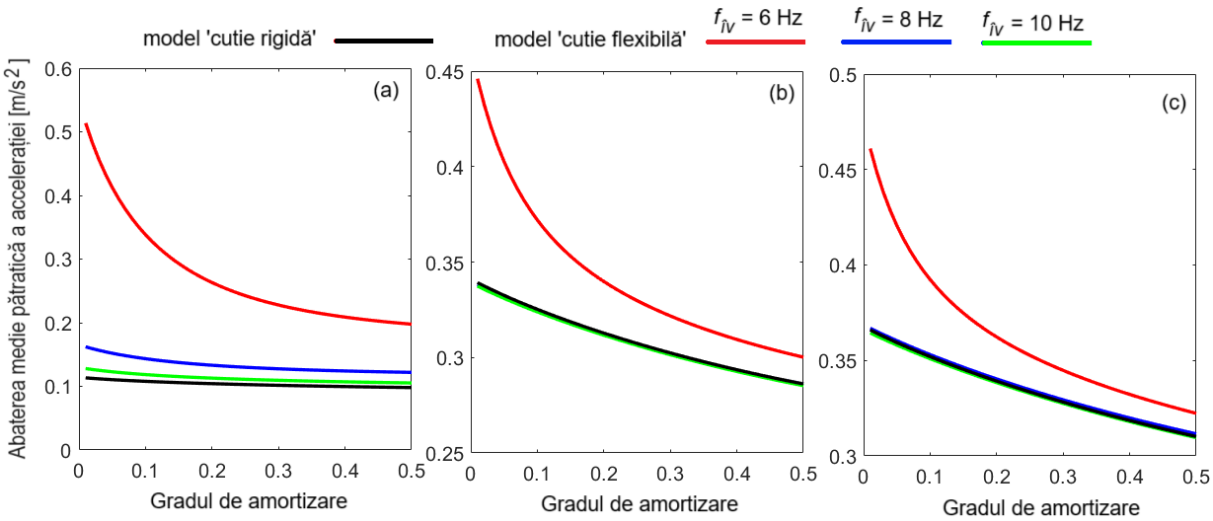

Fig. 3.10. The influence of bending vibrations on the root mean square of the carbody acceleration in correlation with the damping ratio of the primary suspension:
(a) at the middle of the carbody; (b) above to bogie 1; (c) above to bogie 2.

The influence of the vertical bending of the carbody is observed in the rate of decrease of the root mean square of the acceleration. In the case of the "rigid carbody" model, the rate of decrease of the root mean square of the acceleration is higher above the two bogies than of the carbody middle. In contrast, in the case of the "flexible carbody" model, the rate of decrease of the root mean square of the acceleration is higher at the middle of the carbody for any of the three situations considered. Comparing the results obtained for the "flexible carbody" model with those corresponding to the "rigid carbody" model, it is observed that, at the middle of the carbody, the rate of decrease of the root mean square of the acceleration is always significantly higher in the case of the "flexible carbody" model. In contrast, above the two bogies, the rates of decrease of the root mean square of the acceleration in the case of the "flexible carbody" model are practically equal to those corresponding to the "rigid carbody" model.

4. Study on the influence of the suspension model in the simulation of the vertical vibration behaviour of the railway vehicle carbody

4.1. Introduction

In this chapter, the influence of the secondary suspension model on the vertical vibration behaviour of the carbody is investigated based on the results of numerical simulations [11]. Numerical simulation applications are developed based on a rigid-flexible coupled railway vehicle model with seven degrees of freedom, corresponding to the vertical vibration modes of the carbody and the vertical vibration modes of bogies.

Four different secondary suspension models are integrated into the vehicle model. The first model is a simple model, considered as the reference model, consisting of a single Kelvin-Voigt system for vertical translation through which the stiffness and vertical damping of the secondary suspension are represented. The other three models are analysis models, which are obtained by composing in different variants the reference model with systems through which the pith vibrations of the bogies are transmitted to the carbody, influencing its vibration behaviour. The first analysis model consists of the reference model and a Kelvin-Voigt system for rotation that takes the relative angular displacement between the carbody and the bogie. The second analysis model consists of the reference model and a Kelvin-Voigt system for longitudinal translation that models the transmission system of longitudinal forces between the carbody and the bogie. The third analysis model brings together all three Kelvin-Voigt systems described above - the Kelvin-Voigt system for vertical translation, the Kelvin-Voigt system for rotation, and the Kelvin-Voigt system for longitudinal translation.

The evaluation of the influence of the secondary suspension model on the vertical vibration behaviour of the railway vehicle carbody is carried out based on the frequency response functions of the acceleration, the power spectral density of the acceleration an the root mean square of the acceleration.

4.2. Mechanical model of railway vehicle

Figure 4.1 shows the mechanical model for the study of the vertical vibrations of a four-axle passenger railway vehicle with two suspension stages, which runs at a constant speed V on a track with vertical irregularities. Except for the secondary suspension model, this model is similar to the "flexible carbody" model presented in Chapter 3. The vehicle model is a rigid-flexible coupled model in which the vehicle carbody is modelled by a free-free equivalent beam of constant section and uniformly distributed mass, Euler-Bernoulli type, and the chassis of the two bogies and the four wheelsets are represented by rigid bodies.

To give a uniform character to the paper, the same notations as those used in Chapter 3 have been maintained. Thus, on figure 4.1, the vertical displacements of the carbody and the bogies corresponding to the bounce vibrations are marked as follows: z_c – the vertical displacement of the carbody; z_{b1} and z_{b2} – the vertical displacements of the two bogies. The rotation angles corresponding to pitch vibrations are denoted by θ_c for the carbody, respectively by θ_{b1} and θ_{b2} for the bogies. The vertical displacement u_c of a section of the carbody at a distance x_c from the origin of the reference system at time t, resulting from the superposition of the three modes of vibration of the carbody – bounce, pitch and the first vertical bending mode. Other notations common to the models shown in figures 3.1 and 4.1 are carbody length l_c, carbody wheelbase $2a_c$ and bogie wheelbase $2a_b$. With $l_{c1,2}$ the distances from the reference system attached to the carbody to its support points on the secondary suspension were noted. These distances fix the position of the relevant points for the vibration behaviour of the carbody, denoted on figure 4.1 by b_1 and b_2. The third point relevant to the evaluation of the vibration behaviour of the carbody is the point marked in the middle of the carbody and denoted by m.

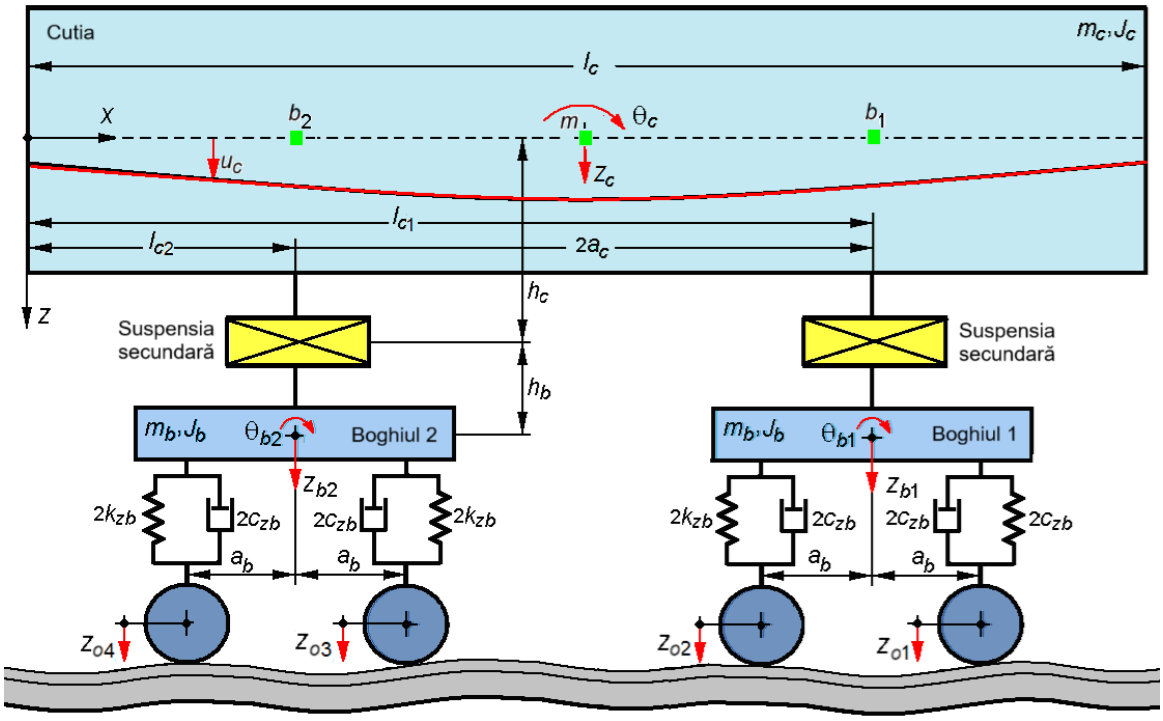

Fig. 4.1. Mechanical model of the railway vehicle [11].

The mass of the carbody and the mass of a bogie are denoted by m_c and m_b, respectively, and the inertia moments of the two bodies are J_c - inertia moment of the carbody and J_b - inertia moment of the bogie. Continuing to accept the assumption of a perfectly rigid track, the vertical irregularities of the track are transmitted directly to the wheelsets, imprinting them with movements in the vertical plane denoted by $z_{o1...4}$.

As with the mechanical model of the vehicle in Chapter 3, the primary suspension corresponding to one wheelset is modelled by a Kelvin-Voigt system for vertical translation, having spring constant $2k_{zb}$ and damping constant $2c_{zb}$.

The differences between the mechanical model of the vehicle presented in the previous chapter and the one in this chapter are found in the model of the secondary suspension. Here, the secondary suspension is represented by four different models, a reference model and three analysis models (figure 4.2).

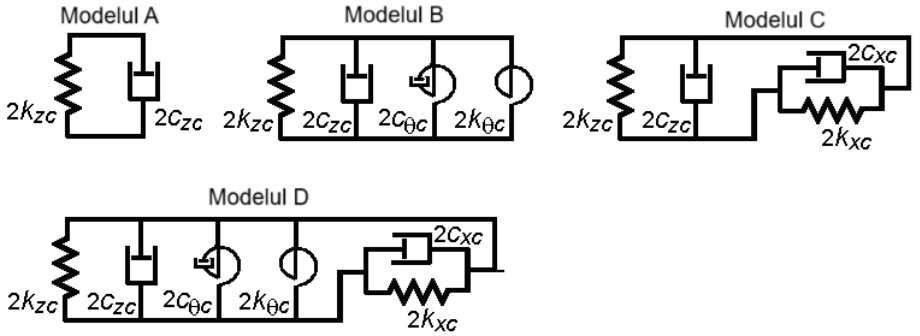

Fig. 4.2. The model of the secondary suspension [11].

The first model (model A) is a simple, reference model, consisting of a Kelvin-Voigt system, for vertical translation, having stiffness $2k_{zc}$ and damping constant $2c_{zc}$. The second model (model B) consists of model A and a Kelvin-Voigt system for rotation, with angular stiffness $2k_{\theta c}$ and damping constant $2c_{\theta c}$, which takes the relative angular displacement between the carbody and bogie. Model C results from the composition of model A with a Kelvin-Voigt system for longitudinal translation, which models the longitudinal force transmission system between the carbody and the bogie. This system is positioned at a distance h_c from the medium fibber of the carbody and at a distance h_b from the centre of gravity of the bogie and has the elastic constant $2k_{xc}$ and the damping constant $2c_{xc}$. The fourth model (model D) is a complete model consisting of three Kelvin-Voigt systems, for vertical translation, for rotation, and for longitudinal translation.

4.3. Analysis of the vertical vibration behaviour of the vehicle carbody

In this section, the results of the numerical simulations regarding the influence of the secondary suspension model on the vertical vibration behaviour of the railway vehicle carbody are presented. The evaluation of the vertical vibration behaviour of the carbody is performed based on the frequency response functions of the acceleration, the power spectral density of the acceleration and the root mean square of the acceleration, for the four models of the secondary suspension – model A, model B, model C and model D. Model A is considered the reference model, and models B, C, and D are the analysis models.

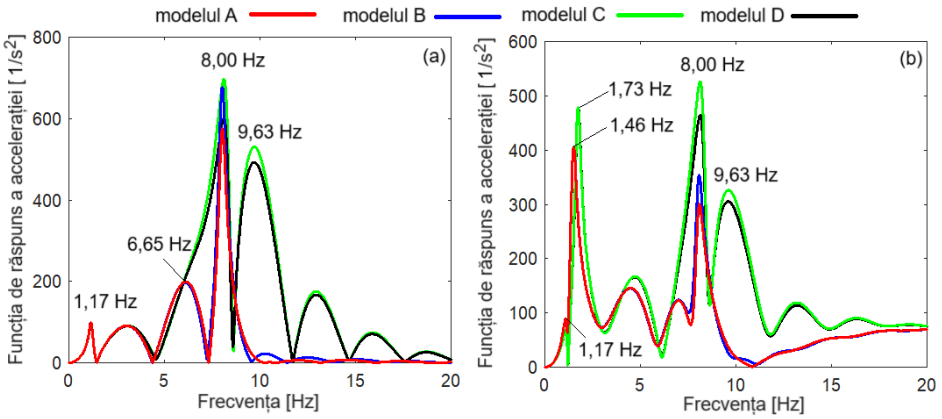

Fig. 4.3. Frequency response functions of the carbody acceleration:
(a) at the middle of the carbody; (b) above the bogie 1.

Figure 4.3 shows the frequency response functions of the acceleration in two of the relevant points for the vibration behaviour of the carbody, namely at its middle (diagram a) and above the bogie 1 (diagram b), for the four models of the secondary suspension. The presented results were obtained for the reference values of the parameters of the numerical model of the vehicle. Both diagrams show peaks corresponding to the eigenfrequencies of the vehicle's vibration modes, as well as a series of minima in the response functions corresponding to the geometric filtering effect. The values of the eigenfrequencies of the vibration modes of the carbody and bogies are centralized in Table 4.1.

Table 4.1. The eigenfrequencies of the vibration modes of the carbody and bogies.

Vibration mode	Secondary suspension model	Frequency [Hz]
Carbody bounce	Model A, Model B, Model C, Model D	1.17
Carbody pitch	Model A, Model B	1.46
	Model C, Model D	1.73
Carbody bending	Model A, Model B, Model C, Model D	8.00
Bogie bounce	Model A, Model B, Model C, Model D	6.65
Bogie pitch	Model A, Model B, Model C, Model D	9.63

It can be seen that the eigenfrequencies of carbody pitch and vertical bending and the eigenfrequencies of the bogie bounce and pitch do not change for any of the three analysis models relative to reference model A. The eigenfrequency of the carbody pitch is maintained at 1.46 Hz in the case of model B. By introducing the longitudinal system in the secondary suspension model, respectively in models C and D, the eigenfrequency of the pitch vibrations of the carbody increases to 1.72 Hz.

From the point of view of the vibration level of the carbody, the influence of the suspension model is manifested at the frequency of 8 Hz – the eigenfrequency of the vertical bending vibration of the carbody, for all three analysis models. The pitch vibrations of the carbody are affected only in the C and D models of the secondary suspension. This can be explained by a poor coupling between the pitch vibrations of the bogies and the pitch vibrations of the carbody in the case of the B model of the secondary

suspension. It is also noted that the vibration level of the carbody increases significantly at the frequency of 9.63 Hz - the eigenfrequency of pitch vibrations of the bogie, only in the case of C and D models of the suspension. The conclusion is that it is the longitudinal system of the secondary suspension that makes an important contribution to the transmission of pitch vibrations of the bogies to the carbody, while the rotational system contributes to a lesser extent. In model D, the contribution of the two systems does not add up, because the two systems work in antiphase. All these observations are also highlighted in the case of the power spectral density of the acceleration in the two relevant points of the carbody, at the speed of 200 km/h, presented in the diagrams in figure 4.4.

According to diagram (a) of figure 4.4, at the middle of the carbody, the secondary suspension model influences the vibration level at the eigenfrequencies of the vertical bending of the carbody and the bogie pitch. At the vertical bending frequency of 8 Hz, all three analysis models – model B, model C and model D – lead to an increase of the vibration level of the carbody compared to the reference model A. At the bogie pitch frequency of 9.63 Hz, only analysis models C and D significantly influence the vibration level of the carbody, which increases relative to the vibration level corresponding to the reference model A. As also shown above, near the bogie (diagram b), the C and D models of the secondary suspension influence the eigenfrequency of the carbody pitch, which increases from 1.46 Hz to 1.73 Hz from cause of the longitudinal system. Based on these last observations, it is interesting to analyse how the stiffness of the system for rotation, respectively the stiffness of the longitudinal system, influences the vibration behaviour of the carbody at the eigenfrequencies of vertical bending, bogie pitch and carbody pitch.

The diagrams from figure 4.5 show the influence of the stiffness of the system for rotation included in model B of the secondary suspension, respectively in model D, on the vibration of the carbody, at the middle of it and above to the bogie, at the eigenfrequency of the vertical bending of the carbody (8 Hz) and at the eigenfrequency of the bogie pitch (9.63 Hz), for the speed of 200 km/h. The increased stiffness of the system for rotation of the model B of the secondary suspension leads to an increase of the vibration level of the carbody at the frequency of 8 Hz. In model D, where the longitudinal system is also included (k_{xc} = 10 MN/m), increasing the stiffness of the rotational system results in a reduction of the carbody vibration level at both 8 Hz and 9.63 Hz, as a result of the compensation effect due to the opposite action of the two systems working in antiphase.

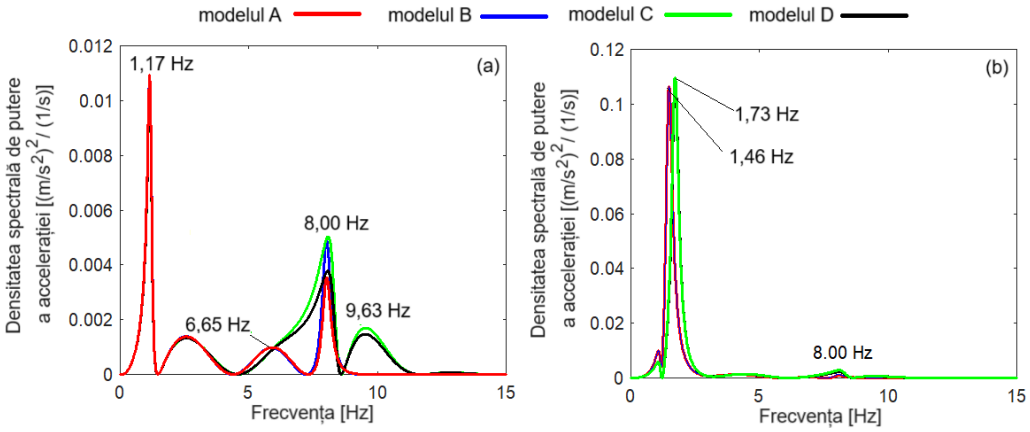

Fig. 4.4. Power spectral density of acceleration at 200 km/h:
(a) at the middle of the carbody; (b) above to bogie 1.

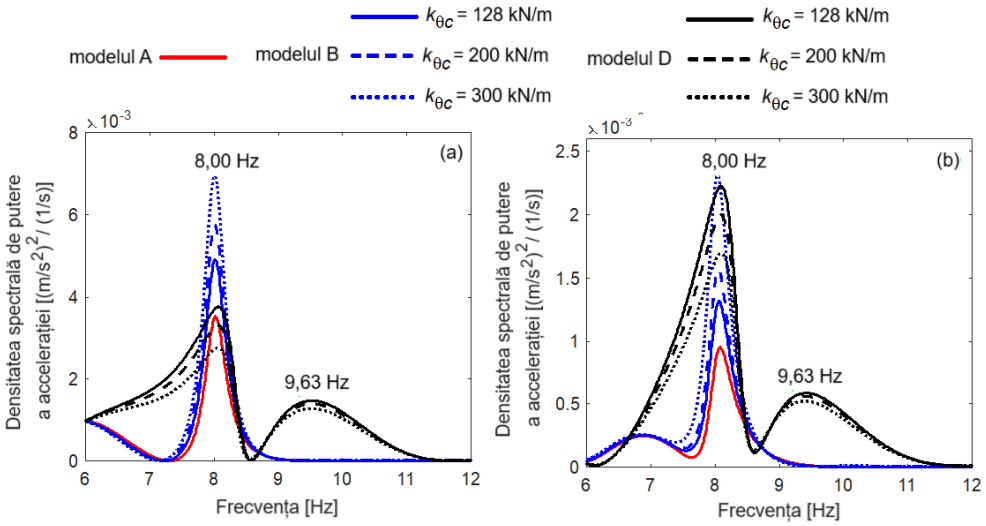

Fig. 4.5. The influence of the angular stiffness of the secondary suspension on the power spectral density of the acceleration: (a) at the middle of the carbody; (b) above to bogie 1.

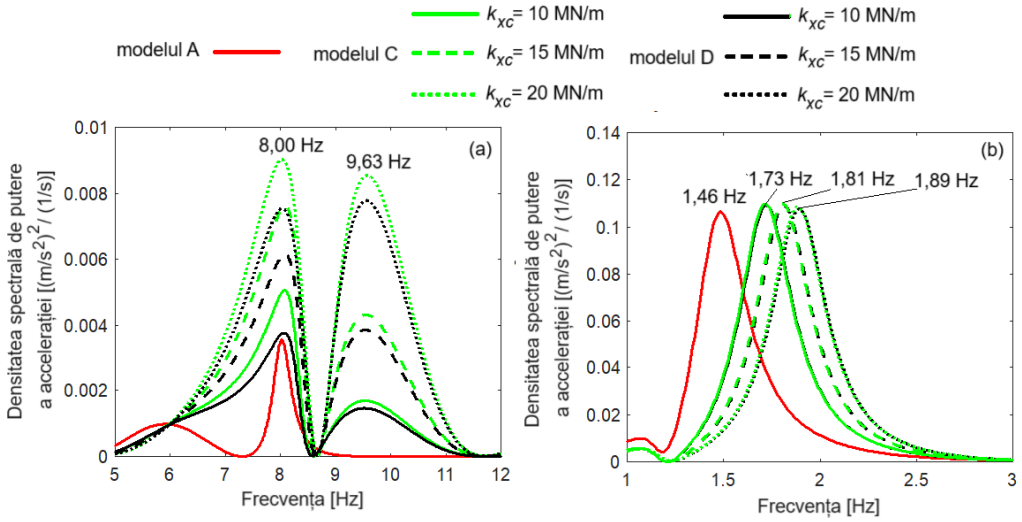

Fig. 4.6. The influence of the longitudinal stiffness of the secondary suspension on the power spectral density of the acceleration: (a) at the middle of the carbody; (b) above to bogie 1.

Based on diagram (a) from figure 4.6, the influence of the stiffness of the longitudinal system, included in the model C of the secondary suspension, on the level of vibrations at the middle of the carbody at the eigenfrequency of the vertical bending of the carbody and at the eigenfrequency of the pitch vibrations of the bogie is analyzed. When increasing the stiffness of the longitudinal system, significant increases of the vibration level are obtained at both eigenfrequencies. Diagram (b) of figure 4.6, in which the power spectral density of the acceleration of the carbody above the bogie is presented, highlights the increase of the eigenfrequency of the pitch vibrations of the carbody as the stiffness of the longitudinal system in the model C of the secondary suspension increases from 1.72 Hz (for k_{xc} = 10 MN/m) at 1.81 Hz (for k_{xc} = 15 MN/m), respectively at 1.89 Hz (for k_{xc} = 20 MN/m), without significant changes in the vibration level of the carbody.

Figure 4.7 shows the root mean square of the acceleration at the carbody middle and above the bogie, calculated on the speed range 10 ... 250 km/h. Here too, the effect of geometric filtering on the root mean square deviation of the carbody's acceleration is observed, which does not increase continuously with speed.

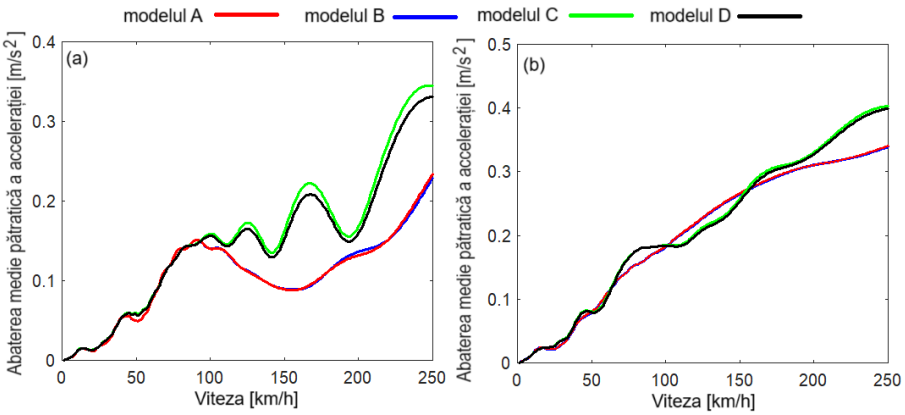

Fig. 4.7. The root mean square of the acceleration:
(a) at the middle of the carbody; (b) above to bogie 1.

Regarding the influence of the secondary suspension model on the vibration behaviour of the carbody, it is highlighted that the rotation system for pitch included in the B model of the suspension does not significantly affect the vertical vibration level of the carbody. The influence of the longitudinal system of the model C of the suspension on the vibration level of the carbody is more pronounced at the middle of the carbody at speeds above 100 km/h. Above the bogie, the influence of the model C of the suspension on the vibration level is noticeable at speeds above 200 km/h. For example, at the carbody middle, at a speed of 165 km/h, the acceleration for the model C is approx. 140% higher than the acceleration obtained for the reference model A, and at the speed of 250 km/h 47% higher. Above the bogie, at the speed of 165 km/h, the root mean square of acceleration for model C is 4.9% higher than for model A, and at the speed of 250 km/h by 18.5%. The values of the root mean square of the acceleration in the case of model D are not significantly different from those corresponding to model C.

According to figure 4.8, the increase the rotation system stiffness does not significantly affect the root mean square of the acceleration corresponding to model B, and in the case of model D, the reduction of the vibration level is modest. For example, at the carbody middle, when increasing stiffness $k_{\theta c}$ from 128 kN/m to 300 kN/m, the root mean square of the acceleration for model D decreases from 0.20 m/s^2 to 0.19 m/s^2 at the speed of 165 km/h, respectively from 0.33 m/s^2 to 0.32 m/s^2 for the speed of 250 km/h.

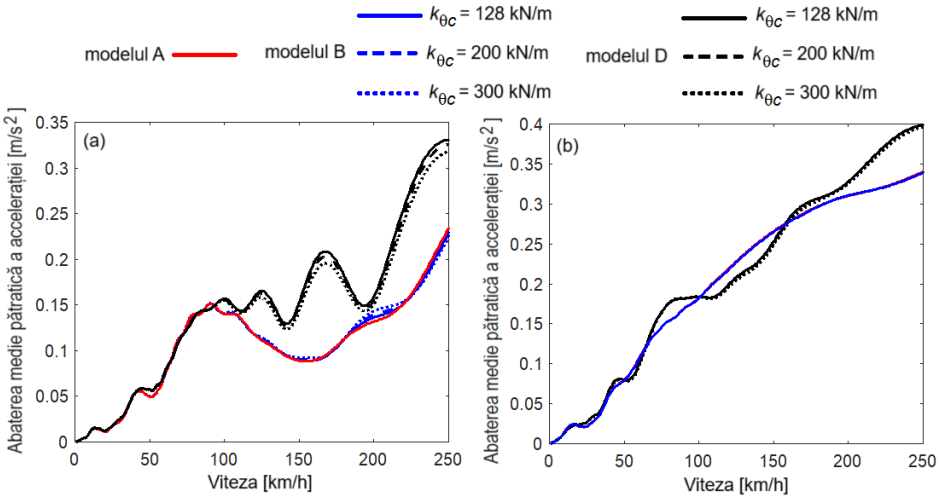

Fig. 4.8. The influence of the angular stiffness of the secondary suspension on the root mean square of the acceleration: (a) at the middle of the carbody; (b) above to bogie 1

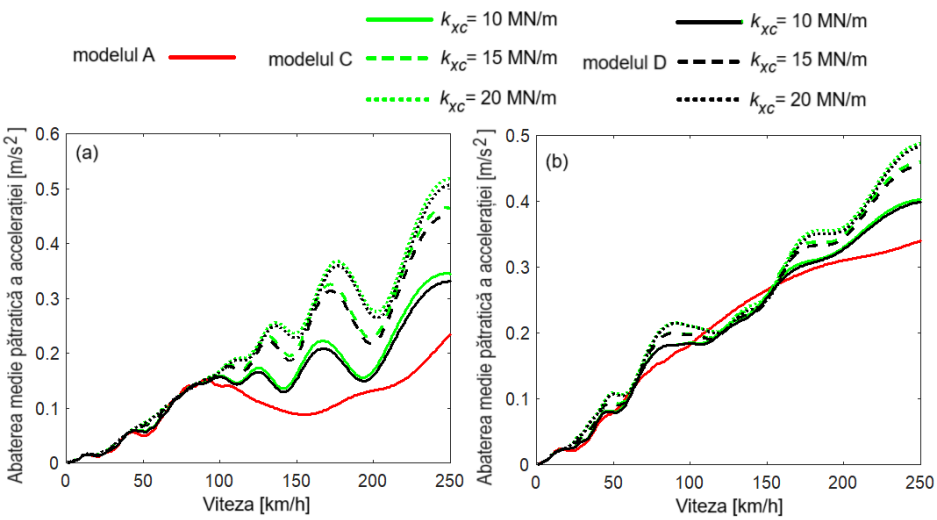

Fig. 4.9. The influence of the longitudinal stiffness of the secondary suspension on the root mean square of the acceleration: (a) at the middle of the carbody; (b) above to bogie 1

The influence of the stiffness of the longitudinal system, included in models C and D of the secondary suspension, on the mean square of the acceleration is highlighted in figure 4.9. As previously shown, the influence of the longitudinal system on the vibration level of the carbody is especially manifested at high speeds, and increasing the stiffness of this system further increases this effect. At the middle of the carbody, when increasing the stiffness k_{xc} from 10 MN/m to 20 MN/m, at the speed of 165 km/h, the acceleration increases from 0.22 m/s^2 to 0.32 m/s^2, and at the speed of 250 km/h, the acceleration increases from 0.34 m/s^2 to 0.52 m/s^2. Above the bogie, at a speed of 165 km/h, the acceleration of the carbody increases from 0.29 m/s^2 to 0.32 m/s^2, and at a speed of 250 km/h from 0.40 m/s^2 to 0.79 m/s^2.

5. Study on the influence of the track model in the simulation the vertical vibration behaviour of the railway vehicle carbody

5.1. Introduction

In this chapter, the influence of the track model on the vertical vibration behaviour of the railway vehicle carbody is analysed based on the results obtained through numerical simulations. For this, the frequency response functions, the power spectral density and the root mean square of the carbody acceleration are compared for two models of the vehicle-track system, namely the "rigid track" model and the "elastic track" model. The model referred to here as "rigid track" is the vehicle-track system model presented in Chapter 4 (figure 4.1) in which the secondary suspension is represented by model C. The "elastic track" model is developed within this chapter and includes the rigid-flexible coupled model type of vehicle, introduced in previous chapters, and the track which is represented by an equivalent model with concentrated parameters.

The "elastic track" model is a 15-degree-of-freedom model corresponding to the vertical vibration modes of the carbody – bounce, pitch and the first vertical bending mode, the vertical vibration modes of the bogies – bounce and pitch, and the vertical displacements of the wheels and rails. This model is described in detail in the next section, which also includes the equations of motion of the bodies that make up the vehicle-track system. The chapter is further structured, like chapters 3 and 4, on sections dedicated to the presentation of the calculation relations of the frequency response functions, the power spectral density of the acceleration and the root mean square of the acceleration at the relevant points of the vibration behaviour of the carbody. In the last section, the results of the numerical simulations for the two models of the vehicle-track system are analysed, and the general conclusion is that the influence of the track model manifests itself in the range of frequencies higher than 20 Hz, i.e. outside the frequency range of interest for the vertical vibrations of the vehicle carbody.

5.2. Mechanical model of the vehicle-track system

Figure 5.1 presents the mechanical model of the vehicle-track system for studying the influence of the track model on the vertical vibration behaviour of a railway vehicle carbody. As in the previous chapters, the case of a four-axle passenger vehicle with two suspension stages, moving at constant speed V on a track with vertical irregularities, is considered.

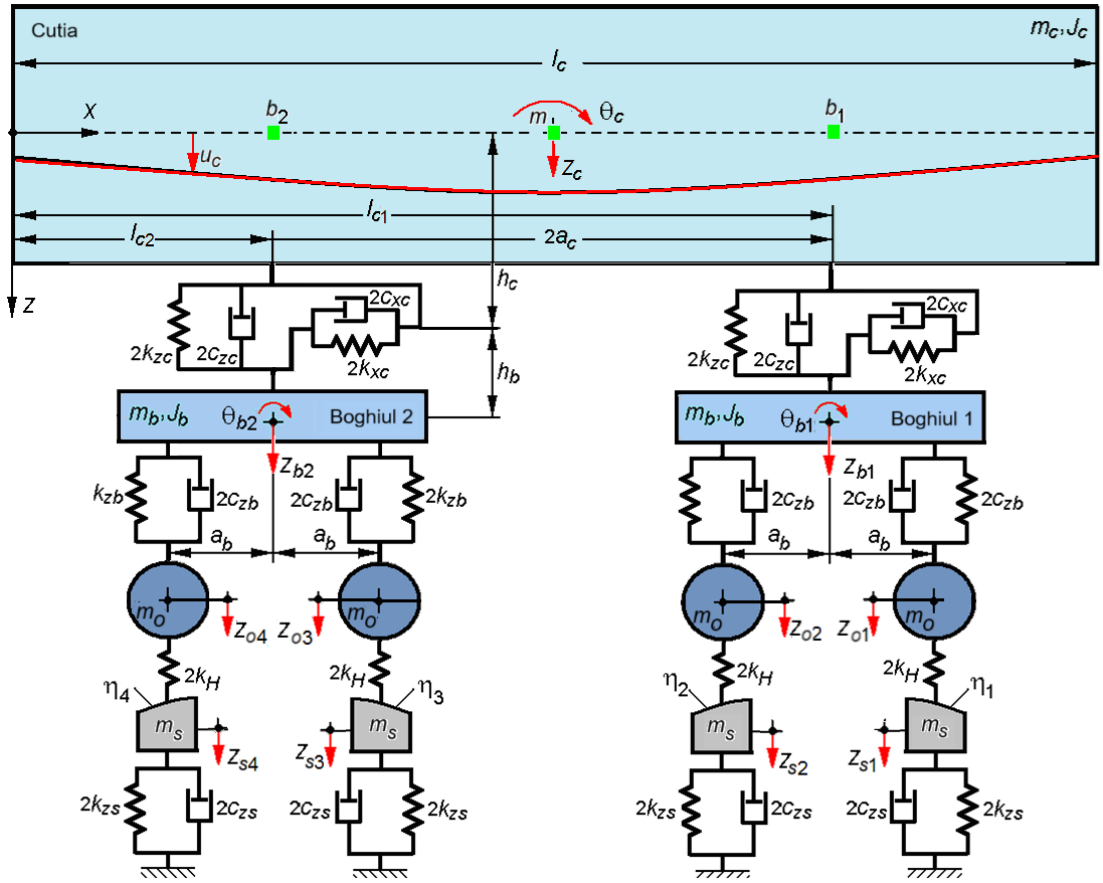

Fig. 5.1. Mechanical model of the railway vehicle – track system.

It is observed that the vehicle model is similar to the model in Chapter 4, in which the secondary suspension is represented by model C. The differences between the two models arise from the fact that here the elastic contact between the wheel and the rail is considered, which is modelled by elastic elements with linear stiffness characteristic $2k_H$. Thus, the wheelsets, of mass m_o, perform vertical displacements, denoted by $z_{o1...4}$.

Neglecting, in the frequency range specific to the vertical vibrations of the vehicle, the coupling effects between the wheels caused by the propagation of bending waves through the rails, an equivalent model with equivalent model with concentrated parameters is adopted for the track. At each wheelset, the track is represented by a system with one degree of freedom in the vertical direction, the corresponding displacement being denoted by $z_{s1...4}$. The equivalent track model has mass m_s, stiffness $2k_{zs}$ and damping constant $2c_{zs}$. The vertical irregularities of the track at each wheel are denoted by $\eta_{1...4}$. The other notations marked in figure 5.8 are the same as those introduced in Chapters 3 and 4.

5.3. Analysis of the vertical vibration behaviour of the vehicle carbody

In this section, the influence of the track model on the vertical vibration behaviour of the railway vehicle carbody is analysed. For this, results obtained through numerical simulations for the vehicle-track system model presented in the figure 5.1 are used, which are compared with the results of numerical simulations obtained for the vehicle-track system model presented in the figure 4.1 in which the secondary suspension is represented by the model C. To simplify the presentation, the two models will be referred to as the "rigid track" model and the "elastic track" model. To evaluate the vertical vibration behaviour of the carbody, the frequency response functions of the acceleration, the power spectral density of the acceleration and the root mean square of the acceleration are analysed in parallel for the two models at the three points relevant for the vibration behaviour of the carbody – point m located in the middle of the carbody and points b_1 and b_2 positioned above the two bogies. The eigenfrequencies of the vertical vibration modes of the carbody and the bogies corresponding to the reference values of the parameters of the numerical model of the vehicle are summarized in Table 5.1.

Table5.1. Eigenfrequencies of the vibration modes of the carbody and bogies.

Vibration mode	Frequency [Hz]
Bounce carbody	1.17
Pitch carbody	1.73
Vertical bending of the carbody	8.00
Bounce bogie	6.65
Pitch bogie	9.63

The eigenfrequencies of the vehicle are also highlighted in figures 5.2 and 5.3, which represent the response functions of the carbody acceleration at its middle and above to the two bogies, for the two models of the vehicle - track system, respectively the "rigid track" model and the "elastic track" model.

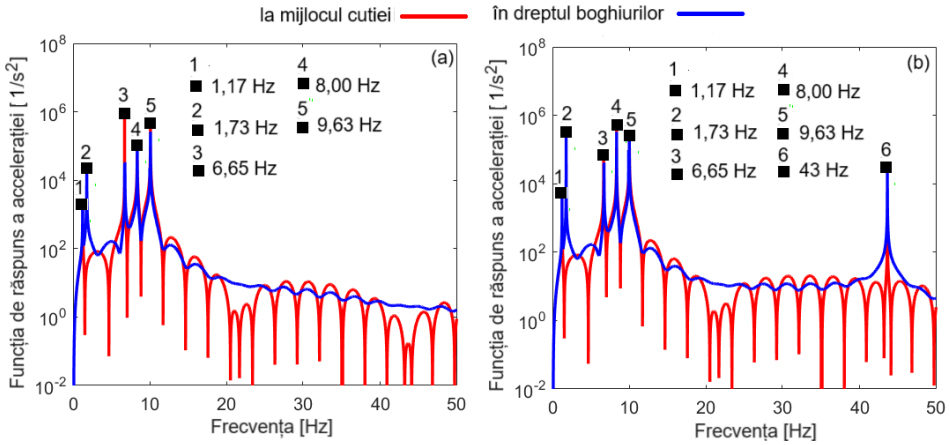

Fig. 5.2. Frequency response functions of the carbody acceleration for the undamped case: (a) for the "rigid track" model; (b) for the "elastic track" model.

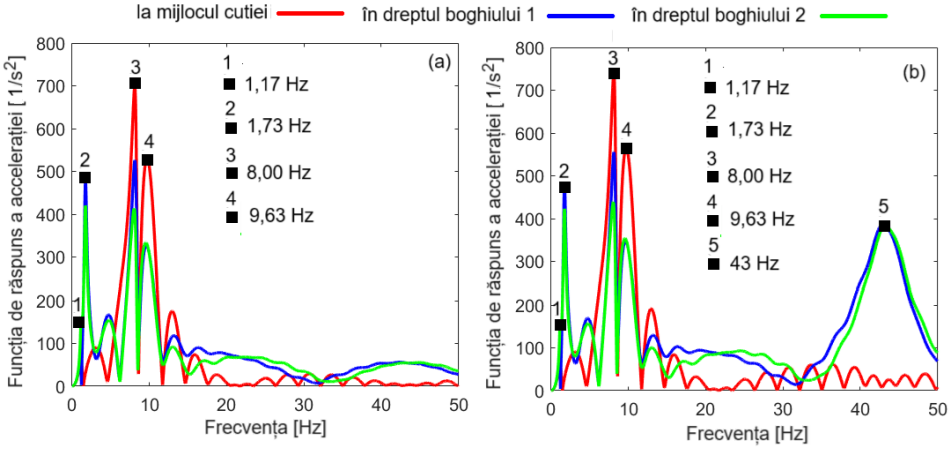

Fig. 5.3. Frequency response functions of the carbody acceleration for the damped case: (a) for the "rigid track" model; (b) for the "elastic track" model.

In figure 5.2, the carbody acceleration response functions are obtained for the undamped case, respectively for $c_{zc} = 0$, $c_{xc} = 0$, $c_{zb} = 0$, $c_m = 0$ and $c_{zs} = 0$ (only for diagram b), and in figure 5.3 for the reference values of the system damping constants. On diagrams (b) of the two figures, the peak of the response functions of the carbody acceleration calculated at the points located above front of the two bogies (points b_1 and b_2), corresponding to the eigenfrequency of the vertical vibrations of the wheelset, at 43 Hz, is marked.

Based on the diagrams in these two figures, a series of conclusions can be synthesized regarding the characteristics of the vibration behaviour at the reference points of the carbody, conclusions that were also highlighted in the analysis carried out in Chapter 3. These refer to: the asymmetry of the frequency response of the carbody above two bogies due to the damping of the system; the greater efficiency of the geometric filtering effect at the middle of the carbody than near the bogies; the greater efficiency of the geometric filtering effect at frequencies higher than 20 Hz.

Figure 5.4 shows the response functions of the acceleration for the "elastic track" model, considering the reference values of the parameters of the numerical model of the vehicle - track system, respectively $\xi_{zs} = 0.18$, and two analysis values of the track damping ratio $\xi_{zs} = 0{,}10$ and $\xi_{zs} = 0{,}30$.

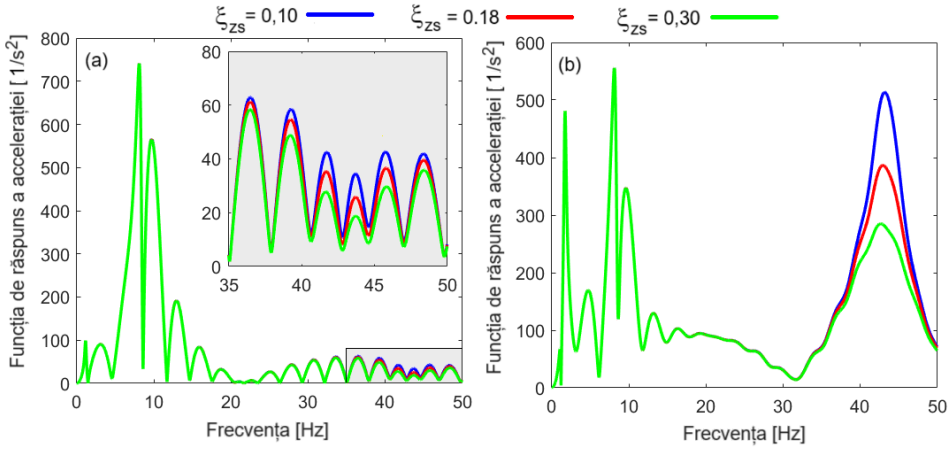

Fig. 5.4. Influence of the track damping ratio on the frequency response function of the carbody acceleration at a speed of 200 km/h: (a) at the middle of the carbody; (b) above the bogie 1.

It is observed, on the one hand, the reduced influence of the track model on the vibration regime of the at its middle and, on the other hand, the significant weight it has on the vibration behaviour of the carbody above the bogie. However, it is observed that the influence of the track model on the carbody response manifests itself around the frequency of 43 Hz (the eigenfrequency of the vertical vibrations of the wheelsets on the track), which is outside the frequency range specific to the vertical vibrations of the vehicle carbody, the upper limit of which is not higher than 10 Hz. In the present case, the frequency range of the vertical vibrations of the vehicle is between 1.17 Hz – the eigenfrequency of the carbody's bounce vibrations, and 9.63 Hz – the eigenfrequency of the bogie's pitch vibrations. Regarding the influence of the track damping on the carbody's response, this is very well highlighted in diagram (b), in the 43 Hz frequency area, where significant increases in the response function of the carbody acceleration are observed when the track damping ratio decreases, in the 43 Hz frequency area.

Figure 5.5 shows the power spectral density of the acceleration calculated at the relevant points for the carbody, for the two models of the vehicle-track system, namely the "rigid track" model and the "elastic track" model. The first observation refers to the fact that the track model does not influence the dominant vibration modes at the relevant points of the carbody. As shown in Chapter 3, at the middle of the carbody, the dominant vibration mode is bounce, but vertical bending also has an important share. Above the bogies, the carbody vibration is dominated by pitch vibrations. The second observation refers to the influence of the track model on the carbody vibration level, which is visible in the high frequency range, above 20 Hz, especially above the bogies.

The diagrams from figure 5.13 show the power spectral density of the acceleration at the eigenfrequencies of the carbody vibration modes for the two vehicle-track system models. They highlight the fact that at the eigenfrequencies of the carbody bounce and pitch vibrations, the track model does not influence the results regarding the carbody vibration level at any of its relevant points. At the eigenfrequency of the carbody bending vibrations (diagram c) there are differences between the results obtained based on the two vehicle-track system models, which are more important at high speeds.

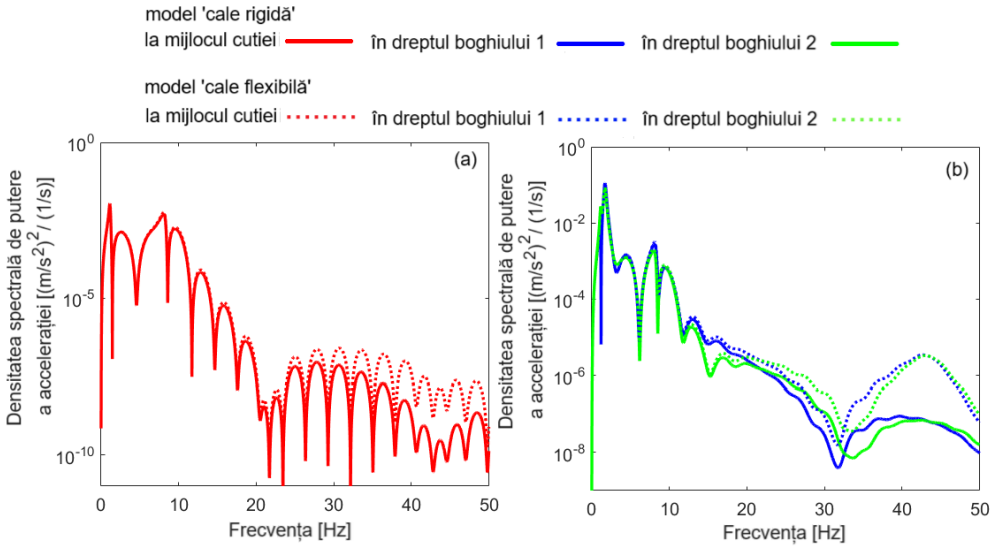

Fig. 5.5. Power spectral density of the acceleration at 200 km/h:
(a) at the middle of the carbody; (b) above the bogies.

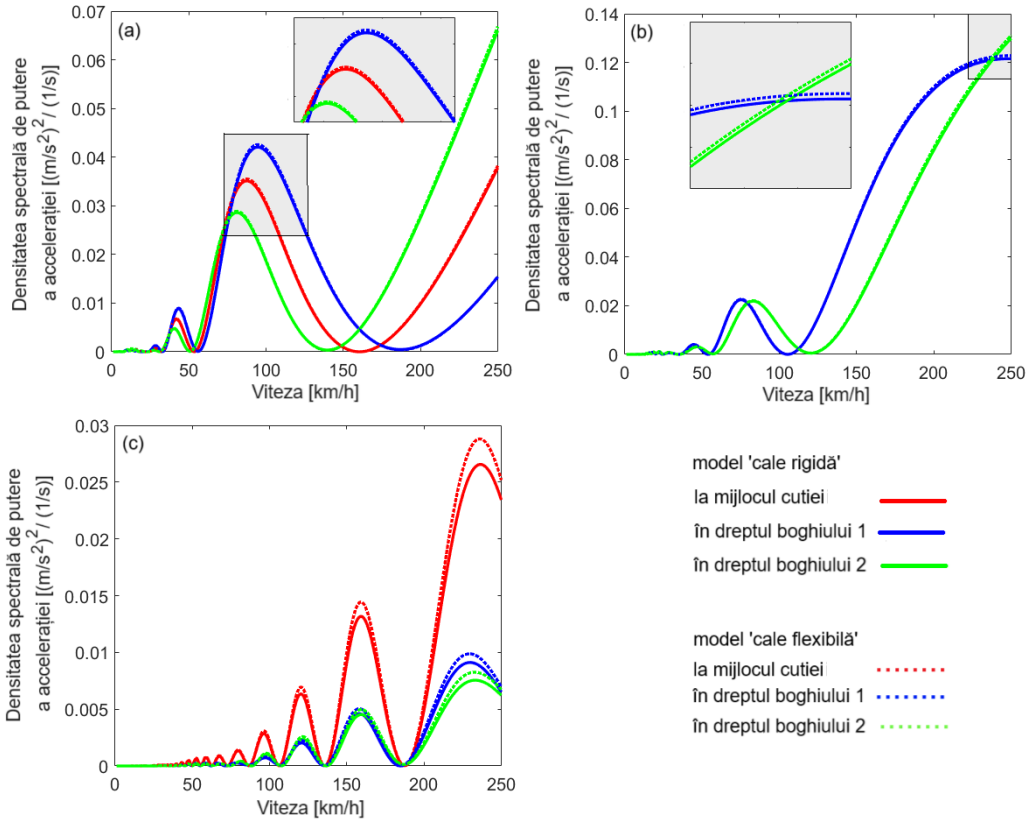

Fig. 5.6. Power spectral density of the acceleration at the eigenfrequencies of the vibration modes of the carbody: (a) at the eigenfrequency of bounce vibrations (1.17 Hz); (b) at the eigenfrequency of pitch vibrations (1.73 Hz); (c) at the eigenfrequency of bending vibrations (8 Hz).

Figure 5.7 shows the influence of the track model on the root mean square of the acceleration at the middle of the carbody and above the bogies. For the “elastic track” model, acceleration increases are obtained only at the middle of the carbody, but these increases are not greater than 4%.

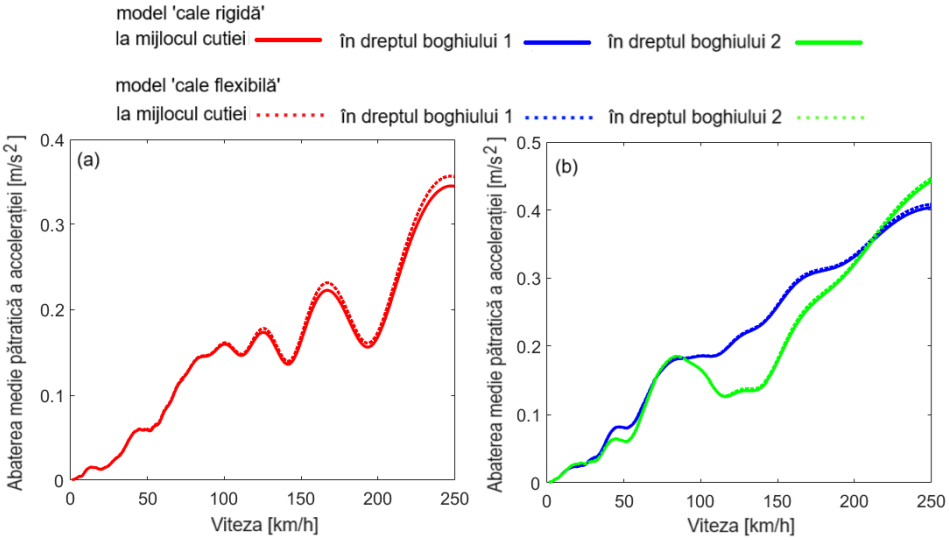

Fig. 5.7. The root mean square of the acceleration:
(a) at the middle of the carbody; (b) above the bogies.

6. Study of the dynamic response of the carbody - anti-bending bars system

6.1. Introduction

One of the passive methods of reducing vertical bending vibrations of light passenger railway carbodies to improve the ride comfort involves the use of a system of anti-bending bars mounted on the longitudinal beams of the carbody chassis. This method was proposed by the doctoral supervisor, prof. Mădălina Dumitriu, in the paper [14].

The operating principle of the anti-bending bar system is schematically shown in Figure 6.1 [64]. Figure 6.1 (a) shows the main components of the vehicle: the carbody (1), the chassis of the two bogies (5), the primary suspension (6), the secondary suspension (7), the vehicle wheels (4) and the track (8). Four rigid supports are mounted on the chassis of the vehicle body, two on each longeron, arranged symmetrically in relation to the middle of the carbody. A steel bar with a circular section, called an anti-bending bar, is attached to the supports of a longeron. When the carbody is deformed by the action of the first vertical bending mode, the cross-sections in which the anti-bend bar supports are fixed, located on either side of the axis of symmetry of the carbody, rotate in opposite directions, as shown in figure 6.1 – (b) and (c). Depending on how the carbody bends, the ends of the supports move apart (figure 6.1 (b)) or closer together (figure 6.1 (c)), so that the anti-bending bars are subjected to stretching or compression. In the anti-bending bars, longitudinal elastic reaction forces are developed acting on the supports, marked in figures (b) and (c) by red arrows. These forces determine, on the neutral axis of the carbody, the longitudinal forces and bending moments marked in figures (b) and (c) by straight arrows and blue arched arrows respectively. As can be seen, the bending moments oppose the vertical bending movement of the carbody. On the other hand, since these moments are

elastic in nature, their effect leads to an increase in the bending rigidity of the carbody, which means an increase in the frequency of its first bending mode. In other words, the eigenfrequency of the vertical bending of the carbody can be increased and brought out of the range in which the human body exhibits high sensitivity to vibrations. For this, the parameters of the anti-bending bar must be established from the condition of achieving the frequency of the first mode of vertical bending of the carbody, convenient from the point of view of ride comfort.

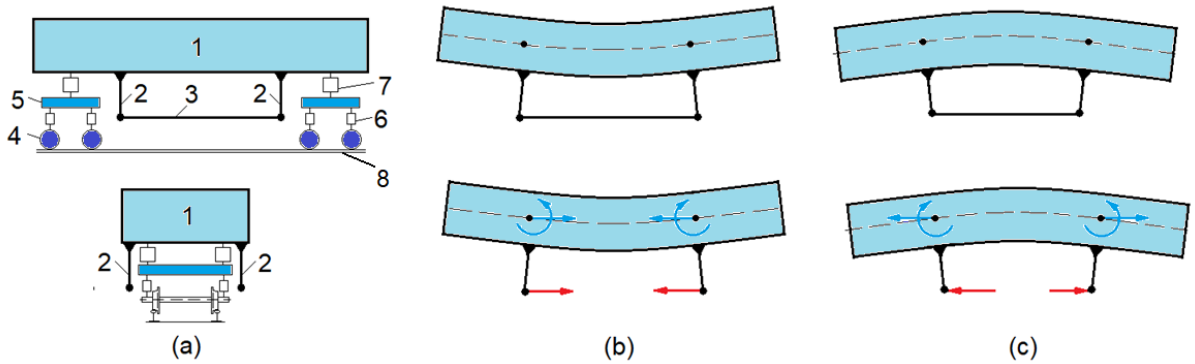

Fig. 6.1. Operating principle of the anti-bending bar system [36]:
1. vehicle carbody; 2. support of the anti-bending bars; 3. anti-bending bar; 4. wheel; 5. the bogie chassis; 6. the primary suspension; 7. secondary suspension; 8. track.

The effectiveness of the anti-bending bar system in terms of reducing the bending vibrations of the carbody and improving the ride comfort of high-speed railway vehicles was investigated by M. Dumitriu in the paper [14], referred to above, based on the results obtained by numerical simulations. The simulation applications were developed based on an original model of the railway vehicle, which includes the carbody – anti-bending bars system. It is important to point out here some aspects related to the modelling of the anti-bending bar system, to which I will refer later, so that I can highlight my contribution to the development of the carbody system model - anti-bending bars and, implicitly, to the development of this method.

First of all, it should be noted that the anti-bending bars have been reduced to linear elastic elements, rigidly fixed in the supports on the longitudinal beams of the carbody chassis. It is also important to remember that in the original model of the carbody - anti-bending bars system, the mass of the anti-bending bars was neglected in relation to the weight of the carbody. However, it was considered to limit the interference between the vertical bending vibrations of the carbody and those of the anti-bending bars by limiting the length of the anti-bending bars. Specifically, the maximum length of the anti-bending bars has been set so that the frequency of the first vertical bending mode of the anti-bending bars is one octave from that of the first bending mode of the carbody. For the calculation of the maximum length of the anti-bending bar, it was separated from the carbody - anti-bending bar assembly and considered a Euler-Bernoulli beam fixed at the ends.

The functionality of the method of reducing the bending vibrations of the railway vehicle carbody by using the anti-bending bar system has been tested in the laboratory, with the help of an experimental demonstrator system.

The experimental demonstrator system was developed between 2022 and 2024 within the research project entitled *Method to reducing the vertical vibration of the railway vehicle carbody based on anti-bending system*, project code PN-III-P2-2.1-PED-2021-0319, funded by contract 724PED/2022. The project was coordinated as director by the doctoral supervisor, Professor M. Dumitriu, and I participated as a member of the research team, occupying the position of PhD student. The results of the theoretical and experimental research obtained within this project were presented in papers [10] and [36], which were published in the journal Applied Sciences, with the mention that I participated as a co-author.

In the short presentation above I tried to motivate the choice to continue, within the doctoral thesis, the research on the possibilities of reducing the vertical bending vibrations of the railway vehicle carbody by using the anti-bending bar system. On the one hand, the method described is an innovative method from a scientific point of view, and from a technical point of view it is a simple method, which has the advantage that it does not require high manufacturing, implementation and maintenance costs. The functionality of this method has been demonstrated both theoretically [8, 14] and experimentally on a scale laboratory model [10, 36], which justifies further research to be able to make the transition to a higher scientific and technical level. On the other hand, I pointed out the experience gained in the theoretical and experimental research activity and the knowledge gained during two years as a member of the research team of the above-mentioned project.

The objective I set myself in my doctoral thesis is to develop the model of the carbody–anti-bending bars system, in order to take into account the effect of the elastic parameters of the fastening elements of the anti-bending bars to the supports, as well as the effect of the rigid and bending modes of the anti-bending bars on the dynamic response of the vehicle carbody. For this, the clamping system of the anti-bending bars of supports has been modelled by ideal elastic elements that take over both vertical and longitudinal translations, as well as rotations in the vertical-longitudinal plane. For vertical motions, the anti-bending bars were modelled as free-free Euler-Bernoulli beams but connected to the elastic elements of the support fasteners. On the longitudinal direction, the inertial effects of the anti-bending bars have been neglected as well, since the eigenfrequencies in this direction are far outside the field of interest, because the longitudinal stiffness of the anti-bending bars is higher than the vertical bending stiffness.

In view of the complexity of the proposed problem, a step-by-step approach is useful so that, in the first step, which is the subject of this chapter, the basic properties of the dynamic response of the carbody - anti-bending bars system are highlighted, and in the second step (see Chapter 7) the effect of anti-bending bars on the vertical vibrations of the railway vehicle carbody is analysed. Therefore, in the following, the model of the carbody - anti-bending bars system is presented, the equations of motion and frequency response functions are deduced, and then the dynamic response of the carbody - anti-bending bars system is analysed. On this basis, the following shall be established: (a) the correlation between the eigenfrequencies of the bounce vibrations and the bending vibrations of the carbody-anti-bending bars system and the stiffness of the fastening of the bars to supports; (b) the characteristics of the harmonic vibration regime of the carbody and of the anti-bending bars according to the rigidity of the fastening of the bars to supports; (c) the identification of possibilities for increasing the frequency of the carbody bending vibrations by means of anti-bending bars.

6.2. Model of the carbody - anti-bending bars system

Figure 6.2 shows the mechanical model of the carbody-anti-bending bars system, in which the vehicle carbody and the anti-bending bars are considered as free-free Euler-Bernoulli beams. The anti-bending bars are attached to the supports fixed to the carbody by ideal elastic elements that work in three directions: vertical translation, longitudinal translation along the anti-bending bars and rotation in the vertical-longitudinal plane. The carbody rests on the elements of the secondary suspension which is modelled with the help of Kelvin-Voigt systems that work only on translation in the vertical direction.

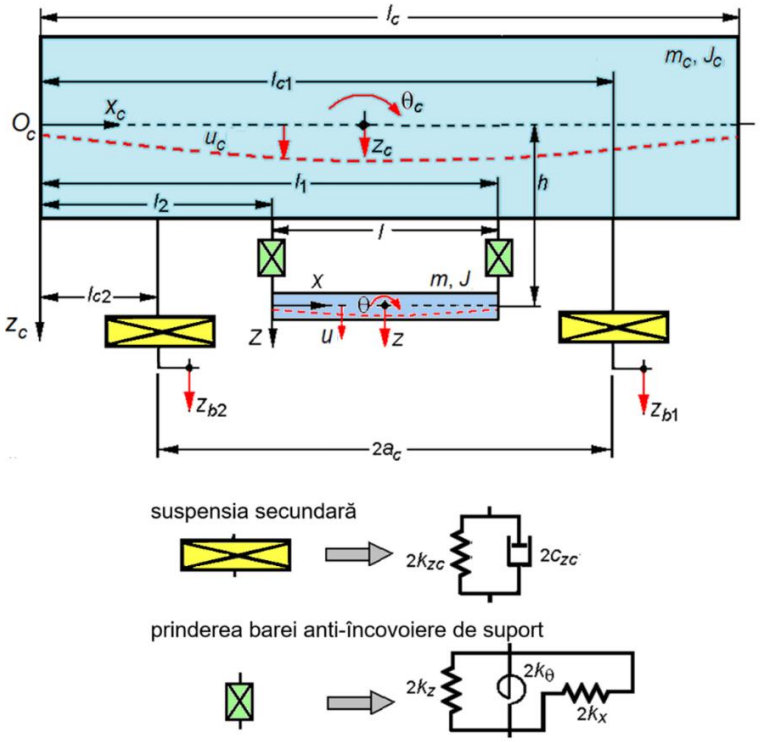

Fig. 6.2. Model of the carbody - anti-bending bars system.

The parameters of the carbody model and those of the secondary suspension are identical to those presented in the previous chapters. These parameters are: E_cI_c – the bending stiffness of the carbody, where E_c is the longitudinal modulus of elasticity of the carbody, and I_c is the moment of inertia of the cross-section of the carbody; ρ_c – the mass of the carbody per unit length; μ_c – the structural damping coefficient of the carbody; l_c – the length of the carbody; $l_{c1,c2}$ – distances that position the elements of the secondary suspension in relation to the $O_cx_cz_c$ reference system attached to the left end of the carbody originating at the level of the neutral axis of the carbody; $2k_{zc}$ – the elastic constant of the secondary suspension at one end of the carbody; $2c_{zc}$ – the damping constant of the secondary suspension at one end of the carbody; h - the distance between the axis of the anti-bending bars and the neutral axis of the carbody.

The parameters of the anti-bending bar system and of the fastening of the anti-bending bars to the supports are: EI – the bending stiffness of a bar, where E is the longitudinal modulus of elasticity of the bars, and I is the moment of inertia of the cross-section of a bar; ρ – the mass of a bar per unit length; μ – the structural damping

coefficient of the bar; d – the diameter of a bar; l – the length of a bar; k_x – the longitudinal stiffness of the fastening of a bar to the support; k_z – the rigidity in the vertical direction of the fastening of a bar to the support; k_θ – angular stiffness for rotations in the vertical-longitudinal plane; $l_{1,2}$ - distances that position the supports of the anti-bending bars in relation to the $O_c x_c z_c$ reference system.

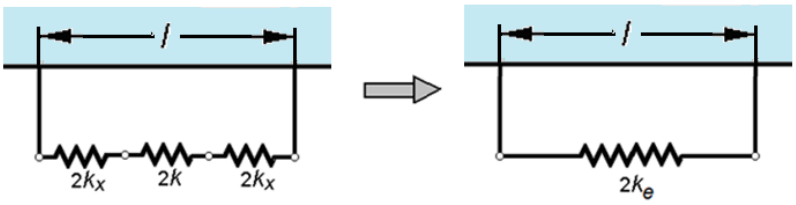

Fig. 6.3. Model of the bars in longitudinal direction.

In the longitudinal direction, the anti-bending bars are reduced to elastic elements of stiffness k (for a bar) that work in series with the longitudinal elastic elements of the bars' fastening to their supports (figure 6.3). The cumulative effect is an elastic element equivalent to stiffness k_e.

The excitation of the carbody – anti-bending bars system comes from the vertical displacements of the bogies, which are presumed to be harmonic movements in phase or out of phase and which are at the level of the secondary suspension elements.

Motion of the carbody is described by the function $u_c(x_c,t)$ which represents the displacement of the x_c section at time t with respect to the $O_c x_c z_c$ reference frame. Motion of the anti-bending bars is described similarly by means of a single function of the form $u(x, t)$ since the two bars move identically due to the symmetry and absence of the rolling motion of the carbody; x locates any section of the bar in relation to the Oxz reference system originating at the left end of the anti-bending bar, at the level of its neutral axis.

The presented model can be considered a simplified model of the railway vehicle, obtained by neglecting the components of the bogies and reducing them to simple vertical displacements imposed on the secondary suspension elements, denoted with $z_{b1,2}$. However, the simplified vehicle model has the particularity of having the same fundamental properties as those of the complete vehicle model. The advantage of the simplified model lies in the possibility of easily establishing the correlation between the characteristics of the attachment of the anti-bending bars to the supports and to evaluate the coupling of the vibrations of the bars with those of the carbody.

6.3. Dynamic response analysis of the carbody-anti-bending bars system

Next, the dynamic response of the carbody – anti-bending bars system is analysed based on the model presented above, respectively since the frequency response functions.

Figure 6.4 shows the frequency response function of the mid-carbody displacement without and with anti-bending bars, calculated in the absence of damping. The dynamic response of the carbody is dominated by the two spikes that correspond to the resonant frequencies of the carbody on the secondary suspension, whose movement presents two degrees of freedom.

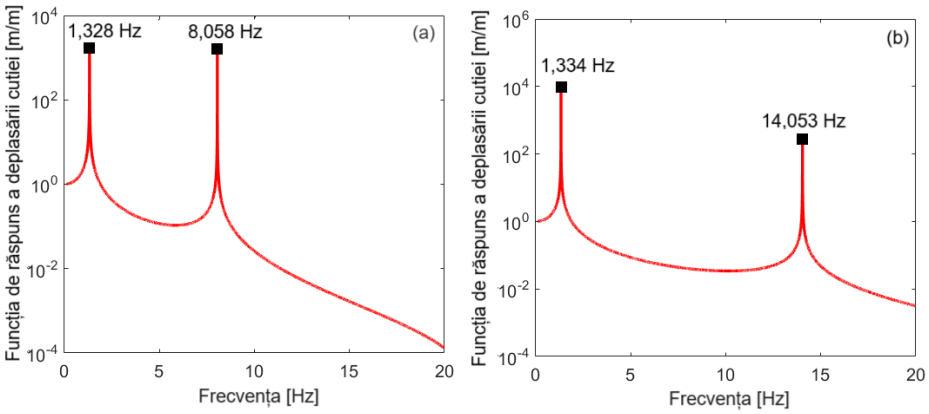

Fig. 6.4. Frequency response function of the displacement at the middle of the carbody:
(a) carbody without anti-bending bars; (b) carbody with anti-bending bars (non-inertia bar model).

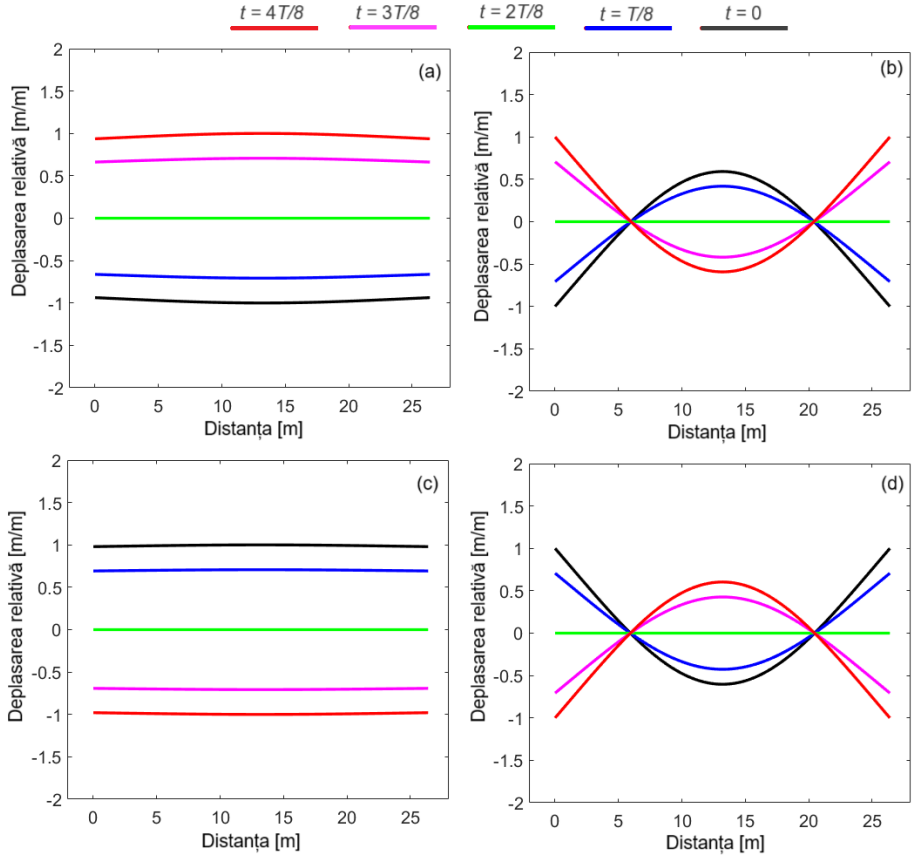

Fig. 6.5. Carbody displacement at the resonance frequencies:
carbody without anti-bending bars - (a) $f = f_j$ = 1.328 Hz; (b) $f = f_h$ = 8,058 Hz;
carbody with anti-bending bars - (c) $f = f_{jb}$ = 1.334 Hz; (d) $f = f_{hb}$ = 14.05 Hz.

Figure 6.5 shows how the vehicle carbody vibrates when the excitation frequency is equal to one of the system's resonant frequencies. Diagrams (a) and (b) show the relative displacement of the carbody axis without anti-bending bars, and diagrams (c) and (d) show the relative displacement of the carbody with anti-bending bars. In both situations analysed, at the low resonant frequency, the vibration of the carbody is dominated by the rigid vibration mode, while at the high resonant frequency, the bending mode predominates, which presents a maxim in the middle of the carbody, and two nodes located symmetrically on either side of the maxim. In terms of vibration shape, no noticeable

differences can be identified between the way the carbody vibrates without/with anti-bending bars. The only observation is that the vibrations in diagrams (a) and (c) are out of phase, and so are the vibrations in diagrams (c) and (d), but this is less important.

Figure 6.6 shows the dynamic response in the middle of the carbody for several values of the vertical stiffness of the fastening of the anti-bending bars to the supports. All diagrams show 4 peaks corresponding to the 4 resonant frequencies of the system. It is interesting to note that, apparently, the frequency response function in the middle of the carbody does not show the fourth peak in diagrams (a) and (b). The explanation lies in the very poor coupling between the vibration of the carbody and that of the anti-bending bar system due to the high elasticity of the fastening system. It is noted that in the case of poor coupling between the vibration of the carbody and that of the anti-bending bar system - diagrams (a) and (b), the resonant frequencies of the carbody bounce and bending, as well as the bending frequency of the anti-bending bars remain practically unchanged. However, the resonance frequency of the bar bounce increases from 0.72 Hz to 2.38 Hz if the vertical stiffness of the fastening goes from 10 kN/m to 100 kN/m. When there is a stronger coupling between the vibrations of the carbody and those of the anti-bending bar system - diagrams (c) and (d), practically only the resonant frequencies of the anti-bending bars are changed while the resonant frequencies of the carbody remain almost unchanged. Thus, the bounce of the anti-bending bars reaches 6.59 Hz for k_z = 1 MN/m and 11.08 Hz for k_z = 10 MN/m. At the same time, the resonance frequency of the bending of the anti-bending bars increases first to 31.91 Hz (k_z = 1 MN/m), and then to 58.40 Hz (k_z = 10 MN/m).

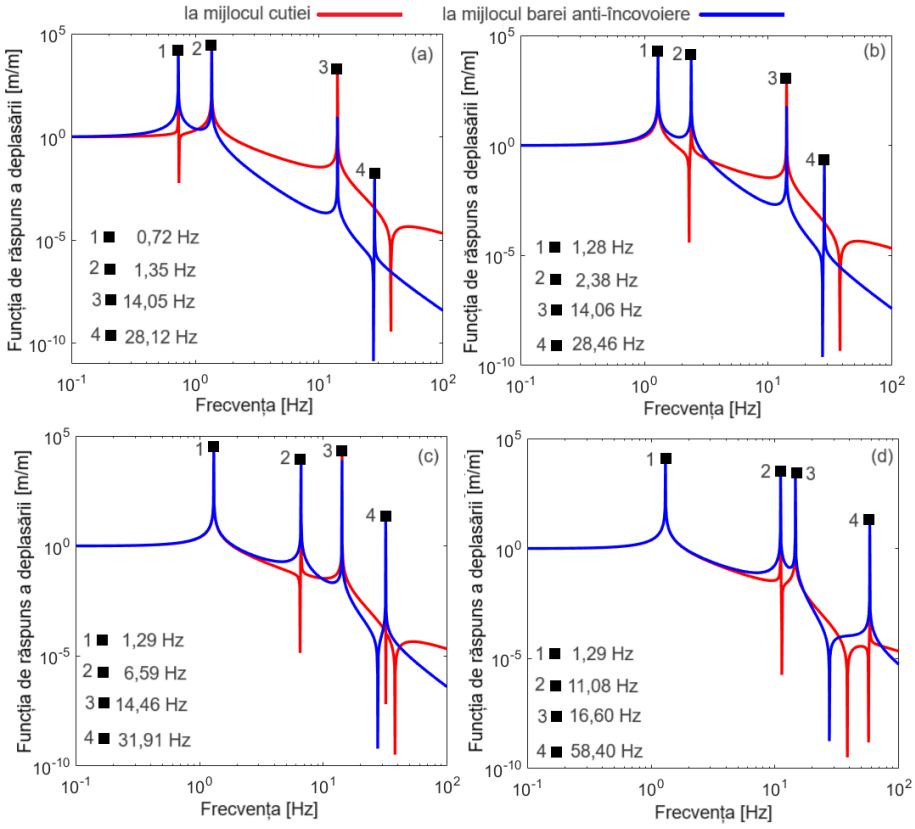

Fig. 6.6. Frequency response function of the displacement at the carbody middle and at the anti-bending bars middle (no-damping model):
(a) k_z = 10 kN/m; (b) k_z = 100 kN/m; (c) k_z = 1 MN/m; (d) k_z = 10 MN/m.

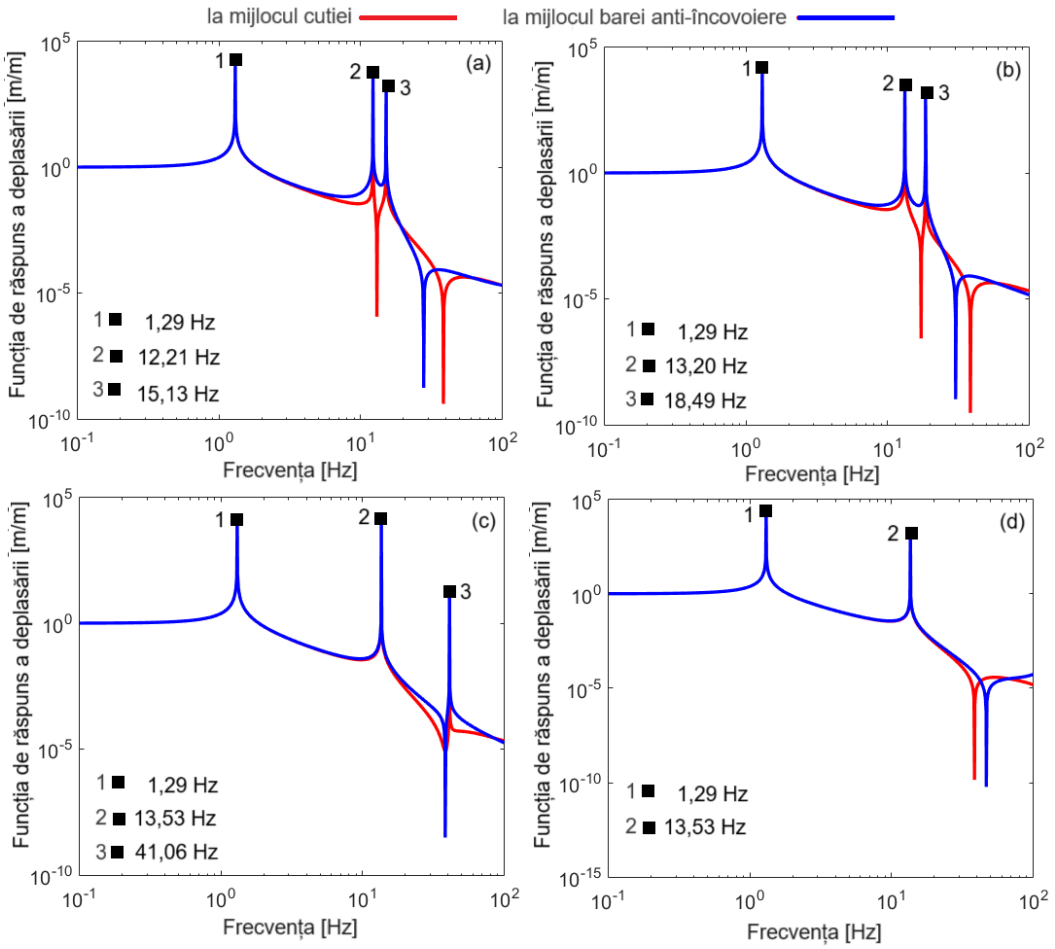

Fig. 6.7. Frequency response function of the displacement at the carbody middle and at the anti-bending bars middle (no-damping model): k_z = 100 MN/m; (b) k_z = 1 GN/m; (c) k_z = 10 GN/m; (d) k_z = 100 GN/m.

Figure 6.7 shows the frequency response functions in the middle of the carbody and in the middle of the anti-bending bars for the situation where the stiffness of the fastening of the anti-bending bars to the supports takes high values. The diagrams show the response functions also in the range 0.1 – 100 Hz, without considering the influence of damping. In diagrams (a), (b) and (c) of figure 6.7, the frequency response functions show three peaks corresponding to the resonant frequencies due to the bounce and bending of the carbody and the bounce of the anti-bending bars. The fourth peak, which is due to the bending of the anti-bending bars, is located outside the range considered for simulation. Diagram (d) shows only the resonance peaks of the carbody, the bounce of the anti-bend bars being outside the frequency range represented.

Based on the analysis of the frequency response of the carbody and the anti-bending bars calculated with the non-damping model, it is concluded that the resonance frequencies of the carbody on the secondary suspension are not significantly influenced by the presence of the anti-bending bar system or by the vertical and rotational rigidity of the anti-bending bar clamping. On the other hand, the same cannot be said about the resonant frequencies of anti-bending bars. They continuously increase as the grip of the support bars is more rigid. The explanation lies in the fact that the mass of the carbody is much greater than the mass of the anti-bending bar system and its movement is slightly

influenced by the presence of the anti-bending bar system. On the other hand, the restriction imposed on the length of the anti-bending bars, resulting from the condition that the resonance frequency at bending the anti-bending bars is at least one octave from the resonance frequency at bending the carbody, is not necessary when the stiffness of the fastening of the anti-bending bars to the supports is sufficiently high, because their bending frequency increases with the rigidity of the fastening of the anti-bending bars to the supports.

Figure 6.8 shows the influence of the model's damping on the frequency response functions of the carbody and anti-bending bars. It is about the damping of the secondary suspension, as well as the structural damping of the carbody and the anti-bending bars. For comparison, the frequency response function of the carbody without/with anti-bending bars is presented, in the latter case, the non-inertia bar type model was used. The effect of the anti-bending bars (the non-inertia bar model) on the frequency response is observed by increasing the bending frequency of the carbody from 8 Hz to 14 Hz. Regarding the results obtained with the inertia bar model, the following observations are made.

In the case of low stiffness of the fastening between the anti-bending bars and the supports, diagrams (a) and (b), the frequency response curve in the middle of the carbody overlaps that calculated with the non-inertia bar model, except for the area around the bounce frequency of the anti-bending bars located either to the left, if k_z = 10 kN/m, or to the right of the carbody bounce resonance, for k_z = 100 kN/m. The vibration behaviour of the anti-bending bars is much more intense than that of the carbody in the low frequency range due to the bounce resonance of the bars. At the same time, the vibration of the anti-bending bars has a poor damping at the bending frequency of approx. 28 Hz.

When there is a stronger coupling between the vibrations of the carbody and those of the anti-bending bar system - diagrams (c) and (d), the characteristics of the frequency response functions of the carbody–anti-bending bars system are preserved, with the difference that the vibration of the anti-bending bars decreases in intensity at its bounce frequency, but increases in the rest, especially at the bending resonance of the anti-bending bars. In diagram (c) the vibration of the anti-bending bars is lower than that of the carbody at the resonant frequency of the carbody, while in diagram (d), when the bounce of the anti-bending bars comes closer to the bending frequency of the carbody, the vibration of the bars is greater than that of the carbody. It is also interesting to note that the bending resonance of the carbody increases to a certain extent compared to the ideal case where the carbody is fitted with spring-type bars (the non-inertia bar model). This aspect is especially visible in diagram (d), where the vertical stiffness of the anti-bending bars to the carbody is 10 MN/m.

Diagrams (e) and (f) correspond to two large values of the vertical stiffness of the fastening of the anti-bending bars to the supports, k_z = 100 MN/m and k_z = 1 GN/m respectively, which shows a strong coupling of the anti-bending bars to the carbody. This situation is characterized by the presence of the bounce resonance of the anti-bending bars near the bending resonance of the carbody, while their bending resonance exceeds the field of interest. The vibration of the carbody therefore has two peaks located at over 10 Hz with the specification that, at k_z = 1 GN/m, the peak due to its own bending has a lower frequency than the frequency given by the bar-type model without inertia, diagram (f). The vibration of the anti-bending bars is more intense than that of the carbody when the excitation frequency is around the two peaks.

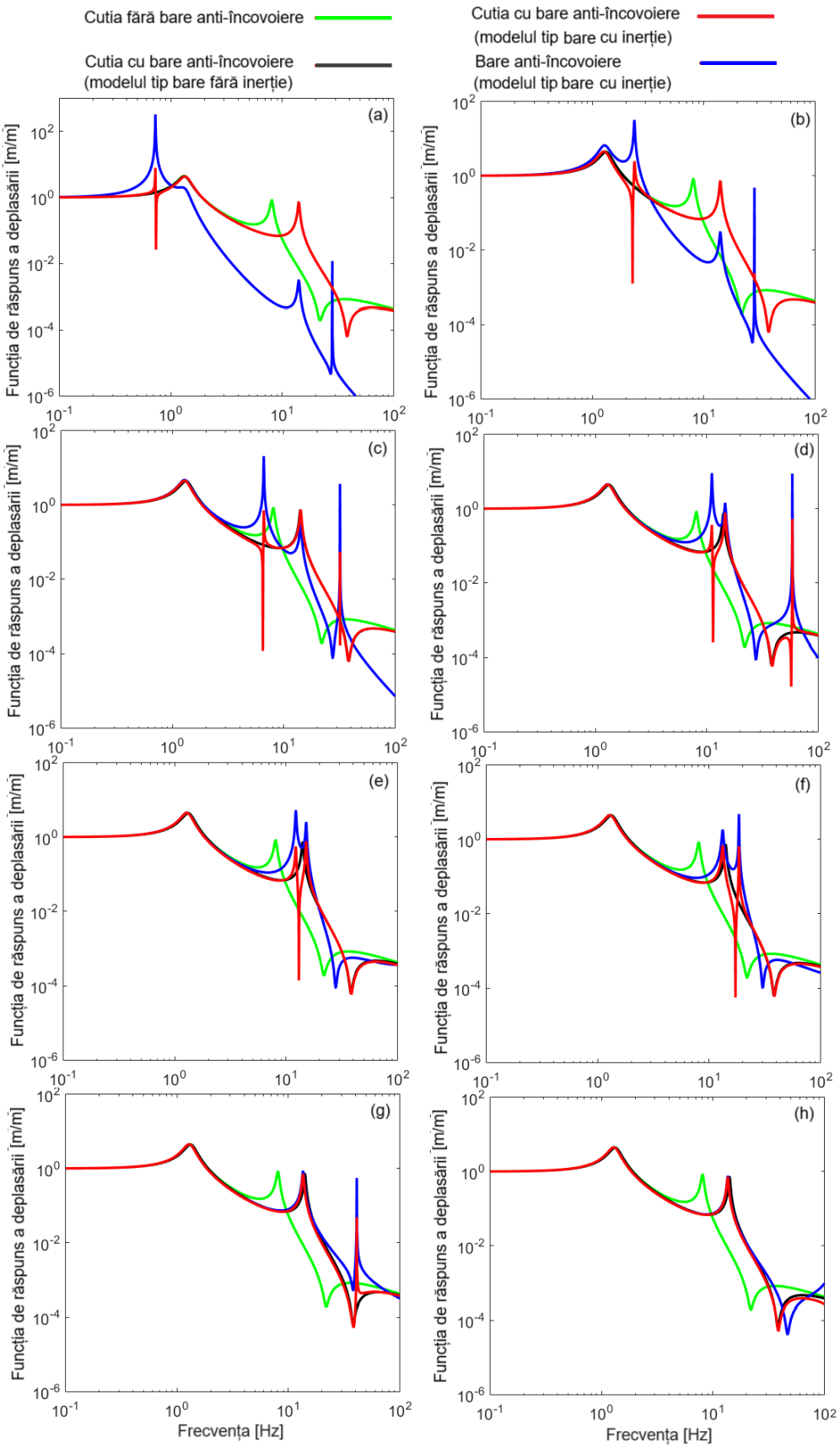

Fig. 6.8. Frequency response function of the displacement at the carbody middle and at the anti-bending bars middle (damping model): (a) k_z = 10 kN/m; (b) k_z = 100 kN/m; (c) k_z = 1 MN/m; (d) k_z = 10 MN/m; (e) k_z = 100 MN/m; (f) k_z = 1 GN/m; (g) k_z = 10 GN/m; (h) k_z = 100 GN/m.

Diagrams (g) and (h) show the frequency response functions for the case of very rigid fastening of the anti-bending bars to the supports. In diagram (g), the frequency response functions of the carbody – anti-bending bars system have three peaks, of which the one located at the highest frequency corresponds to the bounce of the anti-bending bars (k_z = 10 GN/m), and in diagram (h), where k_z = 100 GN/m, these functions have only two peaks because the bounce of the anti-bending bars is outside the range of interest. As regards the vibration of the carbody, the results obtained with the inertia bar model are close to those obtained with the non-inertial bar model with two differences: (a) the peak corresponding to the bending of the carbody has a slightly lower frequency, 13.51 Hz compared to 14.05 Hz resulting from the non-inertia bar model; (b) the vibration of the carbody shows the peak corresponding to the bounce of the anti-bending bars, as shown in diagram (g). The vibration of the anti-bending bars is practically equal to that of the carbody at low frequencies, up to 4-5 Hz, after which, progressively, it becomes higher.

In conclusion, the analysis of the vibrations of the carbody – anti-bending bars system with the help of the damping model highlights the following: the vibration of the carbody is similar to that obtained with the non-inertia bar model, except for the frequency intervals in which the vibration of the carbody interferes with the bounce of the anti-bending bars; the vibration of the carbody is not influenced by interference with the bending of the anti-bending bars, either due to the poor coupling or because the bending frequency of the anti-bending bars is much higher, being located more than an octave from the bending of the carbody; the vibration of the carbody is influenced by interference with the bounce of the anti-bending bars in almost all the cases studied; the vibration of the carbody becomes independent of the vibration of the anti-bending bars only if the stiffness of the fastening of the anti-bending bars to the supports is very high, as shown in diagram (h); the vibration of the anti-bending bars is clearly superior to the vibration of the carbody due to their bounce and bending resonances when the stiffness of the fastening of the bars to the supports is not sufficiently stiff, according to diagrams (a) – (f).

Next, the influence of the longitudinal stiffness of the fastening of the anti-bending bars to the supports is analysed. Figure 6.9 shows the frequency response functions in the middle of the carbody for different values of the stiffness fastening of the anti-bending bars to the supports. The parametric calculation was carried out by choosing the last four values of the vertical stiffness of the fastening between the anti-bending bars and the supports considered in the previous case, so that the bounce frequency of the anti-bending bars is higher than the bending frequency of the carbody. For each value of the vertical stiffness of the fastening of the anti-bending bars to the supports, 5 values of the longitudinal stiffness k_x corresponding to the proportionality factor K were tested (see Table 6.1). In diagrams (a) and (b) by making the anti-bending bars more flexible in the longitudinal direction, against the background of increasing the elasticity of the support's fasteners, the frequency of the peak of the bending resonance decreases from the maximum to the minimum value. Similar aspect is identified in the case of the frequency of the peak corresponding to the bounce of the anti-bending bars, whose decrease is smaller. In contrast, in diagrams (c) and (d), which are similar in the frequency range considered, the peak of the bounce of the anti-bending bars no longer appears, but it can also be seen how the frequency of the bending peak of the carbody shifts to lower values when the longitudinal stiffness of the fastening between the anti-bending bars and the supports decreases. Table 6.1 shows the carbody bending frequencies obtained since figure 6.9.

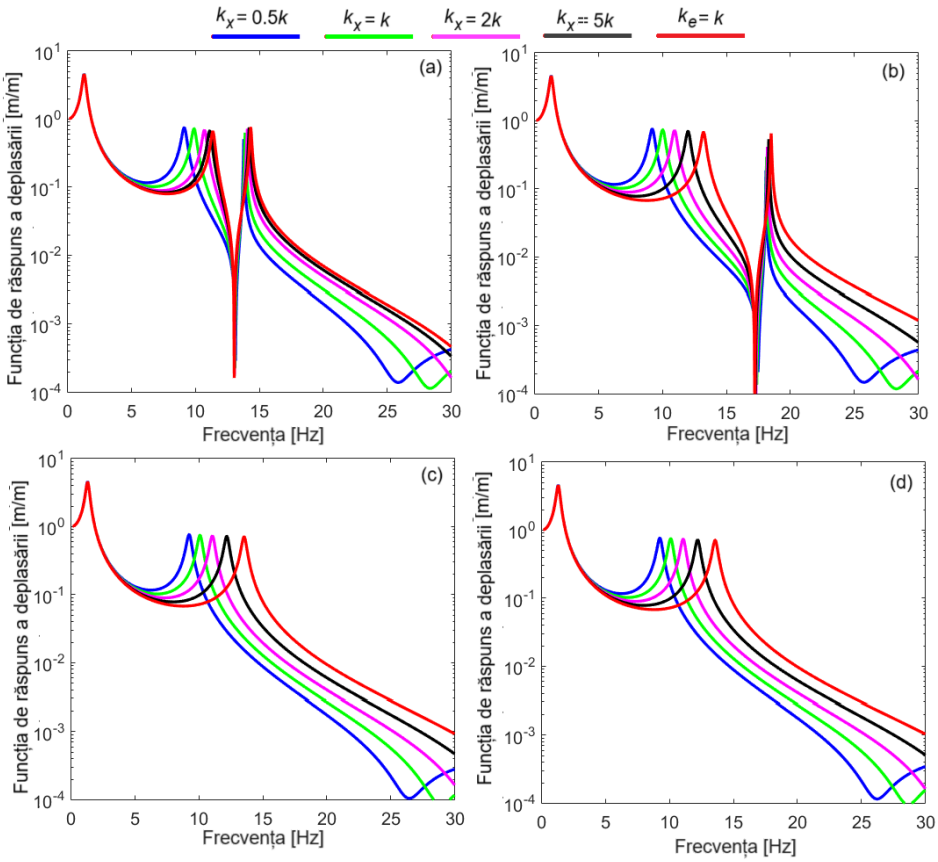

Fig. 6.9. Frequency response functions of displacement to the middle of the carbody for different values of the stiffness of the fastening of the anti-bending bars to the supports:
(a) k_z = 100 MN/m; (b) k_z = 1 GN/m; (c) k_z = 10 GN/m; (d) k_z = 100 GN/m.

If the vertical stiffness k_z is 100 MN/m, then the bending frequency of the carbody decreases from 12.2 Hz to 9.11 Hz. Regarding the last three cases considered, no important differences can be identified between them, the bending frequency of the carbody decreases from approx. 13.5 Hz to about 9.2 Hz. In any case, the results obtained show the importance of ensuring longitudinal stiffness at a sufficiently high level so as not to compromise the functionality of the anti-bending bar system.

Table 6.1. Carbody bending resonance frequencies.

Vertical stiffness k_z	Proportionality factor K				
	∞	5	2	1	0,5
100 MN/m	12.20 Hz	11.51 Hz	10.07 Hz	9.88 Hz	9.11 Hz
1 GN/m	13.21 Hz	11.98 Hz	10.93 Hz	10.00 Hz	9.18 Hz
10 GN/m	13.52 Hz	12.16 Hz	11.04 Hz	10.07 Hz	9.22 Hz
100 GN/m	13.56 Hz	12.19 Hz	11.05 Hz	10.08 Hz	9.23 Hz

The effect of increasing the length of anti-bending bars on the frequency response functions of the carbody and anti-bending bars is further analysed. The analysis is restricted to two cases regarding the vertical stiffness of the fastening of the anti-bending bars to the supports, respectively k_z = 1 GN/m and k_z = 10 GN/m.

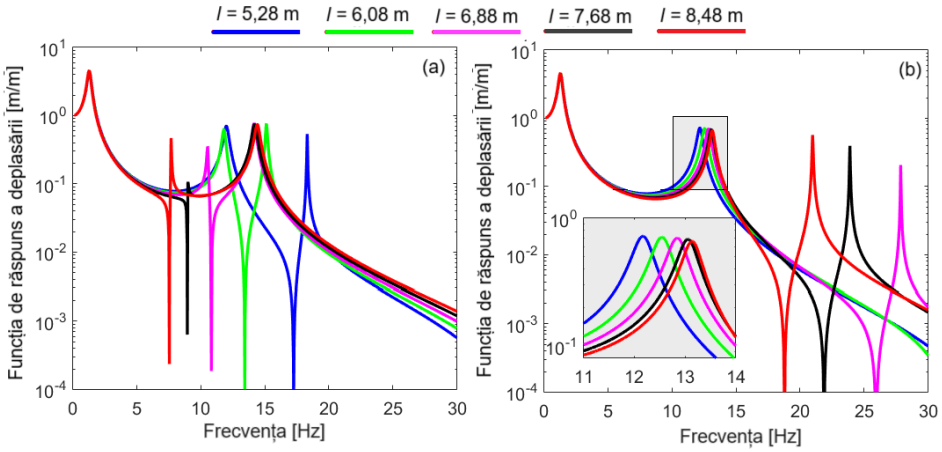

Fig. 6.10. Influence of the length of anti-bending bars on frequency response of the carbody: (a) k_z = 1 GN/m; (b) k_z = 10 GN/m.

Figure 6.10 shows the frequency response function of the carbody for 5 values of the length of the anti-bending bars in arithmetic progression with the ratio 0.8 m starting from the reference value 5.28 m. Diagram (a) is constructed for k_z = 1 GN/m, and the blue curve represents the reference frequency response of the carbody. As the length of the anti-bending bars is greater, the bounce mode frequency of the bars decreases. Diagram (b) is for k_z = 10 GN/m and for the same values of the length of the anti-bending bars. Here, the reduction in the frequency of the bounce mode of the anti-bending bars is noted. Unlike the previous example, there is no longer interference between the bending mode of the carbody and the bounce mode of the anti-bending bars. The effect of increasing the length of the anti-bending bars on the bending frequency of the carbody is observed, which increases from 12.16 Hz for l = 5.28 m to 13.14 Hz for l = 8.48 m.

Based on the results obtained in this chapter, the effect of the inertia of the anti-bending bars and the stiffness of their fastening to the supports on the dynamic response of the carbody and the ride comfort of the passengers is investigated in the next chapter.

7. Effect of anti-bending bars on vertical vibration of the railway vehicle carbody

7.1. Introduction

In Chapters 4 and 5, studies have been developed on the structure of mechanical models that can be used for the study of vertical vibrations of the railway vehicle carbody, in order to establish the appropriate configuration of the secondary suspension model and the track model that would ensure sufficiently accurate results without unnecessarily complicating the analysis of the results by increasing the complexity of the model. Starting from the model of the carbody – anti-bending bars system developed in Chapter 6 and considering the results obtained in the two chapters mentioned above, the model of the integrated carbody–anti-bending bars–bogies–track system is developed.

This model consists of the vehicle carbody fitted with anti-bending bars, which rests on the secondary suspension for which the C model presented in Chapter 4 is adopted, the bogie chassis, the primary suspension, the vehicle wheels and the track, considered rigid based on the results obtained in Chapter 5. The equations of motion of the model of the integrated carbody–anti-bending bars–bogies–track system are then deduced and the frequency response functions are established, considering the harmonic irregularities of the track. Finally, the effect of the anti-bending bars on the vertical vibration behaviour of the railway vehicle carbody when running on a track with random irregularities is evaluated.

7.2. Model of the integrated carbody – anti-bending - bogies – track system

Figure 7.1 shows the mechanical model of the integrated carbody–anti-bending bar–bogies – track system. The railway vehicle travels at constant speed V on a rigid track that presents vertical irregularities, which excite the vertical vibrations of the vehicle.

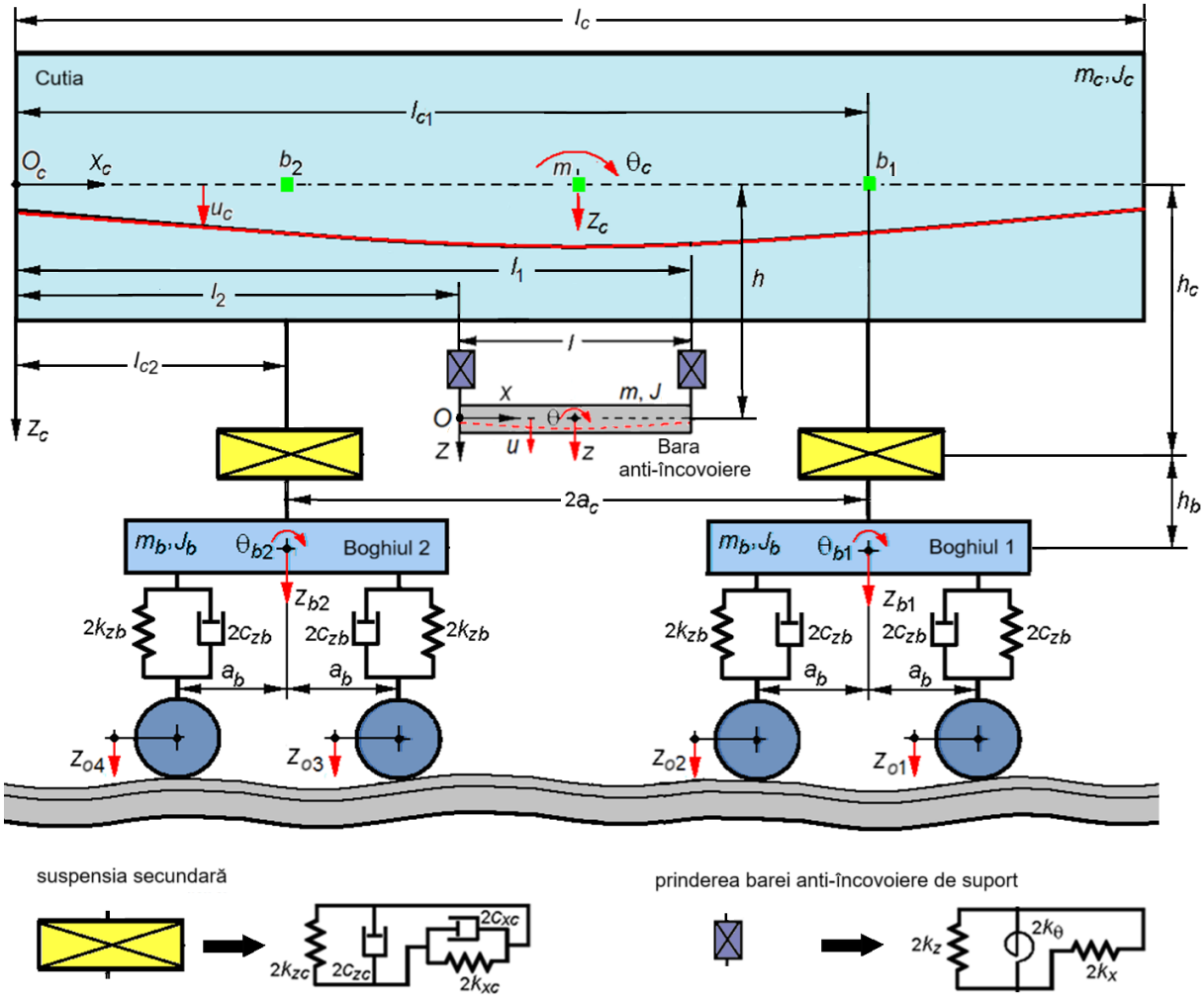

Fig. 7.1. Model of the integrated carbody–anti-bending bars–bogies–track.

As regards the structure of the vehicle model, the representation of the carbody – anti-bending bars system is taken from Chapter 6. It is recalled that both the vehicle carbody and the anti-bending bars are modelled using the theory of the free-free Euler-Bernoulli beam. Unlike the carbody model that does not have connections at the ends, the anti-bend bar model is tied at the ends to the elastic elements of the fastening to the vertical supports that are rigidly fixed to the carbody longerons.

The motion of the carbody is described in relation to the $O_c x_c z_c$ moving reference system by the vertical displacement u_c obtained by composing the rigid modes of vibration – bounce and pitch, and the first bending mode in virtue of the modal analysis method. Motion of the anti-bending bars, presumed identical and vibrating together, is related to the Oxz moving reference system by means of the vertical displacement u which is the result of the overlapping of the rigid modes and the first vertical bending mode.

The carbody is supported by the secondary suspension which is represented by four Kelvin-Voigt systems arranged in a vertical direction, one for each quarter of the carbody. Four other Kelvin-Voigt systems are provided that transmit the longitudinal forces between the carbody and the two bogies. This type of secondary suspension model is identical to the C model discussed in Chapter 4. The same type of model was also used in reference [25], in which the method of reducing the vertical bending vibrations of the railway vehicle carbody by means of the anti-bending bar system was presented.

The chassis of bogies are modelled as rigid bodies with two degrees of freedom each – bounce and pitch. The vertical displacement corresponding to the jump is denoted $z_{b1,2}$, and the rotation in the vertical-longitudinal plane for the pitch is denoted $\theta_{b1,2}$. The chassis of the bogies each rest on the primary suspension modelled by Kelvin-Voigt systems.

Vehicle wheels are rigid bodies that are in permanent contact with the track rails. In this mode, the vertical motion of the wheels, $z_{o1,\ldots,4}$, are identical to the vertical irregularities of the track.

The parameters of the model of the integrated carbody–anti-bending bars–bogies–track system are as follows:

- carbody parameters: $E_c I_c$ – bending stiffness, where E_c is the longitudinal modulus of elasticity, and I_c is the moment of inertia of the cross-section of the carbody; ρ_c – the mass of the carbody per unit length; μ_c – the structural damping coefficient of the carbody, l_c – the length of the carbody, $l_{c1,2}$ – the dimensions of the carbody support points on the secondary suspension, $2a_c$ – the wheelbase of the carbody;

- parameters of anti-bending bars: EI – the bending stiffness of a bar, where E is the longitudinal modulus of elasticity of the bar material, and I is the moment of inertia of the cross-section of the bar; ρ – mass per unit length of the bar; μ – the structural damping coefficient of the bar; k – the longitudinal stiffness of a bar; d – the diameter of a bar; l – the length of the bars;

- Parameters of the elastic fastening of anti-bending bars to the supports: k_z – vertical stiffness; k_x – longitudinal stiffness of the fastening of anti-bending bars to supports; k_θ – angular stiffness for rotations in the vertical-longitudinal plane; h – the distance between the axis of the anti-bending bars and the neutral axis of the carbody;

- parameters of the secondary suspension: $2k_{zc}$ and $2c_{zc}$ – the stiffness and damping constants of the secondary suspension corresponding to a bogie; $2k_{xc}$ and $2c_{xc}$ – the stiffness and damping constants of the longitudinal force transmission system between the

carbody and a bogie; h_c – the distance from the longitudinal force transmission system between the carbody and the bogies to the neutral axis of the carbody;

- bogie chassis parameters: m_b and J_b – mass and moment of inertia; h_b – the distance from the centre of mass of the bogie chassis to the longitudinal force transmission system between the carbody and the bogies; $2a_b$ – the wheelbase of the bogie;

- Primary suspension parameters: $2k_{zb}$ and $2c_{zb}$ – the stiffness and damping constants of the primary suspension corresponding to an axle.

7.5. Dynamic response of the carbody with anti-bending bars to track irregularities

Based on the model presented in the previous section, the dynamic response of the carbody–anti-bending bars system is further analysed, in terms of the frequency response function of the displacement, considering the irregularities of the track in harmonic form.

Figure 7.2 shows, for reference, the frequency response function of the carbody without anti-bending bars and the frequency response function of the carbody with anti-bending bars (non-inertia bar model) when the vehicle speed is 200 km/h. The case without damping was considered to highlight the resonance frequencies of the vehicle's vibration modes.

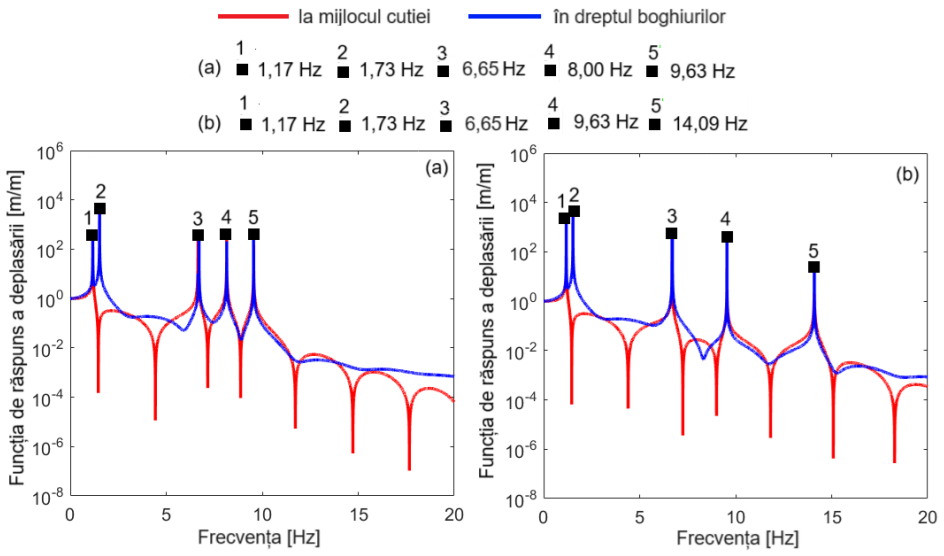

Fig. 7.2. Frequency response function of the displacement at the carbody middle and above the bogies: (a) carbody without anti-bending bars; (b) carbody with anti-bending bars (no-inertia bar model).

Diagram (a) shows the eigenfrequencies of the vehicle's vibration modes, as shown in section 5.5: the carbody bounce frequency at 1.17 Hz, the bogie bounce frequency at 6.65 Hz, the carbody pitch frequency at 1.73 Hz, the bogie pitch frequency at 9.63 Hz and the carbody bending frequency at 8.00 Hz. Bogie pitch and carbody bending are coupled between the system of transmission of longitudinal force between carbody and bogies, which explains the 9.63 Hz resonance in the response function of the carbody.

In diagram (b), the effect of the anti-bending bars upon the carbody bending frequency that increases to 14.09 Hz can be observed. The other eigenfrequencies remain practically unchanged compared to those obtained in the vehicle carbody without anti-bending bars: the carbody pitch frequency at 1.17 Hz, the bogie pitch frequency at 6.65 Hz, the carbody pitch frequency at 1.73 Hz, pitch frequency of the bogie at 9.63 Hz.

Starting from the results obtained in Chapter 6, four values of the vertical stiffness k_z of the fastening of the anti-bending bars to the supports are retained, respectively 10 MN/m, 100 MN/m, 1GN/m and 10 GN/m, for the parametric study of the frequency response functions of the integrated carbody–anti-bending bars–bogies–track system.

Figure 7.3 shows the frequency response function of the displacement in the middle of the carbody, and above to the first bogie, as well as the frequency response function of the displacement in the middle of the anti-bending bars, in the range of 0.1–100 Hz, for speed of 200 km/h. The four values selected above have been considered for the vertical stiffness of the fastening of the anti-bending bars to the supports. Connection between the anti-bending bars and the supports is perfectly rigid, which means that the equivalent longitudinal stiffness k_e equals the longitudinal stiffness of the anti-bending bars. The results were obtained using the inertia bar model.

In all 4 diagrams, the eigenfrequencies of the vehicle with anti-bending bars highlighted in figure 7.2 (b), where the non-inertia bar model was used can be identified, namely: the carbody bounce frequency at 1.17 Hz, the bogie bounce frequency at 6.65 Hz, the carbody pitch frequency at 1.73 Hz, pitch frequency of bogies at 9,63 Hz. In figure 7.3 (a), where the vertical stiffness of the fastening is k_z = 10 MN/m, the bending frequency of the anti-bending bars at 58,55 Hz appears both on the graph of the frequency response function of the displacement in the middle of the carbody and on the graph of the frequency response function of the displacement in the middle of the anti-bending bars. At the same time, the graph of the frequency response function of the carbody displacement above the first bogie also exhibits the pitch frequency of the anti-bending bars at 40.29 Hz. The bending frequency of the carbody at 14.67 Hz and the pitch frequency of the anti-bending bars at 11.18 Hz are also visible.

In the other three diagrams, as the vertical stiffness of the fastening the anti-bending bars to the support's increases, the bending frequency of the anti-bending bars and their pitch frequency leave the frequency range considered. Progressive separation between the bending frequency of the carbody and the pitch frequency of the anti-bending bars occurs. They are located at 12.78 Hz and 16.08 Hz if k_z = 100 MN/m, at 13.52 Hz and 27.94 Hz for k_z = 1 GN/m, and reach 13.60 and 78.47 Hz when k_z = 10 GN/m.

Figure 7.4 shows the influence of damping on the frequency response function of the carbody displacement and on the frequency response function of the anti-bending bar displacement for a speed of 200 km/h. Frequency response function of the displacement is represented in the middle of the carbody and above the two bogies. For anti-bending bars, the frequency response function is calculated in the middle. The same values of the vertical stiffness of the fastening of the anti-bending bars to the supports as in the previous example were considered. As for the damping, its values correspond to the following degrees of damping: 0.015 – the degree of structural damping of the carbody; 0.005 – the degree of structural damping of the anti-bending bars; 0.12 – the degree of damping of the secondary suspension and 0.22 – the degree of damping of the primary suspension.

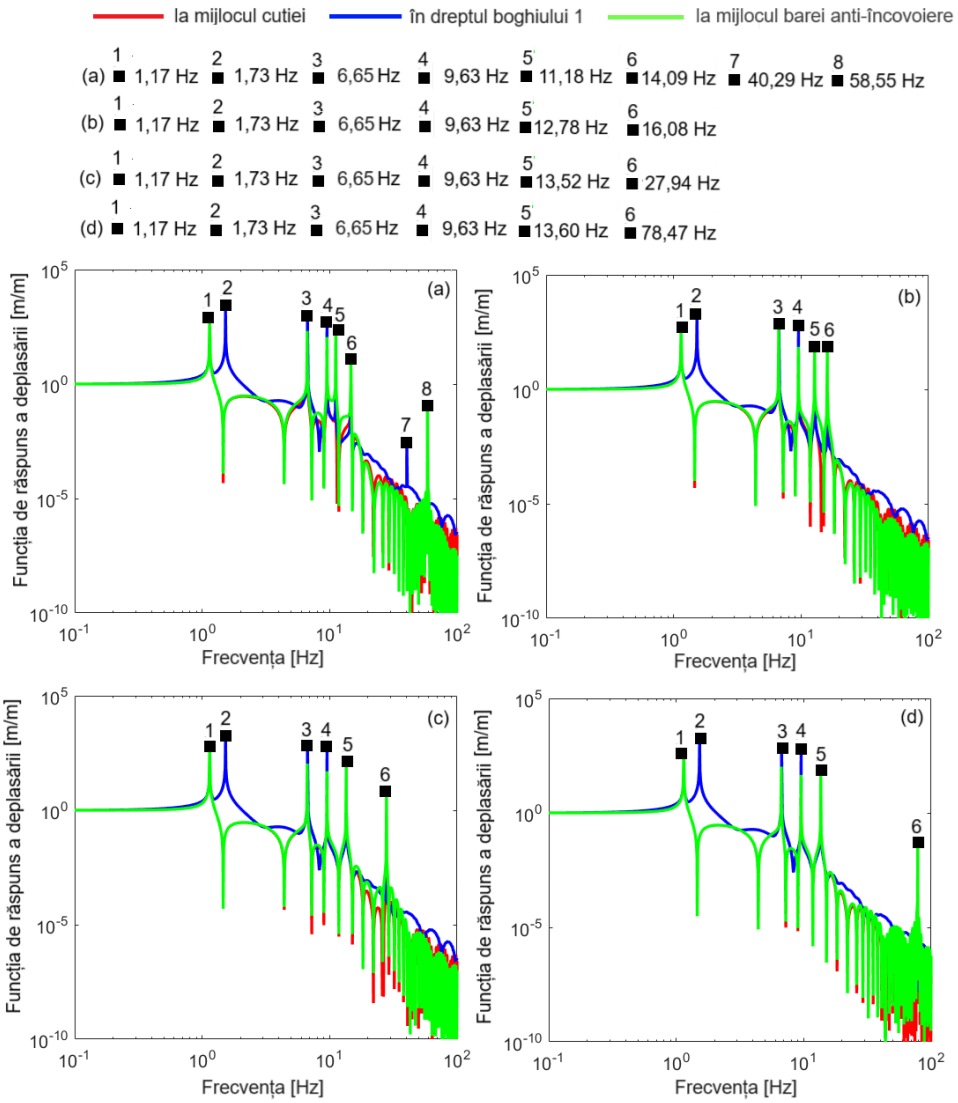

Fig. 7.3. Frequency response functions of the displacement at the carbody middle and above the bogie 1 and the frequency response function of the displacement at the middle of the anti-bending bars at 200 km/h (inertia bar model): (a) k_z = 10 MN/m; (b) k_z = 100 MN/m; (c) k_z = 1 GN/m; (d) k_z = 10 GN/m.

In diagram (a), for k_z = 10 MN/m, the response of the integrated carbody–anti-bending bars–bogies–track system is dominated, at frequencies higher than 10 Hz, by two peaks coming from the bending of the carbody and the bounce of the anti-bending bars. The most intense vibration is signalled in the middle of the anti-bending bars. The peak corresponding to the pitch of the bogies, which could be seen on the graph of the frequency response function of the carbody calculated above the bogies (see figure 7.3 (a)), is now flattened due to damping. On the same diagram, the frequency response function of the carbody displacement calculated in front of the bogies visibly shows the resonance peak due to the gallop of the anti-bending bars, which is located at just over 40 Hz. At the same time, the bending mode of the anti-bending bars appears on the frequency response function of the displacement in the middle of the anti-bending bars in the form of a maximum at 58.6 Hz.

If the vertical stiffness of the anti-bending bars to the supports increases to 100 NM/m (diagram b), then only the two peaks of the carbody bending and the jump of the anti-bending bars are found on the graphs of the frequency response of the system. In diagrams (c) and (d), for k_z = 1 GN/m and k_z = 10 GN/m, respectively, the frequency at which the peak corresponding to the bending of the carbody occurs stabilizes at about 13,5 Hz. The frequency response is also in these two cases higher in the middle of the anti-bending bars compared to that of the carbody, regardless of whether it is calculated in the middle or above the two bogies.

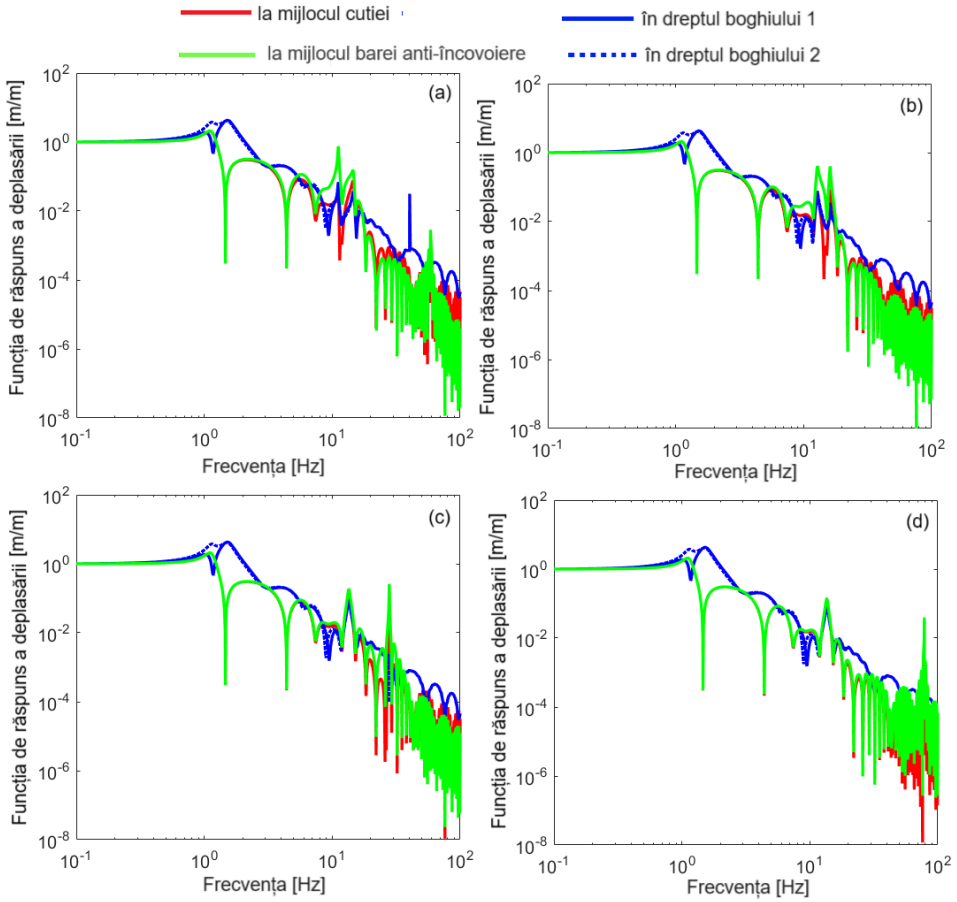

Fig. 7.4. Influence of damping on the frequency response functions of the displacement at the middle of the carbody and above the bogies and on the frequency response function of the displacement at the middle of the anti-bend bars: (a) k_z = 10 MN/m; (b) k_z = 100 MN/m; (c) k_z = 1 GN/m; (d) k_z = 10 GN/m.

As shown in Chapter 6, the reduction in the bending frequency of the carbody as a result of insufficient longitudinal stiffness of the fastening of the anti-bending bars to the supports can be compensated, even if only partially, by increasing the length of the anti-bending bars. Figure 7.5 shows the frequency response of the mid-carbody displacement considering five values of the length of the anti-bending bars that were considered in the previous chapter. In all the cases presented, there is an increase in the frequency of the bending mode of the carbody when the length of the anti-bending bars is longer. On the other hand, there is a decrease in the frequency of the bounce mode of the anti-bending bars because they have higher mass. This aspect cannot be seen in diagram (d) because in this case the frequency of the bounce of the anti-bending bars is higher than the 30 Hz limit of the frequency representation.

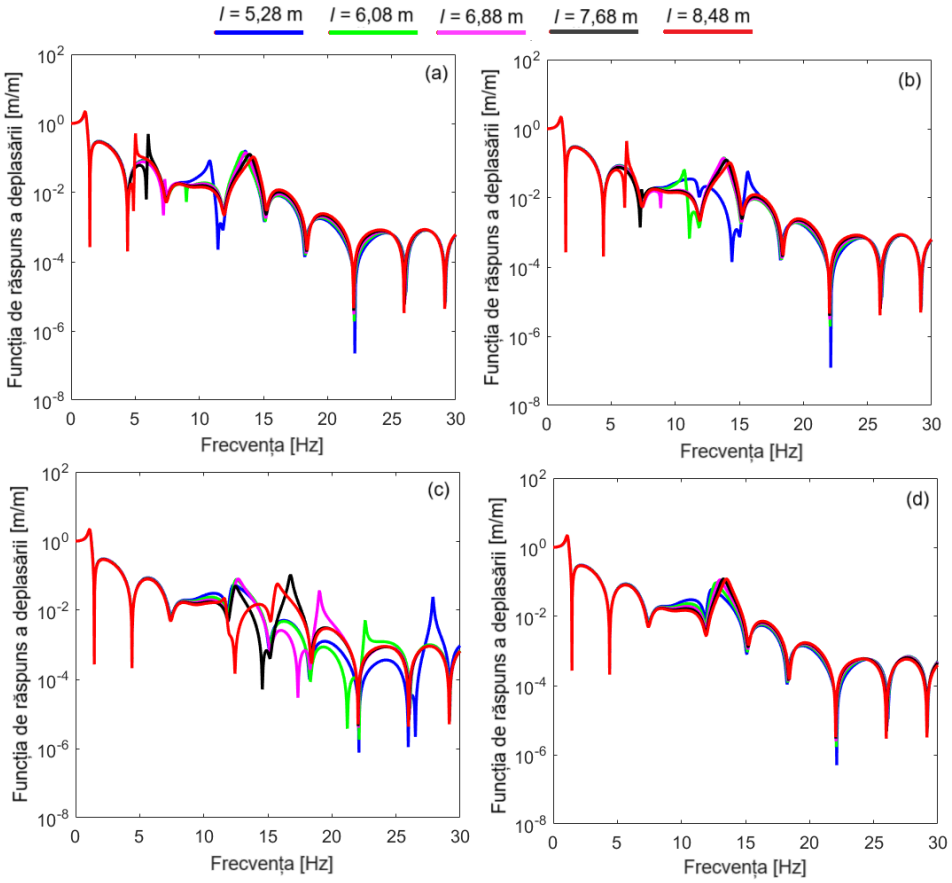

Fig. 7.5. Influence of the length of the anti-bending bars on the frequency response function of displacement at the middle of the carbody (V = 200 km/h): (a) k_z = 10 MN/m; (b) k_z = 100 MN/m; (c) k_z = 1 GN/m; (d) k_z = 10 GN/m.

7.6. Study on the effect of anti-bending bars on vertical vibrations of the railway vehicle carbody

In this section, the effect of anti-bending bars on carbody vibrations and ride comfort when the vehicle runs along a track with random irregularities is evaluated.

Figure 7.6 shows the effect of anti-bending bars (non-inertia bar model) on the root mean square of the carbody acceleration and on the ride comfort index at the relevant points of the carbody in the speed range 0 – 250 km/h. As for the root mean square of the carbody acceleration above the two bogies, the anti-bending bars have a marginal effect. In the middle of the carbody, however, the vibration behaviour improves significantly thanks to the equipment of the carbody with anti-bending bars, especially at speeds above 150 km/h. The largest reductions in vibration behaviour are recorded at 176 km/h, where the root mean square of acceleration decreases to 78%, and at 250 km/h where the same parameter reaches 69% of the value calculated for the carbody without anti-bending bars. The ride comfort index decreases to a certain extent above the bogies due to the presence of anti-bending bars, a more pronounced reduction being observed after 200 km/h especially in above the bogie 2. Comfort improves radically in the middle of the carbody almost over the entire speed range investigated.

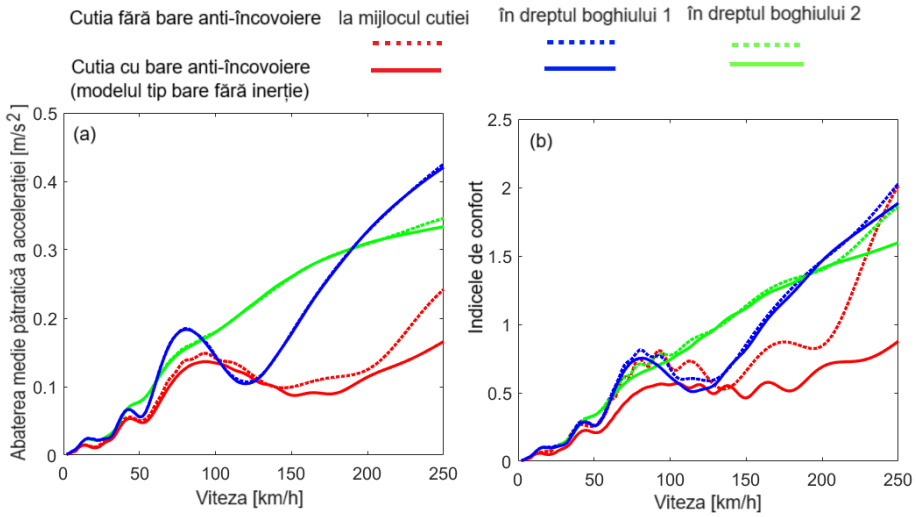

Fig. 7.6. Effect of anti-bending bars (non-inertia bar model):
(a) root mean square of the carbody acceleration; (b) ride comfort index.

There is, however, a narrow speed range around 136 km/h, where the ride comfort index is less influenced by the anti-bending bars. The ride comfort index has been significantly reduced to 178 km/h and 250 km/h, speeds at which it reaches 59% and 44%, respectively, of the value obtained in the absence of anti-bending bars.

Considering that the effect of the anti-bending bars is practically manifested only in the middle of the carbody, the area of analysis is further narrowed, and the investigation focuses on the influence of the anti-bending bars on the vibration regime and the ride comfort index in the middle of the carbody using the inertia bar model.

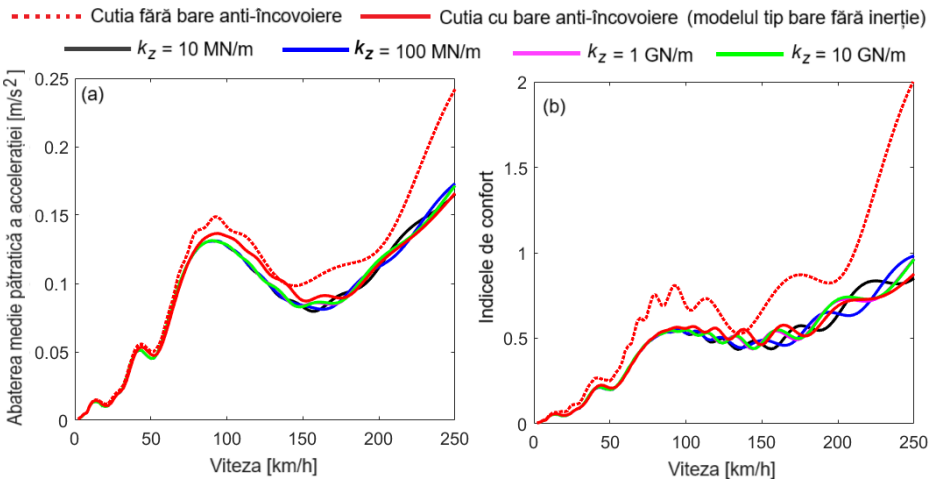

Fig. 7.7. Effect of anti-bending bars in correlation with the vertical stiffness of the fastening of the anti-bending bars to the supports (inertia bar model).

Figure 7.7 shows the influence of the anti-bending bars on the root mean square of the acceleration and on the ride comfort index for four values of the vertical stiffness of the fastening between the anti-bending bars and the supports. The graph of the root mean square of the acceleration and the corresponding graph of the ride comfort index for the carbody without anti-bending bars and for the carbody with anti-bending bars using the non-inertia bar model are also shown.

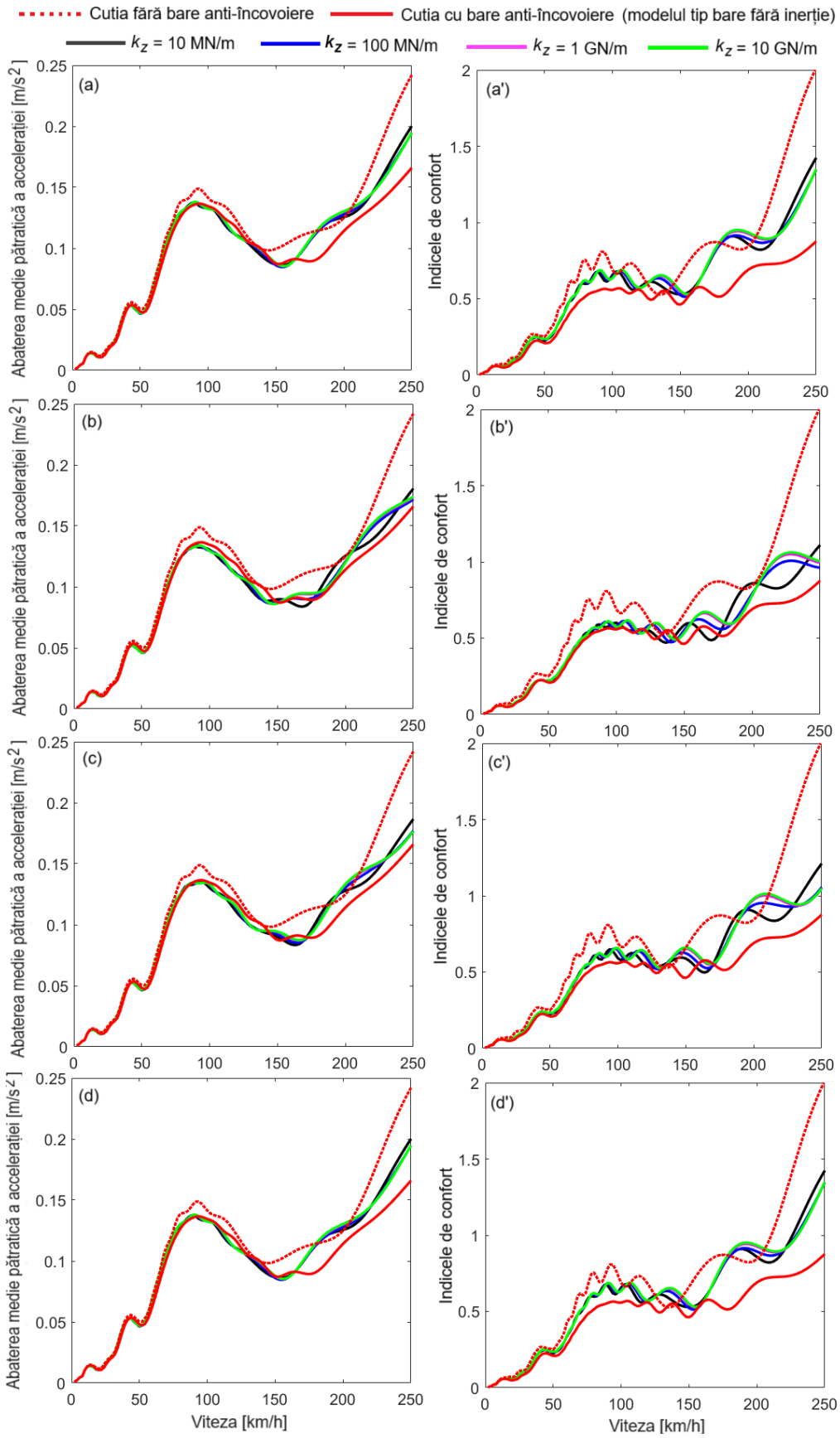

Fig. 7.8. Influence of the longitudinal stiffness of the fastening of anti-bending bars to the supports: (a), (b), (c), (d) the root mean square of the acceleration; (a'), (b'), (c'), (d') ride comfort index; (a), (a') K = 5; (b), (b') K = 2; (c), (c') K = 1; (d), (d') K = 0,5.

The introduction of vertical stiffness of the fastening of the anti-bending bars to the supports influences the results from speed of 80 km/h. In the range between 80 km/h and approx. 175 km/h, the root mean square of the acceleration is lower due to the vertical elasticity of the fastening of the anti-bending bars to the supports. At higher speeds, the root mean square of acceleration calculated with the inertial bar model that takes into account the vertical stiffness of the fastening varies around that obtained with the non-inertial bar model. Similar results are obtained in terms of the ride comfort index.

It is noted that the results presented in figure 7.7 show that the considered values of vertical stiffness do not practically affect the functionality of the anti-bending bars given that in the longitudinal direction the fastening is perfectly rigid.

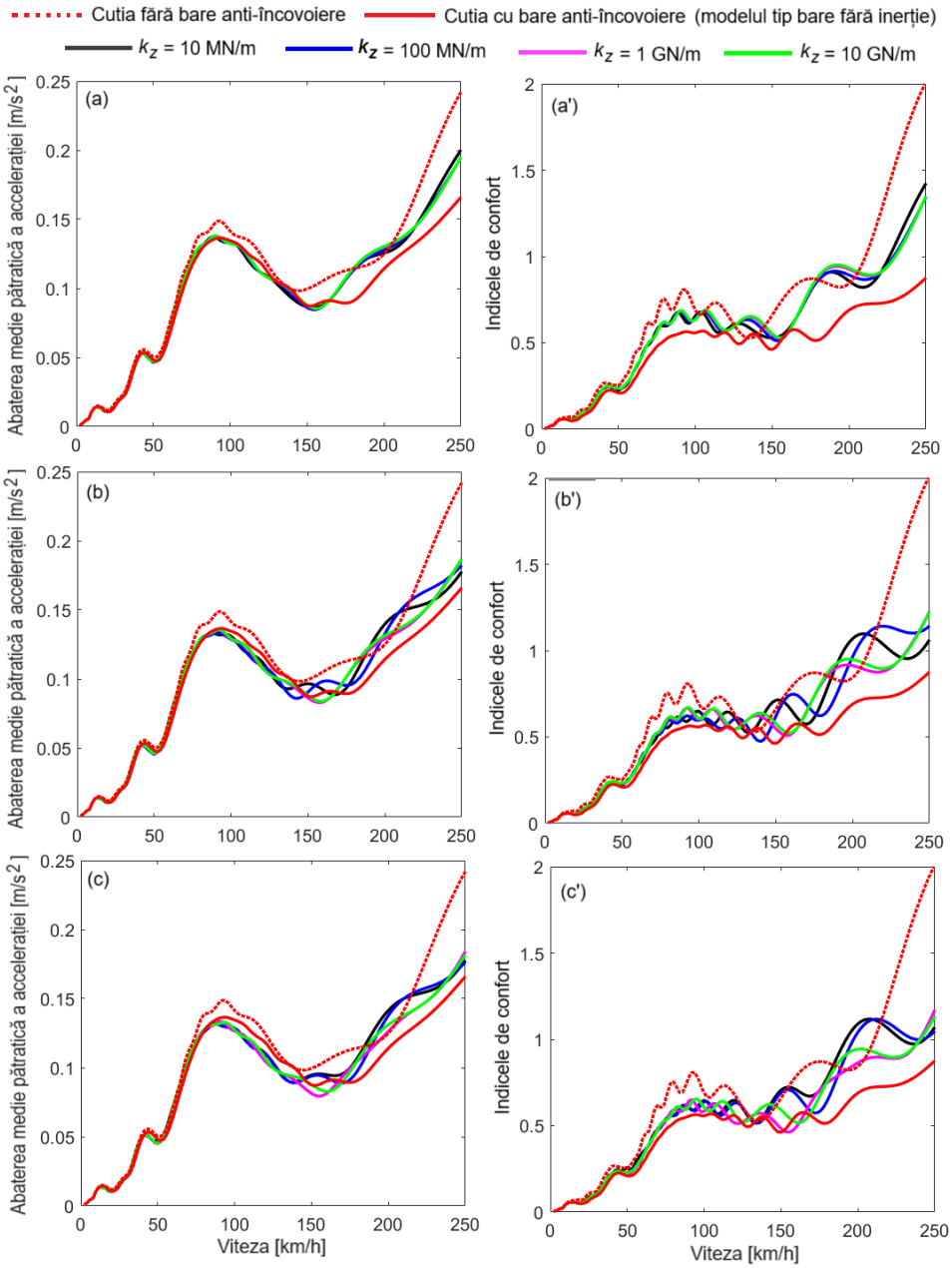

Fig. 7.9. Influence of the length of the anti-bending bars:
(a), (b), (c) the root mean square of the acceleration; (a'), (b'), (c') ride comfort index;
(a), (a') l = 5,28; (b), (b') l = 6,88; (c), (c') l = 8,48.

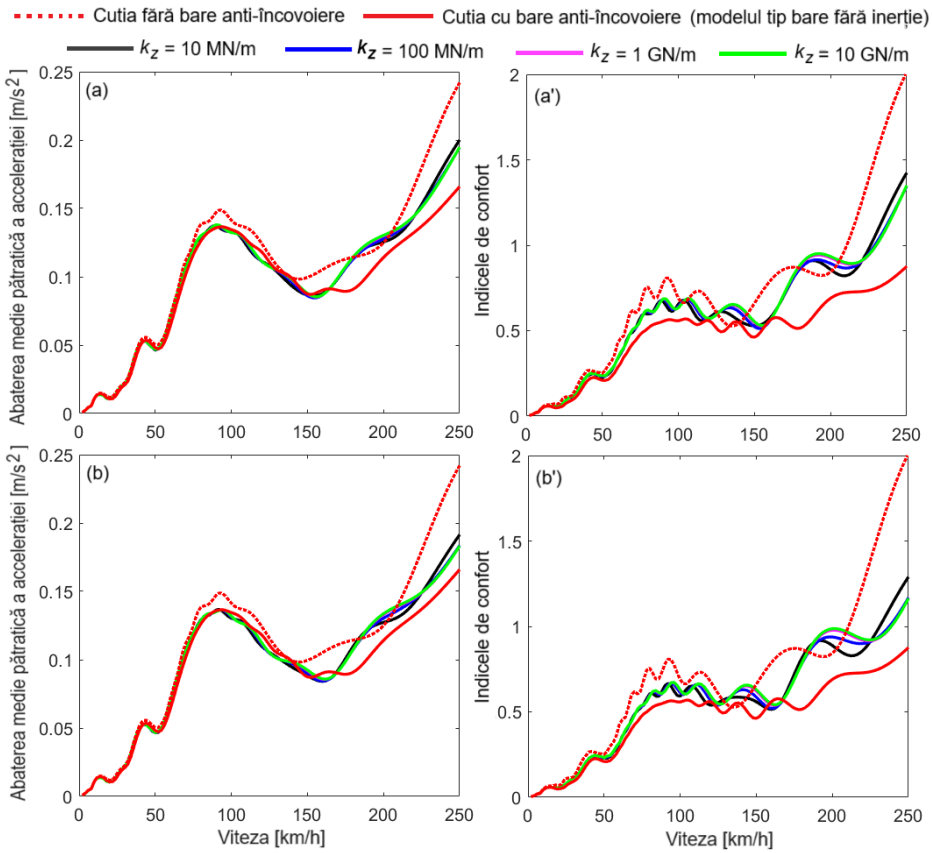

Fig. 7.10. The influence of the distance between the anti-bending bars and the neutral axis of the carbody: (a), (b) root mean square of the acceleration;
(a'), (b') ride comfort index (a), (a') h = 1,2 m; (b), (b') h = 1,4 m.

Figure 7.8 shows the root mean square of the acceleration in the middle of the carbody and the ride comfort index for the four values of the longitudinal stiffness of the fastening of the anti-bending bars to the supports. Examining the two sets of diagrams it follows that as the longitudinal stiffness of the fastening of the anti-bending bars to the support's decreases, both the mean square of the acceleration and the ride comfort index increase, which affects the effectiveness of the anti-bending bars. In addition, the differences between the root mean square of the acceleration and the ride comfort index curves are reduced for different values of the vertical stiffness of the fastening of the anti-bending bars to the supports when the longitudinal stiffness of the fastening is lower. It follows that the reduction in the effectiveness of the anti-bending bars in the case of their more elastic fastening to the supports cannot be counteracted by increasing the vertical rigidity k_z.

In figure 7.9, longitudinal stiffness has the lowest value considered in this parametric study. The length of the anti-bending bars is 5,28 m in diagrams (a) and (a'), 6,88 m in diagrams (b) and (b') and 8,48 m in diagrams (c) and (c') respectively, to evaluate the effect of increasing the length of the anti-bending bars on their ability to reduce the vibration behaviour of the carbody and improve ride comfort. By using longer anti-bending bars, performance improvements are achieved in the medium and high-speed range. The best results are obtained if the vertical stiffness of the fastening of the anti-bending bars to the supports is higher (k_z = 1 GN/m or 10 GN/m) according to diagrams (c) and (c').

Similar effects can be achieved by increasing the distance between the anti-bending bars and the neutral axis of the carbody, as can be seen in figure 7.10. The numerical simulations were also carried out considering the lowest value of the longitudinal stiffness of the fastening of the anti-bending bars to the supports. The length of the anti-bending bars takes the reference value 5.28 m, while the distance between the anti-bending bars and the neutral axis of the carbody is 1.2 m in diagrams (a) and (a') and 1.4 m in diagrams (b) and (b').

8. Experimental determinations

8.1. Introduction

In the previous chapters, the problem of vibrations of the railway vehicle carbody was approached from a theoretical point of view, and numerical simulation software applications were used as an investigation tool. Thus, in the studies developed based on the results of numerical simulations, on the one hand, basic characteristics of the vertical vibration behaviour of the railway vehicle carbody were highlighted, and on the other hand, important effects of the anti-bending bars on the bending vibrations of the railway vehicle carbody. However, observations being limited only to analytical studies, they can be considered speculative, and to be able to be synthesized in the form of conclusions, it is absolutely necessary that they first be corroborated with experimental results.

In this chapter, the experimental determinations carried out both in real physical conditions and in laboratory conditions are described, to verify the theoretical results.

The first part of the chapter is dedicated to the experimental determinations from on a series 21-76 passenger vehicle during the current line circulation on the route Bucharest North - Constanța and return. Two distinct sections are included here, one section describing the vehicle characteristics, measurement conditions, equipment and software used, and another section presenting and analysing results recorded over 20-second time sequences of vertical accelerations measured at the middle of the vehicle carbody. Based on the spectral analysis and the root mean square values of the measured acceleration, the most important characteristics of the vertical vibrations of the vehicle carbody are highlighted, which were also emphasized following the analysis of the results obtained through numerical simulations in Chapters 3, 4 and 5 of the thesis.

The experimental determinations described in the second part of the chapter were carried out to verify the results obtained through numerical simulations regarding the effect of anti-bending bars on the vertical vibrations of the railway vehicle carbody, presented in Chapter 6 of the thesis. These determinations were organized under laboratory conditions, in the Railway Rolling Stock Department of the Faculty of Transport of the National University of Science and Technology Politehnica Bucharest, on a scale model of the carbody with/without anti-bending bars. The scale model of the vehicle carbody is the main element of a demonstrative experimental system, designed and realized within the framework of the research project 724PED/2022 entitled *Method of*

reducing vertical vibrations of the railway vehicle carbody based on an anti-bending system (project code PN- III-P2-2.1-PED-2021-0319), implemented in the period 2022 – 2024, in which, as I have shown, I participated as a PhD student as a member of the research team [74].

The second part of the chapter is structured in three sections. In the first section, the demonstrative experimental system and the measurement and control chain components of this system are described in detail. The second section presents the structure of the software application for the control, acquisition, processing, representation and storage of the measured data, developed in the Matlab programming environment. The last section is reserved to the presentation and analysis of the vertical accelerations measured at the middle of the carbody experimental model with/without anti-bending bars and to summarize the conclusions regarding the agreement between the theoretical and experimental results.

8.2. Experimental determinations under real physical conditions

8.2.1. Characteristics of the passenger vehicle

The experimental determinations under real physical conditions were carried out in a second-class passenger vehicle of the 21-76 series. The vehicles of the 21-76 series are salon vehicles, with 84 seats, intended for medium and long-distance traffic, being used on Regio (R), InterRegio (IR) and InterCity (IC) trains. Figure 8.1 shows the passenger vehicle series 21-76 in train IR1682 (Constanța - Bucharest North). The passenger vehicles of the 21-76 series were built for a maximum speed of 160 km/h and equipped with Y32 R bogies, with monobloc wheels, without electromagnetic shoe brakes.

Fig. 8.1. Passenger vehicle series 21-76 in the composition of train IR 1682.

8.2.2. Description of experimental determinations

The experimental determinations were carried out during the circulation in the current line, on the route Bucharest Nord - Constanța and return (see figure 8.2). On this railway line, passenger trains can run at a maximum speed of 160 km/h.

Fig. 8.2. The railway route Bucharest North - Constanța.

To carry out the experimental determinations, a chain was used to measure the acceleration of the carbody of the passenger vehicle, which brings together specialized equipment and devices produced by Brüel & Kjær (B&K) and National Instruments (NI), and a GPS (Global Positioning System) receiver. for monitoring the speed of the train. The carbody acceleration measurement chain includes the B&K type 4514 accelerometer and the data acquisition system consisting of the assembly NI cDAQ-9171 chassis - NI 9233 module. The data acquisition system is connected to a laptop and is commanded and controlled with a software application for control, acquisition, processing, storage and representation of measured data. The TOPGNSS brand GPS receiver, model GN-803G, was used to monitor and record the speed of the train.

Next, in figures 8.3 – 8.5, images taken during the experimental determinations are presented. In figure 8.3 you can see the B&K accelerometer type 4514 which is fixed by a pin in a nut glued with glue on a metal support. The image in figure 8.4 shows all the components of the carbody acceleration measurement chain described above, namely the B&K accelerometer type 4514 and the assembly NI cDAQ-9171 chassis - NI 9233 module.

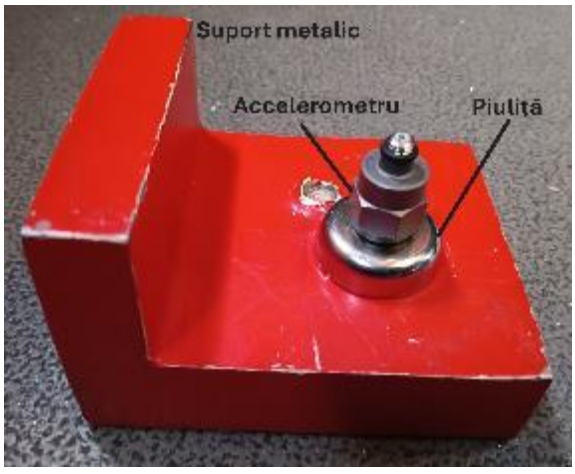

Fig. 8.3. Accelerometer fixation.

Fig. 8.4. Acceleration measuring chain.

8.2.3. Analysis of experimental results

Figures 8.5 - 8.6 show the values of the root mean square of the acceleration for all measurement sequences corresponding to the speeds at which measurements were made for the Constanța - Bucharest North route. Analysing the diagrams, a first observation is highlighted: at the same speed, the root mean square of the acceleration takes values in a relatively wide range. The dispersion of the values of the root mean square of the acceleration can be explained by the variability of the amplitude of the track irregularities along it. A second observation is related to the influence of the traffic speed on the values of the root mean square of the acceleration. Even in the conditions where the acceleration values are dispersed, the general tendency to amplify the vibrations of the carbody when the speed increases are observed.

Based on the diagrams in figure 8.7, the frequency response of the carbody is analyzed for six different values of speed, between 30 km/h and 140 km/h. Although the spectra of the measured accelerations show several peaks, those corresponding to the eigenfrequency of the carbody bounce at 1.75 Hz and the eigenfrequency of the vertical bending of the carbody at 8.45 Hz stand out clearly.

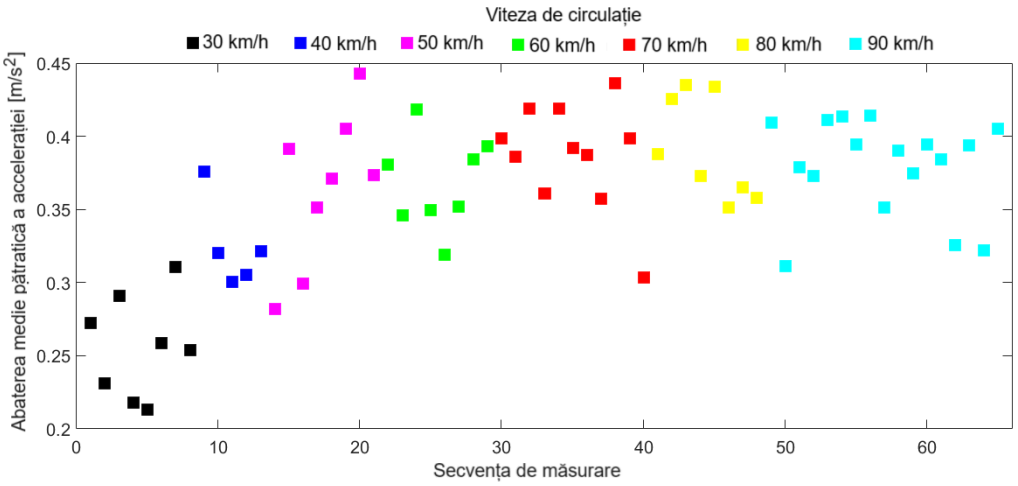

Fig. 8.5. The root mean square of the acceleration recorded on the Constanța - Bucharest North route for speeds between 30 km/h and 90 km/h.

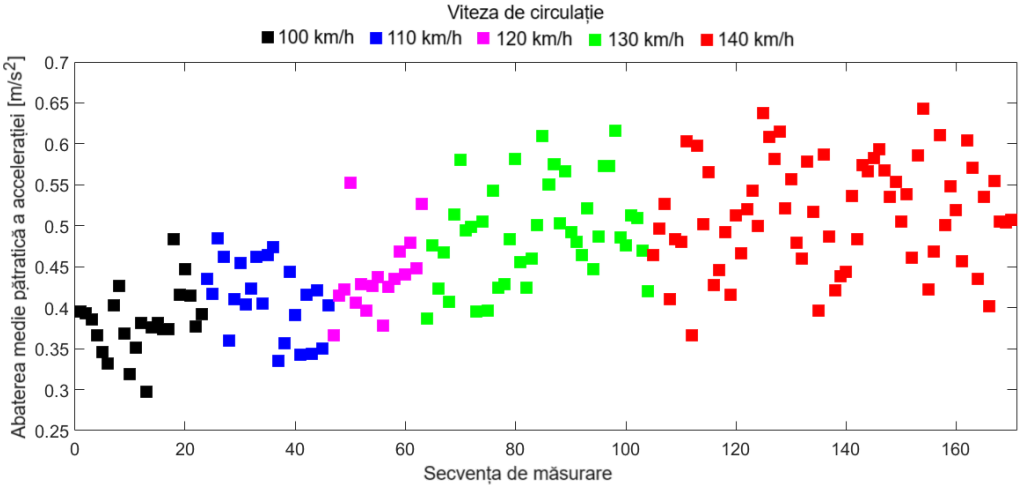

Fig. 8.6. The root mean square deviation of the acceleration recorded on the Constanța - Bucharest North route for speeds between 100 km/h and 140 km/h.

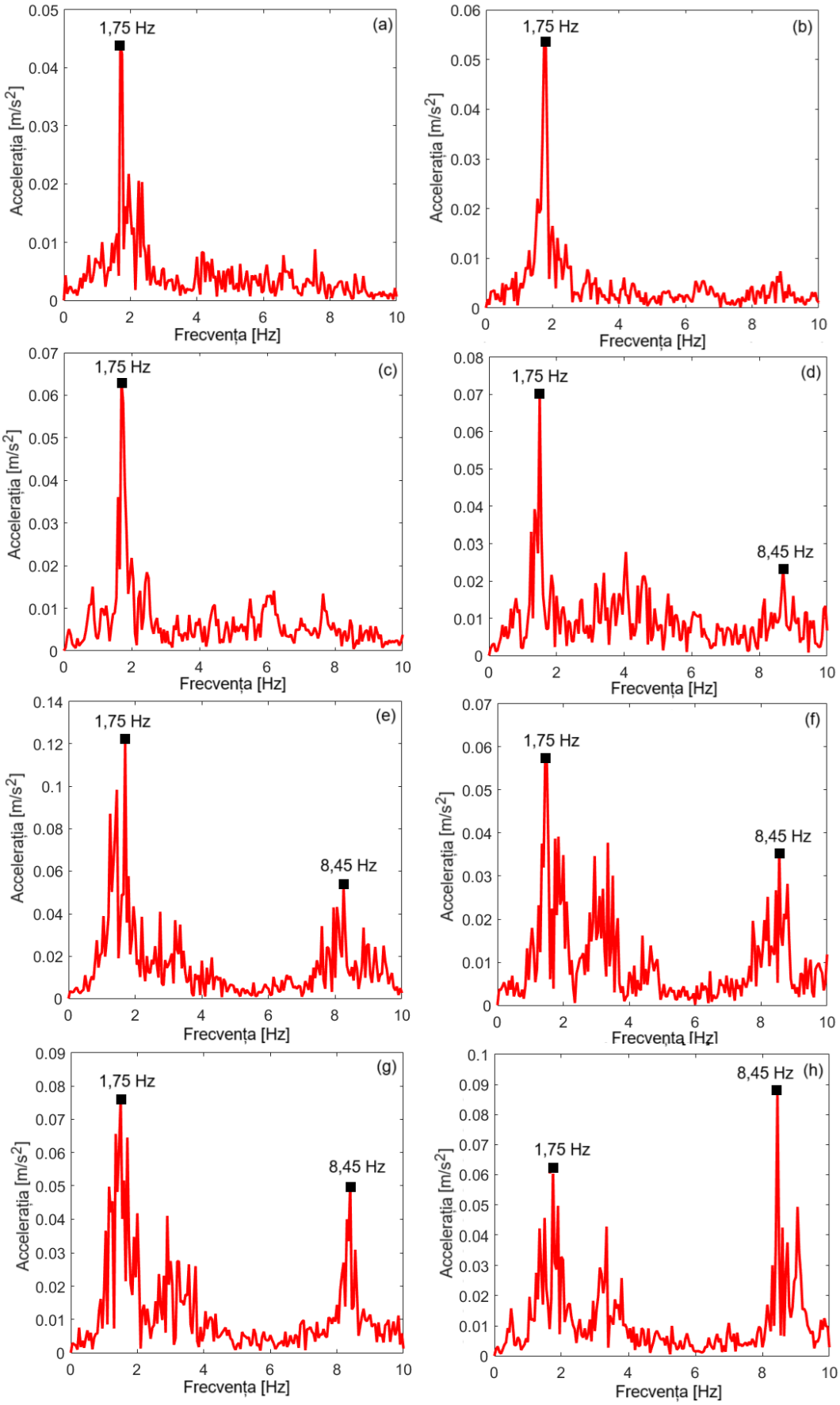

Fig. 8.7. Spectra of the acceleration measured at the speeds: (a) 30 km/h; (b) 40 km/h; (c) 50 km/h; (d) 60 km/h; (e) 100 km/h; (f) 110 km/h; (g) 120 km/h; (h) 140 km/h.

It should be recalled here that in Chapters 3 – 5, for the reference values of the numerical model of the vehicle, the following eigenfrequencies of the vibration modes of the carbody manifesting in the middle of the carbody were identified: 1.17 Hz – eigenfrequency of hopping vibrations; 8 Hz - eigenfrequency of vertical bending vibrations. As with the numerical simulation results in Chapter 3 and Chapter 5, similar observations regarding the dominant vibration modes at the middle of the carbody. In general, bounce is the vibration mode that dominates the acceleration spectrum. As the speed increases, the bending vibrations have an important weight, which can be seen in diagrams (d) – (g), where the peak corresponding to the frequency of 8.45 Hz is well highlighted. At high speeds, as is the case in diagram (h) where the acceleration spectrum for 140 km/h is plotted, bending becomes the dominant vibration mode in the middle of the carbody.

8.3. Experimental determinations under laboratory conditions

8.3.1. Description of the demonstrative experimental system

Experimental determinations carried out to verify the results obtained through numerical simulations regarding the effect of anti-bending bars on the vertical vibrations of the railway vehicle carbody (see Chapter 7) were organized in the laboratory, on a 1:10 scale experimental model of the carbody without anti-bending bars and with anti-bending bars. The scale model of the vehicle carbody is the main element of a demonstrative experimental system, designed and realized within the framework of the research project 724PED/2022 entitled *Method of reducing vertical vibrations of the railway vehicle body based on an anti-bending system* (project code PN-III-P2-2.1-PED-2021-0319), implemented in the period 2022 – 2024 [74]. The project was coordinated as director by the PhD supervisor, professor M. Dumitriu, and I participated as a member of the research team, as a doctoral student.

The experimental model of the carbody, which is reduced to a beam made of aluminum, is supported by means of elastic rubber elements on two metal supports. Anti-bending bars are attached to either side of the scale model of the carbody. Figures 8.8 and 8.9 show the experimental model of the carbody without/with anti-bending bars. Figure 8.10 and figure 8.11 show in detail the anti-bending bar and its attachment system to the experimental carbody model. Figure 8.12 details the elastic rubber elements on which the experimental carbody model rests.

The measurement and control chain of the demonstrative experimental system integrates several specialized components dedicated to the generation of vibrator control signals and the acquisition and processing of experimental data (experimental carbody model acceleration and excitation force).

The vibrations of the experimental carbody model are excited with the Brüel & Kjær type LDS V201 vibrator (figure 8.13) working with the LDS PA25E amplifier (figure 8.14), and the excitation force is measured with the Laumas SA15 force cell (figure 8.15) placed between the vibrator and the experimental model of the carbody. The vibrator - amplifier - force cell assembly is presented in figure 8.16.

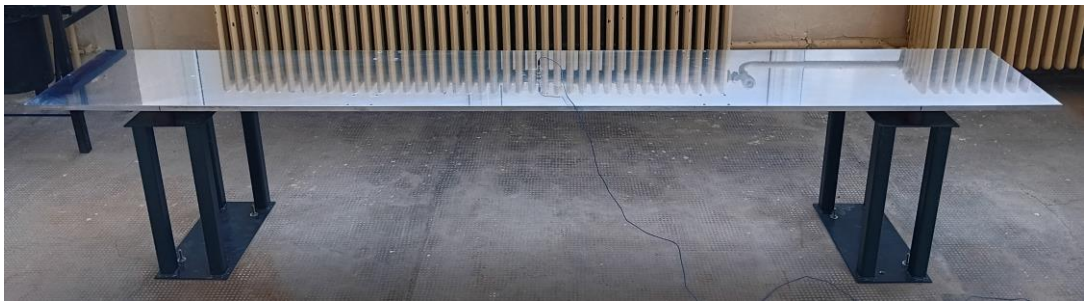

Fig. 8.8. The experimental model of the carbody without anti-bending bars [36].

Fig. 8.9. The experimental model of the carbody with anti-bending bars [36].

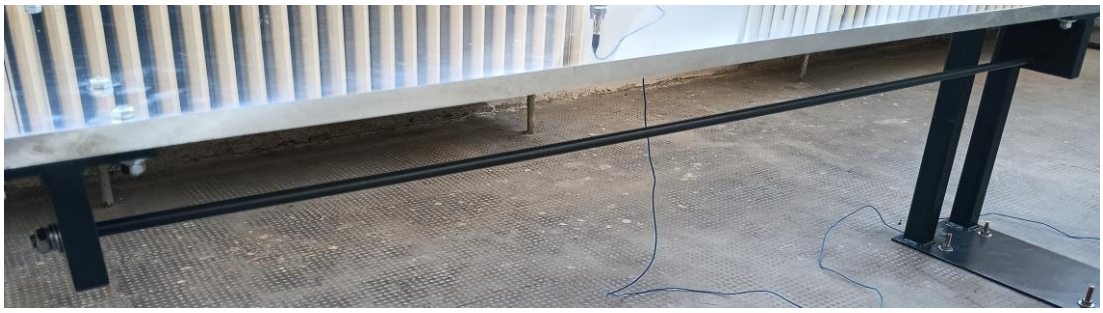

Fig. 8.10. Anti-bending bar [36].

Fig. 8.11. Anti-bending bar clamping system [36].

Fig. 8.12. Elastic rubber elements [36].

To apply the excitation force to one end of the experimental carbody model, the vibrator-force cell assembly is placed on a special support (figure 8.17). The acceleration measurement of the experimental model of the carbody is done with a Brüel & Kjær type 4514 accelerometer mounted in the middle of it (figure 8.18).

In the demonstrative experimental system, several specialized components are integrated, dedicated to the acquisition and processing of experimental data (acceleration of the experimental carbody model and the excitation force) or the generation of the control signals of the vibrator.

Fig. 8.13. Vibrator LDS V201.

Fig. 8.14. Amplifier LDS PA25E.

Fig. 8.15.Force cell Laumas SA15.

Fig. 8.16. The vibrator – amplifier – force cell assembly.

Fig. 8.17. Location of the vibrator – force cell assembly.

Detail – location of the vibrator – force cell assembly.

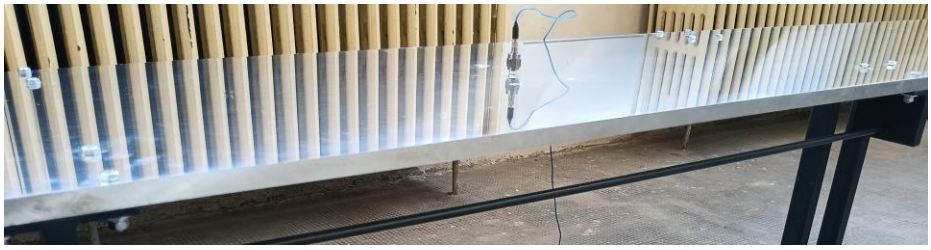

Fig. 8.18. Mounting the accelerometer on the experimental model of the carbody.

Fig. 8.19.Chassis NI cDAQ-9174.

NI 9234 module.

NI 9263 module.

NI 9219 module.

Fig. 8.20. Serial modules.

It is the assembly consisting of the NI cDAQ-9174 type chassis (figure 8.19) and three modules with specialized functions (figure 8.20): the NI 9234 module for receiving and synthesizing the data flow from the three accelerometers, the specialized NI 9263 module for generating signals control of the vibrator and the NI 9219 module intended for voltage or current measurements with applications in electrical resistive tensometry.

8.3.2. Analysis of experimental results

The verification of the results obtained through numerical simulations regarding the effect of anti-bending bars on the vertical vibrations of the railway vehicle carbody, presented in Chapter 7 of the thesis, involves measuring the acceleration of the experimental model of the carbody, in a first phase, without anti-bending bars and, subsequently, with anti-bending bars. To ensure the statistical representativeness of the measurement results, six recordings of the experimental data (vertical accelerations and excitation forces) were made for each value of the frequency of the harmonic excitation force considered in the field of interest, respectively the field between 5 Hz and 20 Hz.

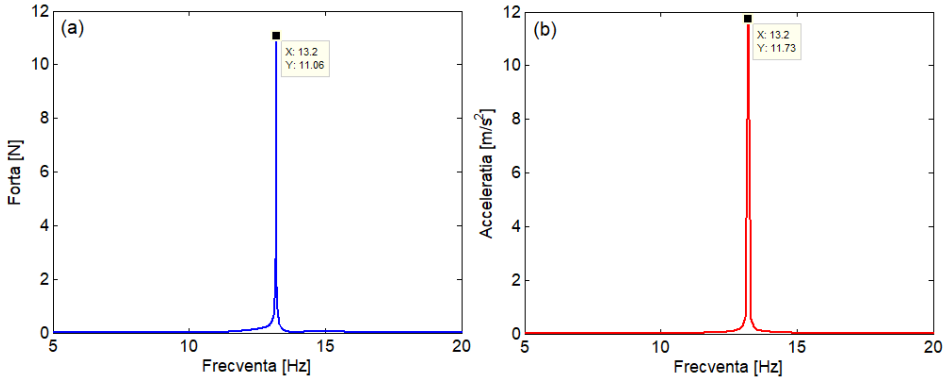

Fig. 8.21. Amplitude spectrum: (a) of acceleration measured at middle the experimental model of the carbody; (b) of the excitation force.

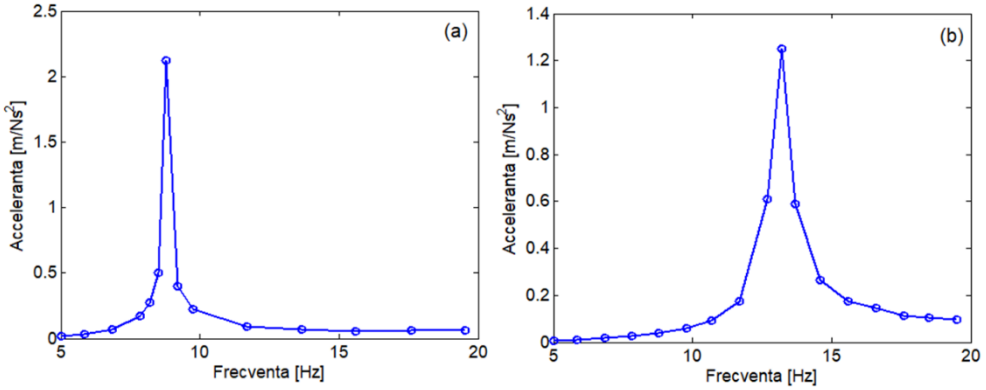

Fig. 8.22. Accelerance in the middle of the experimental carbody model: (a) without anti-bending bars; (b) with anti-bending bars.

The frequency spectrum of the vertical acceleration measured at the middle of the experimental model of the carbody with anti-bending bars at the frequency of 13.2 Hz and the frequency spectrum of the corresponding excitation force are shown in the diagrams in figure 8.21. The analysis of the diagrams indicates that the two spectra are dominated by the peaks appearing at the excitation frequency, the other spectral components having an

insignificant weight. For each recording, accelerance was calculated as the ratio of the maximum amplitude of the acceleration to the maximum amplitude of the excitation force determined from the frequency spectrum. Finally, the accelerance corresponding to a certain frequency of the excitation force was calculated as the average of the accelarances obtained from all the recordings made at that frequency.

Diagrams (a) and (b) in figure 8.22 show the frequency response functions determined based on the accelerations measured at the middle of the experimental carbody model without anti-bending bars and with anti-bending bars, respectively. To simplify the processing of experimental data, the frequency response function is presented in the form of accelerance. In both cases, the vibration regime of the experimental carbody model is dominated by the first vertical bending mode. For the experimental carbody model without anti-bending bars the eigenfrequency of the first vertical bending mode is at 8.8 Hz and the measured resonance peak is 2.119 m/Ns^2. After fitting the anti-bending bars, the eigenfrequency of the first vertical bending mode increases to 13.2 Hz, i.e. by 50%. Regarding the amplitude of the vibration, the acceleration has a value of 1.25 m/Ns^2. Based on the accelerance values, the vertical bending vibration reduction rate is calculated, which is 41%.

9. Conclusions, original contributions and future research directions

9.1. Conclusions

For elaboration of the doctoral thesis I consulted a rich bibliographic material, including 131 scientific works (articles, monographs, doctoral theses) and 11 technical works (technical documentation, railway standards and regulations) covering the thematic area of the thesis. The analysis of the bibliographic material contained in Chapter 1 and Chapter 2 of the paper led to the following important conclusions from the perspective of the topic addressed:

- The weight reduction criterion represents a general valid criterion in the design of railway vehicles so that they travel at the highest possible speeds and the energy consumption is as low as possible. By reducing the weight of railway vehicles other benefits are obtained, such as reducing vibrations transmitted through the ground, reducing manufacturing costs or maximizing the use of axle loads.
- To apply the weight criterion, one of the following solutions can be chosen during the design stage of railway vehicles: the use of light materials or the modification of the mechanical structures of the vehicle.
- The use of light materials resulted in a significant decrease in the structural rigidity of the carbody. Favorable conditions were thus created for the excitation of structural vibrations in the long carbodies of passenger vehicles.
- The vibration behaviour of the carbody is strongly influenced by structural vibrations, with important effects on passenger comfort. Also, structural vibrations stress the carbody to fatigue, which leads to a reduction in its service life.

- The structural vibrations of the railway vehicle carbody are particularly complex, with local and global modes, which can have different modal shapes and eigenfrequencies. From the point of view of passenger comfort, the structural modes of vibration are important, whose frequencies are in the low frequency range, in which the human body shows a high sensitivity to vibrations. The first mode of vertical bending of the carbody is of particular importance, having its own frequency in the range of 7 ... 12 Hz, a range in which the human body is more sensitive to vertical vibrations.
- To reduce the structural vibrations of long and light carbodies of passenger vehicles, the weight criterion must be correlated with the stiffness criterion. The "key" to designing the carbody structure is to achieve greater stiffness for less weight.
- The simplest solutions for reducing the carbody structural vibrations involve reducing the length of the carbody, increasing the cross-section or increasing the rigidity of the carbody. These solutions are not efficient, being in contradiction with other requirements imposed in the design of long and light carbodies of passenger vehicles.
- The methods proposed in the specialized literature for the reduction of flexible vibration modes relevant from the point of view of ride comfort can be grouped, depending on the approach, into methods for "vibration isolation" or methods for "vibration damping". The methods that fall into the first category - methods for "vibration isolation" - aim to isolate the carbody from the vibrations transmitted from the wheelsets and bogies through the vehicle's suspension. In the second category - methods for "vibration damping", methods that lead to an increase in the structural damping of the carbody can be included. Regardless of the category they fall into, these methods can be developed based on passive, semi-active or active concepts.
- The problem of vibrations of flexible carbodies, particularly important from the point of view of the impact it has on the dynamic performance of railway vehicles, has opened up a vast area of research, which has developed over time, as research directions have diversified, and investigative methods and tools have become increasingly complex and sophisticated.
- With the introduction of the concept of the anti-bending bar system, which was the basis for the development of a new method of reducing the vertical bending vibrations of the carbody of high-speed railway vehicles, a new direction of research that has not been sufficiently explored until now has opened. Research in this direction can be developed to answer the questions regarding the influence of the self-vibration modes of the anti-bending bars and the elastic elements of fastening to the carbody chassis struts on the carbody vibrations and ride comfort.

In Chapter 3 of the thesis, the results of a study were presented in which the influence of the first vertical bending mode on the vibration behaviour of the railway vehicle carbody is analyzed, in correlation with the bending stiffness of the carbody, speed and suspension damping. Based on these results, conclusions regarding:

- The characteristics of vertical vibrations in the relevant points of the carbody.
- Geometric filtering effect.
- The dominant vibration modes of the carbody.
- The influence of bending vibrations on the carbody vertical vibration behaviour.
- The influence of the speed on the vertical vibration behaviour of the carbody.
- The influence of the vertical bending of the carbody in correlation with the damping of the secondary/primary suspension on the vertical vibration behaviour of the carbody.

In Chapter 4, the influence of the secondary suspension model on the vertical vibration behaviour of the carbody is investigated based on the results of numerical simulations. The conclusions that can be summarized based on the studies included in Chapter 4 are:

- The influence of the secondary suspension model manifests itself especially on the vertical bending vibrations of the carbody.
- The carbody pitch vibrations are influenced only by the longitudinal system of transmission of longitudinal forces between the carbody and the bogie, included in the models C and D of the secondary suspension, and are manifested by increasing the eigenfrequency of the pitch vibration, without significant changes in the vibration level.
- The vibration level of the carbody increases significantly at the eigenfrequency of the pitch vibrations of the bogie, in the case of models C and D of the suspension. It is concluded that the longitudinal system in the secondary suspension has an important contribution in transmitting the pitch vibrations of the bogies to the carbody, while the rotational system contributes to a lesser extent.
- The longitudinal system, introduced in model C and model D, significantly changes the vertical vibration level, especially at the carbody middle.

Chapter 5 is dedicated to a study on the influence of the track model - on the vertical vibration behaviour of the railway vehicle carbody evaluated on the basis of the results obtained through numerical simulations. The conclusions drawn from the study carried out in Chapter 5 can be grouped according to the problems treated as follows:

- The influence of the track model on the vibration behaviour of the carbody. The track model has little influence on the vibration behaviour of the carbody in its middle, but has an important weight above the bogies at frequencies higher than 20 Hz.
- The influence of track damping on the vibration behaviour of the carbody is manifested above the bogies, at the eigenfrequency of the vertical vibrations of the wheelset on the track.
- Influence of the track model on the dominant vibration modes of the carbody. The track model does not influence the dominant modes of the carbody.
- The influence of the track model on the vibration level of the carbody. At the eigenfrequencies of the bounce and pitch vibrations of the carbody, the track model does not influence the results regarding the vibration level of the carbody

Chapter 6 represents a first stage in the development of research on the possibilities of reducing the vertical bending vibrations of the carbody of railway vehicles by using anti-bending bars. The main conclusions summarized based on the presented results are:

- Carbody eigenfrequencies are not significantly influenced by the anti-bending bar system or anti-bending bar clamping stiffness.
- Eigenfrequencies of anti-bending bars increase continuously as the clamping of the bars to the supports is more rigid.
- The inertia of the anti-bending bar system is much lower than that of the carbody, which explains the features highlighted above.
- If the clamping stiffness of the anti-bending bar system is high enough, interference between the bending modes of the carbody and the anti-bending bars is avoided. Under these conditions it follows that it is no longer necessary to limit the length of the anti-bending bars to ensure that their eigenfrequency is sufficiently far from the bending frequency of the carbody.

- Insufficiently increasing the rigidity of the attachment of the anti-bending bar system to the supports can cause interference between the vibrations of the carbody and the vibration corresponding to the bounce mode of the anti-bending bars. This results in the need to stiffen the connection between the anti-bending bars and the supports.
- The vibration of the anti-bending bars is amplified if the stiffness of the connection between the anti-bending bars is not high enough.
- Longitudinal elasticity of anti-bending bars attachment to supports reduces the carbody bending frequency and may even compromise the functionality of the carbody vibration reduction method using the anti-bending bar system.
- Compensation for the unfavorable influence of the longitudinal elasticity of the attachment of the anti-bending bars to the supports can be done by adopting longer bars with a larger diameter, mounted at a greater distance from the neutral axis of the carbody.

In Chapter 7, the scientific steps carried out in Chapters 4, 5 and 6 initiated in order to build the theoretical model for the study of the vibrations of the integrated system of the carbody with anti-bending bars – bogies – track are exploited.

Based on the parametric study of the frequency response functions of the carbody, the following conclusions were drawn: (a) The vibration behaviour of the carbody is not significantly influenced by the vertical stiffness of the anti-bending bars; (b) The resonance peaks move along the frequency axis as the grip of the anti-bending bars to the supports becomes more rigid in the vertical direction;

According to the analysis regarding the influence of the bending vibration of the anti-bending bars on the dynamic response of the vehicle carbody, the conclusions were synthesized: (a) The root mean square of the acceleration and the ride comfort index are not significantly influenced by the vertical stiffness of the grip of the anti-bending bars to the supports if the grip is perfectly rigid in the longitudinal direction. If the grip of the anti-bending bars to the supports becomes more elastic in the longitudinal direction, then both the vibration behaviour of the carbody and the ride comfort are affected. (b) An improvement in the carbody vibration behaviour and ride comfort can be achieved by increasing the length of the anti-bending bars or by increasing the distance between the anti-bending bars and the neutral axis of the carbody.

Chapter 8 describes the experimental determinations carried out both in real physical conditions and in laboratory conditions, to verify the theoretical results presented in the doctoral thesis. The results of the experimental determinations carried out in real physical conditions, on a passenger vehicle in regular line traffic, constituted the reference basis in the verification process of the results obtained through numerical simulations in Chapters 3, 4 and 5.

The conclusions synthesized following the spectral analysis and the root mean square of the acceleration measured at the middle of the carbody are in agreement with those highlighted in the analysis of the vertical vibration behaviour of the vehicle carbody:

- The values of the eigenfrequencies of the main vertical vibration modes of the carbody identified on the acceleration spectrum measured at the middle of the carbody are quantitatively comparable with those obtained theoretically.
- In general, at the middle of the carbody, bounce is the vibration mode that dominates the acceleration spectrum. As the speed increases, bending vibrations also have an important share. At high speeds, bending becomes the dominant vibration mode at the middle of the carbody.

Experimental determinations carried out under laboratory conditions on a scale model of the carbody without/with anti-bending bars were carried out to verify the results obtained through numerical simulations regarding the effect of anti-bending bars on the vertical vibrations of the railway vehicle carbody, presented in Chapter 6 of the thesis.

- The frequency of the first bending mode of the scale model of the carbody without anti-bending bars is at 8.8 Hz, which proves that the model was correctly dimensioned.
- The frequency of the first bending mode of the scale model of the carbody with anti-bending bars is at 13.2 Hz, thus demonstrating the ability of the anti-bending bars to increase the frequency by 50%.
- The vibration decrease rate at the frequency of the first bending mode of the scale model of the carbody is 41% due to the use of anti-bending bars, which represents the experimental verification of the functionality of the anti-bending bars.

9.2. Personal contributions

The original approaches to the problems studied in the doctoral thesis can be summarized in the form of relevant personal contributions from the perspective of the research topic addressed, as shown below.

1. Development of a study on the influence of bending vibrations on the vertical vibration behaviour of the vehicle carbody, with the following original contributions:
   - development of the mathematical model and processing of the corresponding equations of motion of two different mechanical models of the vehicle - the "rigid carbody" model and the "flexible carbody" model;
   - development of the numerical model for calculating the frequency response functions and the root mean square of the acceleration of the vehicle carbody;
   - development of software applications for simulating the vibration behaviour of the carbody for the "rigid carbody" model and for the "flexible carbody" model;
   - comparative analysis of the vibration behaviour of the carbody for the "rigid carbody" model and for the "flexible carbody" model;
   - analysis of the influence of bending vibrations, in correlation with the speed, the damping of the secondary suspension and the damping of the primary suspension, on the vibration behaviour of the carbody.
2. Development of a study on the influence of the suspension model in simulating the vertical vibration behaviour of the vehicle carbody, with the following contributions:
   - development of four rigid-flexible coupled vehicle models, corresponding to four different secondary suspension models – a reference model and three analysis models;
   - development of mathematical models for each of the four vehicle models and processing of the equations of motion;
   - development of numerical models for calculating the frequency response functions of the carbody, corresponding to the four vehicle models;
   - development of four software application packages for simulating the vibration behaviour of the carbody, corresponding to the four vehicle models;

- comparative analysis of the vibration behaviour of the carbody for the four vehicle models;
- identification of the secondary suspension model that ensures sufficiently precise results in the evaluation of the vibration behaviour of the carbody, without making the analysis of the results difficult by increasing the complexity of the model.

3. Development of a study on the influence of the track model in simulating the vertical vibration behaviour of the vehicle carbody, with the following contributions:

- development of a complex mechanical model of the vehicle - track system, the "elastic track" model, which includes the rigid-flexible coupled model of the vehicle and the equivalent model with concentrated parameters of the track, the connection between the two models, respectively between the wheels and the rails, being achieved by a linear Hertzian elastic element;
- development of the mathematical model and processing of the equations of motion;
- development of the numerical model for calculating the frequency response functions of the carbody, corresponding to the "elastic track" model;
- development of software applications for simulating the vibration behaviour of the carbody, corresponding to the "elastic track" model;
- comparative analysis of the vibration behaviour of the carbody for the "elastic track" model and for the "rigid track" model.

4. Development of research on the possibilities of reducing vertical bending vibrations of the carbody by using an anti-bending bar system.

- development of the model of the carbody - anti-bending bars system, which takes into account the effect of the elastic parameters of the anti-bending bars attachment elements to the supports and the effect of the rigid and bending modes of the anti-bending bars on the dynamic response of the vehicle carbody;
- development of the mathematical model of the carbody - anti-bending bars system and processing of the equations of motion;
- development of the numerical model for calculating the frequency response functions of the carbody and anti-bending bars;
- development of software applications for simulating the dynamic response of the carbody for the " carbody without anti-bending bars" model, the " carbody with anti-bending bars without inertia" model, the " carbody with anti-bending bars with inertia" model;
- comparative analysis of the dynamic response of the carbody for the model " carbody without anti-bending bars", the model " carbody with anti-bending bars without inertia", the model " carbody with anti-bending bars with inertia";
- establishing the basic properties of the dynamic response of the carbody - anti-bending bars system;
- establishing the characteristics of the harmonic vibration regime of the carbody and anti-bending bars depending on the rigidity of the support bars;
- establishing the correlation between the eigenfrequencies of the bounce vibrations and bending vibrations of the carbody - anti-bending bars system and the rigidity of the support bars;
- identifying the possibilities of increasing the frequency of bending vibrations of the carbody using anti-bending bars;
- integration of the carbody - anti-bending bars system model into the general carbody - anti-bending bars - bogies - track system model used to evaluate the effect of anti-bending bars on the vertical vibrations of the carbody;

- development of the mathematical model of the carbody - anti-bending bars - bogies - track system and processing of the equations of motion;
- development of the numerical model for calculating the frequency response functions of the carbody and anti-bending bars;
- development of software applications for simulating the dynamic response of the carbody with anti-bending bars;
- analysis of the dynamic response of the carbody with anti-bending bars;
- comparative analysis of the effect of anti-bending bars on the vertical vibrations of the railway vehicle carbody based on the " carbody without anti-bending bars" model, the " carbody with anti-bending bars without inertia" model and the " carbody with anti-bending bars with inertia" model.

5. Carrying out experimental determinations under real physical conditions, on a passenger vehicle operating on a current line, with the following contributions:

- synthesis of experimental results and creation of a data archive containing the vertical accelerations measured at the middle of the carbody;
- creation of software applications for processing the measured accelerations;
- analysis of experimental results;
- synthesis of conclusions regarding the agreement between theoretical and experimental results based on criteria that take into account: the eigenfrequencies of the main vertical vibration modes at the middle of the carbody; the dominant vibration modes at the middle of the carbody identified on the acceleration spectra.

9.3. Future research directions

The results presented in this thesis highlight important aspects regarding the modelling of the vehicle-track system in simulating the vertical vibration behaviour of flexible carbodies of passenger railway vehicles, respectively the possibilities of reducing vertical bending vibrations by mounting anti-bending bars on the carbody chassis. Considering the results obtained, there are prospects regarding the development of the research topic treated in this paper in new directions oriented towards:

- Development of the concept of anti-bending bars on which the method of reducing bending vibrations of the carbody of railway vehicles is based and its transition to a higher technological maturity level (TRL). The concept of anti-bending bars was formulated as a result of theoretical research, corresponding to TRL2, and then was verified based on the results obtained experimentally in laboratory conditions, thus moving to the technological maturity level TRL3.
- Developing new concepts and integrating them into methods for reducing carbody bending vibrations and improving ride comfort based, for example, on optimizing secondary suspension damping or increasing the structural rigidity of the carbody.
- Development of studies on the influence of vehicle-track system modeling in simulating the vibration behaviour of flexible carbodies of passenger vehicles.

Selective bibliography

1. Bokaeian V., Rezvani M.A., Arcos R., *The coupled effects of bending and torsional flexural modes of a high-speed train car body on its vertical ride quality*, Proceedings of the Institution of Mechanical Engineers Part K Journal of Multi-body Dynamics, 2019, Vol. 233, Issue 4, 979-993.
2. Chen Z., Zhu G., *Dynamic evaluation on ride comfort of metro vehicle considering structural flexibility*, Archives of Civil and Mechanical Engineering, 2021, Vol. 21, 162.
3. Corradi R., Mazzola L., Ripamonti F., *Optimisation of secondary suspension dampers to improve the ride comfort of high-speed rail vehicles*, The 23rd International Congress on Sound and Vibration ICSV23, Athens (Greece), 10-14 July 2016.
4. Diana G., Cheli F., Collina A., Corradi R., Melzi S., *The development of a numerical model for railway vehicles comfort assessment through comparison with experimental measurements*, Vehicle System Dynamics, 2002, Vol. 38, No. 3, 165-183.
5. Dumitriu M., *Izolarea și amortizarea vibrațiilor la vehiculele feroviare*, Editura Matrix Rom, București, 2021.
6. Dumitriu M., *Confortul vibratoriu la vehiculele feroviare*, Editura Matrix Rom, Bucureşti, 2019.
7. Dumitriu M., Sebeşan I., *Calitatea mersului la vehiculele feroviare*, Editura Matrix Rom, București, 2016.
8. Dumitriu M., Sorohan Ș., **Apostol I.I**., *Finite element models for the analysis of the effectiveness of the vertical vibration reduction method of the railway vehicle carbody with anti-bending system - Applications for an experimental scale model*, Acta Technica Napocensis, Series: Applied Mathematics, Mechanics, and Engineering, 2024, Vol. 67, Issue 2S, 613-620.
9. Dumitriu M., **Apostol I.I.,** *The effect of the traction rod on the vertical vibration behavior of the railway vehicle carbody*, Vehicles, 2023, Vol. 5, Issue 4, 1482-1504.
10. Dumitriu M., Mazilu T., **Apostol I.I.**, *Scale models to verify the effectiveness of the methods to reducing the vertical bending vibration of the railway vehicles carbody: Applications and design elements*, Applied Sciences, 2023, Vol. 13, Issue 4, 2368.
11. Dumitriu, M., **Apostol, I.I.,** Stănică, D.I**.**, *Influence of the suspension model in the simulation of the vertical vibration behavior of the railway vehicle car body*, Vibration, 2023, Vol. 6, Issue 3, 512-535.
12. Dumitriu M., Stănică D.I., *Vertical bending vibration analysis of the car body of railway vehicle*, IOP Conf. Series: Materials Science and Engineering, 2019, Vol. 564, 012104.
13. Dumitriu M., *Study on improving the ride comfort in railway vehicles using anti-bending dampers*, Applied Mechanics and Materials, 2018, Vol. 880, 207-212.
14. Dumitriu M., *A new passive approach to reducing the carbody vertical bending vibration of railway vehicles*, Vehicle System Dynamics, 2017, Vol. 55, No. 11, 1787-1806.
15. Dumitriu M., Cruceanu C., *Influences of carbody vertical flexibility on ride comfort of railway vehicles*, Archive of Mechanical Engineering, 2017, Vol. LXIV, Issue 2, 119-238.
16. Dumitriu M., *Analysis of the dynamic response in the railway vehicles to the track vertical irregularities. Part II: The numerical analysis*, Journal of Engineering Science and Technology Review, 2015, Vol. 8, Issue 4, 32-39.
17. Dumitriu M., *On the critical points of vertical vibration in a railway vehicle*, Archive of Mechanical Engineering, 2014, Vol. LXI, Issue 4, 115-140.
18. Foo E., Goodall, R.M., *Active suspension control of flexible bodied railway vehicles using electro-hydraulic and electromagnetic actuators*, Control Engineering Practice, 2000, Vol. 8, No. 5, 507-518.

19. Gong D., Wang K., Duan Y., Zhou J., *Car body floor vibration of high-speed railway vehicles and its reduction*, Journal of Low Frequency Noise, Vibration and Active Control, 2020, Vol. 39, 925-938.
20. Gong D., Zhou J., Sun W., Sun Y., Xia Z., *Method of multi-mode vibration control for the carbody of high-speed electric multiple unit trains*, Journal of Sound and Vibration, 2017, Vol. 409, 94-111.
21. Gong D., Zhou J., Sun W., *Passive control of railway vehicle car body flexural vibration by means of under frame dampers*, Journal of Mechanical Science and Technology, 2017, Vol. 31, Issue 2, 555-564.
22. Gong D., Zhou J.S., Sun W.J., *On the resonant vibration of a flexible railway car body and its suppression with a dynamic vibration absorber*, Journal of Vibration and Control, 2013, Vol. 19, Issue 5, 649-657.
23. Gong D., Gu Y.J., Song Y.J., Zhou J., *Study on geometry filtering phenomenon and flexible car body resonant vibration of articulated trains*, Advanced Materials Research, 2013, Vol. 787, 542-547.
24. Hansson J., Takano M., Takigami T., Tomioka T., Suzuki Y., *Vibration suppression of railway car body with piezoelectric elements (A study by using a scale model)*, JSME International Journal, Series C, 2004, Vol. 47, No. 2, 451-456.
25. Huang C., Zeng J., Luo G., Shi H., *Numerical and experimental studies on the car body flexible vibration reduction due to the effect of car body-mounted equipment*, Proceedings of the Institution of Mechanical Engineers, Part F: Journal of Rail and Rapid Transit, 2016, Vol. 232, Issue 1, 103-120.
26. Hui C., Weihua Z., Bingrong M., *Vertical vibration analysis of the flexible carbody of high speed train*, International Journal of Vehicle Structures & Systems, 2015, Vol. 7, No. 2, 55-60.
27. Iwnicki S., *Handbook of railway vehicle dynamics*, Taylor & Francis Group, LLC, 2006.
28. Jing L., Wang K., Zhai W., *Impact vibration behavior of railway vehicles: A state-of-the-art overview*, Acta Mechanica Sinica, 2021, Vol. 37, 1193-1221.
29. Johnsson A., Berbyuk V., Enelund M., *Pareto optimisation of railway bogie suspension damping to enhance safety and comfort*, Vehicle System Dynamics, 2012. Vol. 50, No. 9, 1379-1407. **46**
30. Kamada T., Hiraizumi T., Nagai M., *Active vibration suppression of lightweight railway vehicle body by combined use of piezoelectric actuators and linear actuators*, Vehicle System Dynamics, 2010, Vol. 48, 73-87**.**
31. Kamada T., Kiuchi R., Nagai M., *Suppression of railway vehicle vibration by shunt damping using stack type piezoelectric transducers*, Vehicle System Dynamics, 2008, Vol. 46, Supplement, 561-570.
32. Knothe K., Stichel S., *Rail vehicle dynamics*, Springer International Publishing AG, 2017.
33. Kozek M., Benatzky C., Schirrer A., Stribersky A., *Vibration damping of a flexible car body structure using piezo-stack actuators*, Proceedings of the 17th World Congress The International Federation of Automatic Control, 2008, 8284-8292.
34. Liu Y., Gong D., Zhou J., *Research on resonance mechanism of articulated train car body based on modal vibration extraction method*, Journal of Vibration and Control, 2024, doi:10.1177/10775463241256017.
35. Mazilu T., *Vibraţii roată-şină*, Editura Matrix Rom, Bucureşti, 2008.
36. Mazilu T, Dumitriu M., Sorohan Ș., Gheți M.I., **Apostol I.I.,** *Testing the effectiveness of the anti-bending bar system to reduce the vertical bending vibrations of the railway vehicle carbody using an experimental scale demonstrator,* Applied Science, 2024, Vol. 14, Issue 11, 4687.
37. Melero M., Nieto A.J., Morales A.L., Palomares E., Chicharro J.M., Ramiro C., Pintado P., *Experimental analysis of constrained layer damping structures for vibration isolation in lightweight railway vehicles*, Applied Sciences, 2022, Vol. 12, 8220.

38. Morales A.L., Chicharro J. M., Palomares E., Ramiro C., Nieto A.J., Pintado, P., *Experimental analysis of the influence of the passengers on flexural vibrations of railway vehicle carbodies*, Vehicle System Dynamics, 2021, Vol. 60, Issue 8, 2825-2844.
39. Miao B.R., Luo Y.X., Peng Q.M., Qiu Y.Z., Chen H., Yang Z.K., *Multidisciplinary design optimization of lightweight carbody for fatigue assessment*, Materials & Design, 2020, Vol. 194, 108910.
40. Miao B.R., Zhang W., Zhang J., Jin D., *Evaluation of railway vehicle car body fatigue life and durability usingmulti-disciplinary analysis method*, International Journal Vehicle Structures & Systems, 2009, Vol. 1, Issue 4, 85-92.
41. Nakagawa C., Suzuki H., *Effects of train vibrations on passenger PC use*, QR of RTRI, 2005, Vol. 46, Issue 3, 200-205.
42. Schandl G., Lugner P., Benatzky C., Kozek M., Stribersk M., *Comfort enhancement by an active vibration reduction system for a flexible railway car body,* Vehicle System Dynamics, 2007, Vol. 45, No. 9, 835-847.
43. Schirrer A., Kozek M., *Co-simulation as effective method for flexible structure vibration control design validation and optimization,* 16th Mediterranean Conference on Control and Automation Congress Centre, Ajaccio, France, June 25-27, 2008, 481-486.
44. Schirrer A., Kozek M., Schöftner J., *MIMO vibration control for a flexible rail car body: Design and experimental validation, vibration analysis and control – new trends and development*, Chapter 15, 2011.
45. Sebeşan I., *Dinamica vehiculelor feroviare*, Editura Matrix Rom, Bucureşti, 2011.
46. Sebeşan I., Mazilu T., *Vibraţiile vehiculelor feroviare,* Editura Matrix Rom, Bucureşti, 2010.
47. Shi H.L., Wu P., *Flexible vibration analysis for car body of high-speed EMU*, Journal of Mechanical Science and Technology, 2016, Vol. 30, No. 1, 55-66.
48. Singh S.K., Vishwakarma A., Singh S.R., Racherla V., *Effect of suspension parameters on dynamics of a metro coach: A parametric study*, Journal of Mechanical Science and Technology, 2023, Vol. 37, Issue 6, 2741-5753.
49. Singh S.K., Danawe H.G., Racherla V., Singh S.R., Prasad A., *Ride index for metro coaches: Experimental evaluation and vehicle dynamics results*, ASME 2019 International Mechanical Engineering Congress and Exposition, November 11–14, 2019, Paper No: IMECE2019-11128, V004T05A075.
50. Stănică D.I., Dumitriu M., Leu M., *The geometric filtering effect on ride comfort of the railway vehicles*, UPB Scientific Bulletin, Series D: Mechanical Engineering, 2021, Vol. 83, Issue 3, 137-154.
51. Stănică D.I., Dumitriu M., *Critical points numerical analysis of ride comfort of the flexible railway carbody*, IOP Conf. Series: Materials Science and Engineering, 2019, Vol. 682, 012004.
52. Sugahara Y., Kojima T., *Suppression of vertical vibration in railway vehicle carbodies through control of damping force in primary suspension: Presentation of results from running tests with meter-gauge car on a secondary line*, Computers in Railways XVI, 2018, Vol 181, 329-337.
53. Sugahara Y., Watanabe N., Takigami T., Koganei R., *Vertical vibration suppression system for railway vehicles based on primary suspension damping control – system development and vehicle running test results*, QR of RTRI, 2011, Vol .52, No. 1, 13-19.
54. Sugahara Y., Watanabe N., Takigami T., Koganei R., *Development of primary suspension damping control system for suppressing vertical bending vibration of railway vehicle car body*, 9th World Congress on Railway Research, 2011.
55. Sugahara Y., *Suppression of vertical bending vibration in railway car bodies by primary suspension damping control* (*Results of running tests using Shinkansen vehicles*), Proceedings of the 21th International Symposium on Dynamics of Vehicles on Roads and Tracks (IAVSD'09), Stockholm, Sweden, Aug. 17-21, 2009, Paper No. 13.

56. Sugahara Y., Kazato A., Koganei R., Sampei M., Nakaura S., *Suppression of vertical bending and rigid-body-mode vibration in railway vehicle car body by primary and secondary suspension control: Results of simulations and running tests using Shinkansen vehicle*, Proceedings of the Institution of Mechanical Engineers, Part F: Journal of Rail and Rapid Transit, 2009, Vol. 223, No. 6, 517-531.
57. Sun Y., Gong D., Zhou J., Sun W., Xia Z., *Low frequency vibration control of railway vehicles based on a high static low dynamic stiffness dynamic vibration absorber*. Science China Technological Sciences, 2019, Vol. 62, 60-69.
58. Takigami T., Tomioka T., *Bending vibration suppression of railway vehicle carbody with piezoelectric elements (Experimental results of excitation tests with a commuter car)*, Journal of Mechanical Systems for Transportation and Logistics, 2008, Vol. 1, No. 1, 111-121.
59. Takigami T., Tomioka T., Hanson J., *Vibration suppression of railway vehicle carbody with piezoelectric elements (A study by using a scale model of Shinkansen)*, Journal of Advanced Mechanical Design, Systems, and Manufacturing, 2007, Vol.1, No. 5, 649-660.
60. Takigami T., Tomioka T., *Investigation to suppress bending vibration of railway vehicle carbodies using piezoelectric elements*, QR of RTRI, 2005, Vol. 46, No. 4, 225-230.
61. Takigami T., *Investigation into suppressing the bending vibration of railway vehicle carbody with piezoelectric elements*, Railway Technology Avalanche, 2005, No. 9.
62. Takigami T., Tomioka T., *Vibration suppression of scale model of railway carbody with piezoelectric element (A study focused on designing shunt circuits)*, 12th SPIE International Symposium Smart Structures and Materials, 2005, Vol. 5760, San Diego, California, 1254-1262.
63. Tomioka T., Takigami T., Suzuki Y., *Numerical analysis of three-dimensional flexural vibration of railway vehicle car body*, Vehicle System Dynamics, 2006, Vol. 44, Supplement, 272-285.
64. Wen Y., Sun Q., Zou Y., You H., *Study on the vibration suppression of a flexible carbody for urban railway vehicles with a magnetorheological elastomer-based dynamic vibration absorber*, Proceedings of the Institution of Mechanical Engineers, Part F: Journal of Rail and Rapid Transit, 2020, Vol. 234, 749-764.
65. Wu Z., Zhang N, Yao J, Poliakov V., *Analysis of train car-body comfort zonal distribution by random vibration method*, Applied Science Sciences, 2022, Vol. 12, Issue 15, 7442.
66. Wu P., Zeng J., Dai H., *Dynamic response analysis of railway passenger car with flexible carbody model based on semi-active suspensions*, Vehicle System Dynamics, 2004, Vol. 41 (Suppl.), 774-783.
67. Xu H., Xiao X., Liu X., Jin X., *Study on the influence of car-body flexibility on passengers' ride comfort*, Vehicle System Dynamics, 2024, Vol. 62, Issue 8, 1952-1989.
68. Yang G., Wang C., Xiang F., Xiao S., *Effect of train carbody's parameters on vertical bending stiffness performance*, Chinese Journal of Mechanical Engineering, 2016, Vol. 29, No. 6, 1120-1126.
69. Younesian D., Nankali A., *Spectral optimization of the suspension system of high-speed trains*, International Journal Vehicle Structures & Systems, 2009, Vol. 1, Issue 4, 98-103.
70. Zhang D., Tao Z.Y. Zhou K., Zhou F.R., Peng Q.Y, Tang Y.Y., *Improving the energy efficiency and riding comfort of high-speed trains across slopes by the optimized suspension control*, Energy, 2024, Vol. 307, 132660.
71. Zheng X, *Active vibration control of flexible bodied railway vehicles via smart structures*, Doctoral Thesis, 2011, Loughborough University.
72. Zhou J., Goodall R., Ren L., Zhang H., *Influences of car body vertical flexibility on ride quality of passenger railway vehicles*, Proceedings of the Institution of Mechanical Engineers, Part F: Journal of Rail and Rapid Transit, 2009, Vol. 223, 461-471.
73. Zhou J., Wenjing S., *Analysis on geometric filtering phenomenon and flexible car body resonant vibration of railway vehicles*, Journal of Tongji University, 2009, Vol. 37, Issue 12, 1653-1657.
74. http://www.mrcf.pub.ro/prezentare-proiect-724ped-2022/